NANOPARTICLE INTEGRATED MICROBIAL WATER SPLITTING FOR CARBONATE REDUCTION IN CO2 CAPTURING

M. Sc. Thesis

2020

For partial fulfilment of the requirement for the Master of Science in Biotechnology

Submitted to
Central Department of Biotechnology
Tribhuvan University
Kirtipur, Kathmandu, Nepal

Submitted by
Rita Kumari Oli
Roll no: BT 415/073
T.U.Regd No: 5-2-0038-0021-2012

NANOPARTICLES INTEGRATED MICROBIAL WATER SPLITTING FOR CARBONATE REDUCTION IN CO_2 CAPTURING

M. Sc. Thesis

2020

For partial fulfilment of the requirements for the Master of Science in Biotechnology

Submitted to
Central Department of Biotechnology
Tribhuvan University
Kirtipur, Kathmandu, Nepal

Submitted by
Rita Kumari Oli
Roll No.: BT 415/073
T.U. Regd. No.: 5-2-0038-0021-2012

Supervisors

Dr. Pramod Aryal
Visiting Senior Scientist
Central Department of Biotechnology
Tribhuvan University, Kirtipur
Kathmandu, Nepal

Prof. Dr. Rajani Malla
Former Head of Department
Central Department of Biotechnology
Tribhuvan University, Kirtipur
Kathmandu, Nepal

ACKNOWLEDGEMENTS

I am very much grateful to my supervisor **Dr. Pramod Aryal**, Senior Scientist, Central Department of Biotechnology for his eternal effort and guidance throughout my research work. I am always thankful to his brilliant ideas and his incessant enthusiasm to work. His valuable support and motivation during the phase of my thesis work; this research could not be possible without him. Moreover I am indebted to his suggestions and discussion that set the new door to research carbon dioxide and nitrogen reduction, water splitting concept and cloning concept via microorganism.

I would like to give my gratitude to **Prof.Dr.Rajani Malla**, Central Department of Biotechnology, Tribhuwan University, for her valuable support, motivate me and encourage me during my thesis.

I would like to give my gratitude to **Prof.Dr.Krishna Das Manandhar**, Head of Department, Central Department of Biotechnology, Tribhuwan University, providing platform for performing thesis as assignment.

I would like to give my gratitude to **Prof.Dr.Jarina Joshi**, Acting Head of Department, Central Department of Biotechnology, Tribhuwan University, providing platform for performing thesis work.

I am thankful to **Alpha agro Pvt.Ltd.** Birgunj for providing me some of the chemicals required for synthesis of cobalt nano-particle. I am also thankful to Nepal Academy of Science and Technology (NAST) for XRD characterization of cobalt nano-particle and also to Central Department of Chemistry, TU, Kirtipur for FTIR.

It is my pleasure to acknowledge all our respected professors, external and internal teachers and all staff members of Central Department of Biotechnology.

I would like to especially thanks to my seniors Mrs. Manju Pun, Ms. Sabina Thapa, Ms. Sita Ghimire and my friend Pooja Pathak and my sister Kabita Kandel for their logical ideas, continuous support and motivate me to complete my thesis.

I would also like to thanks to my brothers Samiran Subedi, Sawan Chaudhary, Siddhartha Gautam and Devraj Mainali for helping me during conduction of my thesis work.

I am grateful to my loving parents who always tried to make me feel a lucky and privileged person and without their unconditional love and support this study would not have been possible. Thank you very much for always being there for me.

Finally, I need to thank all my friends, seniors and juniors and those who had directly or indirectly helped me during the entire thesis work.

Rita Kumari Oli

ACRONYMS

PGA	Phosphoglyceric acid
CO_2	Carbon dioxide
O_2	Oxygen
CCM	Carbon dioxide Concentrating Mechanism
CAM	Crassulacean Acid Metabolism
NAD	Nicotinamide Adenosine Dinucleotide
ATP	Adenosine Tri Phosphate
ADP	Adenosine Di Phosphate
Pi	Inorganic phosphate
PSII	Photosystem II
PSI	Photosystem I
H_2O	Water
NADPH	Nicotinamide Adenosine Diphosphate Hydrogen
LHC	light-Harvesting Complex
RuBisCO	Ribulose1-5Bisphosphate Carboxylase/Oxygenase
N_2	Nitrogen
TCA	Tri-Carboxylic Acid
ED	Entner-Doudoroff pathway
OEC	Oxygen-Evolving Complex
PEC	Photo Electro Chemical
MFC	Microbial Fuel Cells
OER	Oxygen Evolution Reaction
NH_3	Ammonia
BNF	Biological Nitrogen Fixation

N_2O	Nitrous Oxide
N_3	Azide
C_2H_2	Acetylene
OEC	Artificial Evolving Complex
XRD	X-ray Diffraction
FTIR	Fourier Transform Infrared
LB	Lauria Bertani
sps	Species
mg/l	Milligram/litre
g/l	Gram/litre
NCF	Nitrogen Carbon Free
Nfb	Nitrogen free basal
µl	Microlitre
ml	Millilitre
nm	Nanometer
min	Minute
mM	Millimole
Conc.	Concentration
mix	Mixture
d/w	Distilled water
α	Alpha
rpm	Revolution per minute
%	Percentage
IR	Infrared
KPi	Potassium inorganic phosphate
Co nano-particle	Cobalt oxy hydroxide

LIST OF FIGURES

LIST OF TABLES

TABLE OF CONTENTS

ABSTRACT

The global population is increasing day by day and the problems generated by them also increasing in the same proportion. The global warming mainly due to the anthropogenic activities is among them and innovative approaches are required to tame this. Among the agents involved in global warming are nitrous oxide (N_2O), carbon dioxide (CO_2) but N_2O has around 300 times the heat-trapping capacity than CO_2 and could be released in atmosphere through nitrogen cycling of nitrogenous chemical fertilizers. Moreover, having heterotrophic bacterial bio-fertilizer supplement that has ability to utilize ammonia and nitrate could be an alternative to prevent N_2O release. Thus, bio-fertilizer could be alternative to counter the negative impact of indiscriminate use of chemical fertilizers. Hence, one of the bio-fertilizers, *Azospirillum* species, was isolated and characterized through Gram's staining and biochemical tests. Then ammonium ions present in nitrogen free broth (Nfb) culture media were quantified to select the best strain for development as bio-fertilizer. Similarly, syntrophic growth ability of isolates in modified nitrogen and carbon free (NCF) media indicated that the isolates can reduce atmospheric CO_2. Then, protocol was optimized for the development of cellulose producing strain directly from reduce carbon source obtain from CO_2 reduction by isolates. Water splitting mechanism also done by using MFCs where the bacterial culture was incubated. Genomic DNA extracted from the DH5α *E.coli* and *bcsA* and *adrA* gene were amplified by using designed primers. Cellulose genetic engineering was performed using these genes upon digestion and ligation of *bcsA* gene and *adrA* gene in pET28a+ vector. Transformation was successfully done in *E.coli* DH5α. Finally transforming was validated through single restriction digestion of extracted plasmids. Thus, it is suggested that engineering of the isolate for higher CO_2 reduction and cellulose production could support micro cellulose production.

Keywords: Bio-fertilizer, *Azospirillum*, Syntrophic growth, CO_2 reduction, water splitting mechanism, Cellulose genetic engineering

CHAPTER 1
INTRODUCTION

1.1 Background

Global food security is being threatened by increasing population and food demands and diminishing availability of arable land and gains in agricultural productivity (Sharwood *et al.,* 2016). The agriculture productivity could be explored through more environment friendly bio-fertilizers as bio-fertilizers are selective live micro-organism like bacteria, fungi that colonize the rhizosphere or the interior of the plant and promote growth by increasing the availability of primary nutrient and growth stimulus to the target crop, when applied to seed, plant surfaces or soil. They provide a cost effective, eco-friendly and renewable source of nutrients. It improves and increase the nutrient availability to the crop production in which biological process is involved with replacement of chemical fertilizers. They play a vital role in improving soil fertility and ensure maintaining long term sustainability. This could be an alternative because bio-fertilizer overall produced higher growth rates and yield compared with chemical fertilizer (Agbodjato *et. al*., 2018).

Numerous species of soil bacteria which flourish in the rhizosphere of plants, but which may grow in, on, or around plant tissues, stimulate plant growth and are collectively known as plant growth promoting rhizobacteria (PGPR). Modes of PGPR action include fixing N_2. solubilize phosphate from complex organic compounds, and mobilize various metals from rocks such as P, Mg, Zn, positively influencing root growth with morphology and promoting other beneficial plant-microbe symbiosis. The combination of these modes of actions in PGPR is also addressed, as well as the challenges facing the more widespread utilization of PGPR as bio fertilizers (Alam & Kumar Seth, 2012).

The bio-fertilizer can be manufactured both in solid as well as in liquid form. Carbon Source such as Malic acid, Sucrose, Glucose, Manitose and Nitrogen source like Yield extract, Ammonium sulphate, Peptone. Micro-Nutrients, such as Mg sulphate, Zn sulphate, Co nitrate. For the formulations, stabilizers/surfactants, such as Polyethylene Glycol, Glycerol, and PVP could be explored. Moreover, some microorganism to be used in the said facility for production of the bio-fertilizer ranges are *Rhizobium*, *Pseudomonas*, *Azotobacter*, *Azospirillium*, Phosphate Solubilising bacteria such as *Bacillus* (PSB), Potash Mobilizing Bacteria (KMB) and *Trichoderma* for compost production (Rajasekaran *et al.,* 2015). In addition, cellulose is the most abundant biopolymer on earth, recognized as the major component of plant biomass, but also a representative of microbial extracellular polymers (McNamara *et al.,* 2015).

Bacterial cellulose (BC) belongs to specific products of primary metabolism and is mainly a protective coating. Cellulose is synthesized by bacteria (Römling & Galperin, 2015).

Cellulose is an unbranched polymer of β-1, 4 linked glucopyranose residues. Bacterial cellulose has found a multitude of applications in paper, textile, and food industries and as a biomaterial in cosmetics and medicine (Tayeb *et al.,* 2018) that gives the characteristics of the cellulose molecules organized in the cell walls in the form of microfibrils. One of the bacterial sps known to be producing is *Azospirillum* sps and is an important organism when studying their inherent capacity (Onyeze *et. al*., 2013).

Furthermore, *Azospirillum* species are commonly found in soils and in association with roots of plants namely rice, maize, wheat and vegetables. In addition, rhizosphere colonization by *Azospirillum* species has been shown to stimulate the growth of a variety of plant species. To which the success of the *Azospirillum* plant interaction depends on the survival and persistence of this bacterium in soil and the effective colonization of the rhizosphere (Fukami *et al.,* 2018). It is now presumed to be that an understanding of microbial diversity perspectives in agricultural is the indicators of soil quality and plant productivity (Steenhoudt & Vanderleyden, 2000). Thus, soil microbiome is of an importance. But, the increased population worldwide and the anthropogenic activities have been supposed to be the adverse effect of global warming. This has prompted to reduce CO_2 as and making it as the alternative source or research prime concern. The thrus is off without giving any external light source or minimal energy if bacterial cellulose could be formed in electro-chemical synthesis would be an area to explore. Where the use of cobalt nano-particles that could help for enhanced water splitting for carbon dioxide reduction could be an alternative. Thus, since Nepal has a lot of water naturally, it could be used for bio-fertilizer production if the present research supports. One of the molecules to be biologically synthesized could be cellulose as it has myriad of utility and also supports carbon dioxide sequestration. One of the areas of our research is to produce more amount of bacterial cellulose through cellulose biosynthesis engineering.

1.2 Hypothesis:

1.2.1 Null hypothesis (H_0):

The specific nitrogen fixing bacterium couldn't be used for nano based water splitting (cellulose) for carbon dioxide reduction by electrochemical synthesis.

1.2.2 Alternative Hypothesis (H_1):

The specific nitrogen fixing bacterium could be used for nano based water splitting (cellulose) for carbon dioxide reduction by electrochemical synthesis.

1.3 Objectives

1.3.1 General Objective

- To amplify eco-friendly nano based water splitting for carbon dioxide reduction for electrochemical synthesis (cellulose) and bacterial engineering as prototype

1.3.2 Specific Objectives

- To synthesize cobalt nano-particle for augmented carbon dioxide reduction in Microbial fuel cell
- To develop syntrophic growth for better carbon reduction (inorganic to organic)
- To modify the water splitting mechanism
- To clone bacterial cellulose synthesis under constitutive promoter

1.4 Rationale and scope of the study

By using microbial fuel cells device for the production of cellulose as the final product by adding different buffer and media into anodic and cathodic chambers respectively. Inside the anodic chamber electrode used and formed hydrogen as proton and electron. Similarly, in cathodic chamber there could be the chemical reaction using nitrogen free media by adding carbonate as the sole source of carbon and formed white precipitate of cellulose. Atmospheric carbondioxide CO_2 is fixed as carbonate CO_3 form by using putative *Azospirillum* sps which is nitrogen and carbon fix organisms. For more production of cellulose there can be used another technique as syntrophic growth in single camber and double chamber as MFCs. In anodic chamber there could be the conversion of NAD^+ to NADH and bacterial cell release proton and electron. This can be moved through another chamber through semipermeable membrane and electric circuit while not giving external electricity.

The increased population worldwide day by day have main adverse effect faced in termed as global warming. So need the reduced CO_2 as the alternative source or process in our research. This warming affect all of the living and non living things which may cause problem in direct and indirect in world as in the field of agricultural crop production, human health and many more but here focused on the side of biofertilizer through splitting water and have final results as cellulose production from cabondioxide reduction in dark condition. Without giving any external light source or having any sunlight directly bacterial cellulose was formed having different cycle obtained through MFC device with transfer electron and proton passed through membrane and electro catalyst material as in the use of cobalt nano particles which help to enhance the production of biochemical process in there. Main target of our research is to produce more amount of bacterial cellulose through cellulose engineering. Normally cellulose is

produce through plant in nature but in this process it takes more time and cost so we thought why not we find alternative method through bacteria to produce cellulose. This is also only possible through the water splitting mechanism, syntrophic growth and using Microbial Fuel cells. However, studies of novel bacterial strains and optimization of culture conditions promise to make commercial production of bacterial cellulose and its derivatives economically feasible in the near future.

CHAPTER 2

LITERATURE REVIEW

2.1 Uses of water for the food production and carbon reduction

Water has their unique property which is also known as universal solvent (Pohorille *et. al*., 2012). It is essential element in biological, economical and social systems. About 71% of the earth's surface is covered with water (Universe today, 2014). Humans, animals and plants and other living organisms need water for survival. Although its uses have high value for nutrition, health (Matassa *et al.,* 2015) and also has uses in various purposes like food fuel and feed. Its demand is increasing in agricultural, industrial as well as urban settings (Meinzen-dick & Jackson, 1996).

FAO and world water council (Lenton *et. al*., 2008) said that with appropriate investment and policy interventions, food production will be sufficient to support a global population of 9-10 billion in 2050 but without the use of water it cannot be possible for the production of food for global demand (Pate, 2001) and with increased demand for population growth to meet their standard of living water could be limited as only after their demand then it can be diverted for food and irrigation. Moreover, water has multiple benefits in determining natural ecosystem's health and sustainability (Cosgrove & Loucks, 2015).

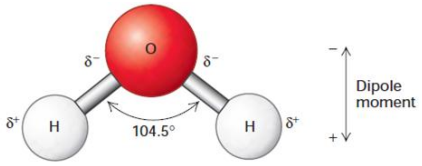

Figure (1): The dipole nature of a water molecule adopted from (Latner, 1970)

Water is dipoles that form electrostatic, non-covalent interactions with one another and with other molecules. It is constituents of all living systems, and they are liberated by many reactions that take place between organic molecules within cells. So in osmosis process water moves across such a semi permeable membrane from a solution of low solute (high water) concentration to one of high solute (low water) concentration until the water concentrations on both sides are equal. Under normal in vivo conditions (Rosiak, 1999) ion channels in the plasma membrane control the movement of ions into and out of cells so that there is no net movement of water and the usual cell volume is maintained. Thus, the movement of water in and out of cells is an important feature of the life of both plants and animals (Latner, 1970). To maintain the water in cells, most biological membranes are semi permeable, more permeable to water than to ions or most other solutes.

2.2 Autoionization of water

The term autoionization, also known as self-ionization of water, means the dissociation of two water molecules itself into hydronium ion and hydroxide ion ($H_2O + H_2O \leftrightarrow H_3O^+ + OH^-$) that exist for a femtosecond (Geissler *et al.,* 2001). This ionization reaction occurs in liquid water as intermediate state. As in the wire connection, hydrogen bond between water molecules keep them intact (Deng, 2004). In neutral condition, water only dissociates as the form of hydrogen and oxygen molecules instead of ionization but because of solvent generated electric field, a proton gets transferred to another molecule of water giving rise to respective ions. The proton transfer is classified as adiabatic and non-adiabatic, respectively, due to the quantum tunnel splitting effect (Uddin *et al.,* 2014).

The protons and hydroxide ions are one of the fastest diffusing ions in liquid water and proton mobility is four times faster than the mobility of water molecules (Bankura & Chandra, 2015). The H-bonding between the acceptor and donor water molecule plays an important role in proton transfer and stabilization of the H_3O^+ and OH^- ion pairs. This only happens when a strong electric field is generated by local water molecules and initiates the dissociation of the water molecules (Lentz & Garofalini, 2018). This process is very important in the different areas of biology and chemistry (Moqadam *et al.,* 2018) because water plays an important role with the solvent properties and can show both acidic and basic characters. Though the mobility of a (Kazarian *et. al*., 2015) hydronium ion is two times greater than that of a hydroxide ion at room temperature (Br & Acid, 2009).

2.3 Types of plants

2.3.1 C3 plants

Plants that does not require to reduce photorespiration is called C3 plants (Borland *et al.,* 2014). About 85% of plant species in this planet are made from C3 plants including, rice wheat soybeans and all trees. The C3 mechanism works well in cool environment (Drennan *et. al*., 1997). In this plant, firstly Calvin cycle fixed the CO_2 by RuBisCo and produces 3 carbon compounds (3PGA).

2.3.2 C4 Plants

The evolution of C4 photosynthesis that arose during periods of low CO_2 is based on the plant hydraulic system and have impacted plant life history, biogeography and the distribution of ecosystems (Lei, 1983). This could have been evolved from C3-C4 intermediate metabolism (Sack, 2012). The first carboxylation product in these types of plants is a 4 carbon compound and such plants are called C4 plants and metabolism is named as C4 cycle (Bräutigam et. al., 2017). This plant helps to reduce the wasteful

reaction of photorespiration. In C4 plants like sugarcane, CO_2 fixation and calvin cycle reaction takes place in two cells, is mesophyll cell and bundle of sheath, respectively. The rate of photorespiration in C4 plants is much lower than in C3 plants (Cousins et. al., 2020). In C4 plants, CO_2 is fixed initially in the outermost mesophyll cells by reaction with phosphoenolpyruvate (PEP). Then the four-carbon molecules so generated are shuttled to the interior bundle sheath cells, whereas the CO_2 is released and then used in the Calvin cycle.

The main characteristics of C4 plants are high growth rates and growth at higher temperature, low photorespiration rates (Keeley et. al., 2003). Most of the crops are C4 plants. This type of plants needs extra ATP to pump CO_2 but still they are more productive. C4 crop plants are also found in warmer area and are sensitive to cold stress. Some examples of C4 plants are maize, sorghum millet and sugarcane. (Lei, 1983) So, C4 photosynthesis is the operation of a CO_2-concentrating mechanism (CCM) which suppresses photorespiration by raising CO_2 around Rubisco (Pinto *et al.,* 2014). The main function of C4 cycle is CO_2 pumps around enzyme. Different types of CO_2 pumps occurs in BS (Bundle of sheath) cell based on the primary C4 decarboxylase enzyme (Pinto *et al.,* 2014).They are C4 –NADP- Malate enzyme type, C4- MALATE- NAD enzyme type and C4-PEP -CARBOXYKINASE enzyme type.

2.3.3 CAM plants and its metabolism

CAM has been detected in more than 1000 angiosperms of 17 different families and it is found in plants like Bromeliaceae, cacteceae, crassulaceae, euphorbiaceae, liliaceae, orchidaceae whereas in CAM plants like pineapple and cacti are adapted in dry environments, use the CAM pathway to minimize photorespiration (Borland *et al.,* 2014). These plants are typically dominant in very hot dry areas like deserts. CO_2 fixation and Calvin cycle takes place in same cell but in different time that is day and night respectively. These types of plant grow in dry place and have developed mechanism to save water and reduce the loss of unnecessary water (Bräutigam *et. al*., 2017). During dark time stomata is open and acidification in night due to the accumulation of malate in vacuole produced by carboxylation of PEP occurs in cytosol. In this time CO_2 fixation can happen (Keeley *et. al*., 2003). So, during in day time stomata is closed to reduce transpiration and deacidification starts on morning by decarboxylation of malic acid in chloroplast. CO_2 released is used in Calvin cycle and then PEP is produced in chloroplast from pyruvate and transported to cytosol but most of the PEP comes from glycolysis (Pate, 2001). Therefore this cycle only happens at day time, both process works in simultaneously (Guralnick *et al.,* 2008).

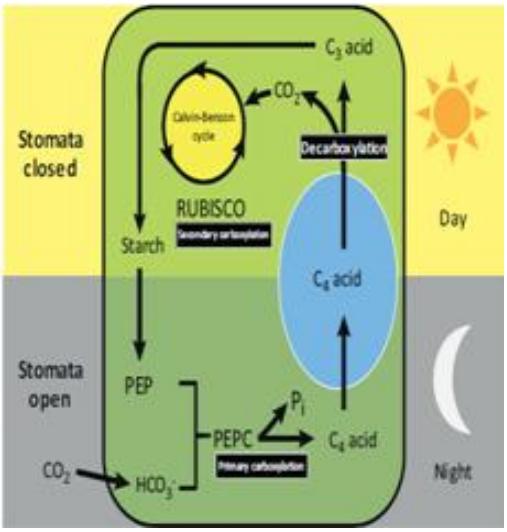

Figure (2): CAM cycle (Lodish *et. al*., 2001)

2.4 Rubisco enzyme

The term ribulose 1,5-bisphosphate carboxylase oxygenase (Rubisco) was coined in 1979 by David Eisenberg at a seminar honouring the retirement prominent RuBisco researcher Sam Wildman (Spreitzer *et. al*., 2002). The enzyme Rubisco mediates conversion from inorganic carbon to organic carbon. It is hexadecameric structure composed of large and small subunits (Andersson, 2008). It is found in more than 99.5% autotrophic (Bathellier *et. al*., 2018) organisms and photosynthetic bacteria, cyanobacteria, algae and plants.

Annual CO_2 fixation resulting from Rubisco's activity amounts for more than 10^{11} tons of atmospheric CO_2. From the evolutionary part Rubisco is one of the ancient enzymes responsible for carboxylation/oxygenation and are present in different forms, form I,II,III and IV (Slesak & Slesak, 2017). This enzyme is present in all domains of life with different forms and the most widespread clad is form I (Iñiguez *et. al*., 2020). The rubisco kinetics varies with changing intracellular concentrations of CO_2 in C3 and C4 plants but in CAM plants it is poorly investigated (Hermida-carrera *et al.,* 2020).

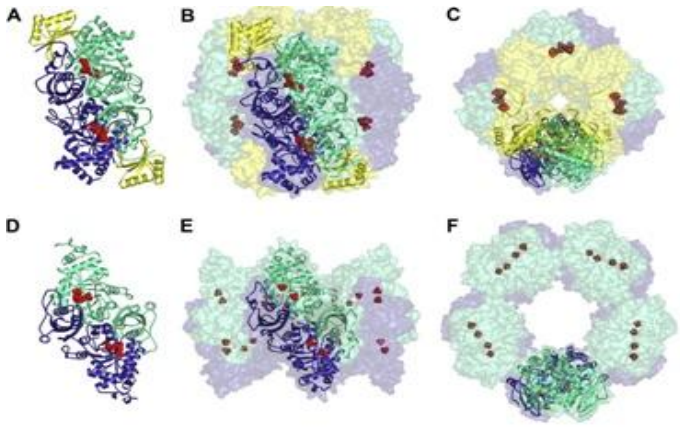

Figure (3): Different forms of Rubisco (Andersson & Backlund, 2008)

Rubisco activase is one of the proteins that are required in higher-plants to maintain and regulate the activity of Rubisco. Rubisco is so important to plants that it makes up 30% or more of the soluble protein in a typical plant leaf and it serves as in the first entry point of CO_2 then into the Calvin cycle and leads to the production of sugar (Rubisco *et al.,* 2019). But, this enzyme has the limitation of photosynthesis under high temperature and water deficit (Perdomo *et al.,* 2017).

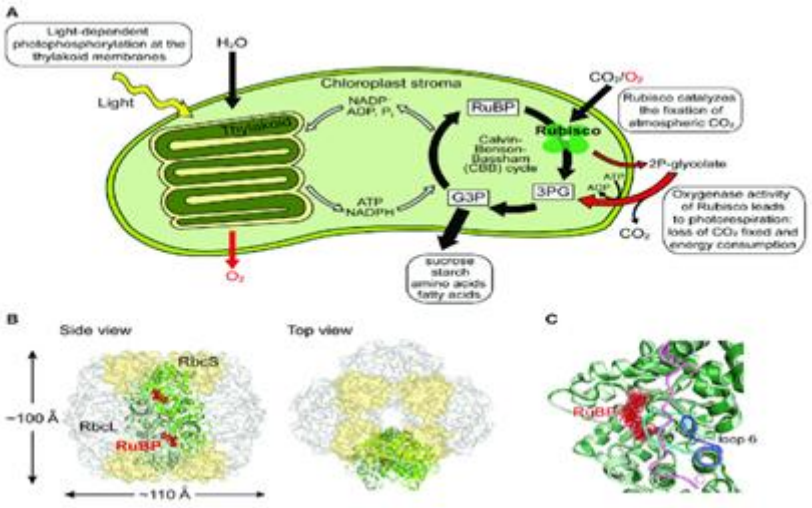

Figure (4): Structure and function of Rubisco (Tabita *et al.,* 2007)

2.5 Photosynthesis

Photosynthesis is one of the primary metabolic process that converts light energy into chemical energy which derives plant growth and biomass production (Colombo *et al.,* 2016).

In case of animals, the free energy in sugars and other molecules comes from food is released in the process of respiration. All synthesis of ATP in animal cells and in non-photosynthetic microorganisms results from the chemical transformation of energy-rich compounds in the diet as in the form of glucose or starch (Tomimatsu & Tang, 2016). But, in photosynthesis, plants and certain microorganisms can trap the energy from light and use it to synthesize ATP from ADP and Pi. Much of the ATP produced in photosynthesis is hydrolyzed to provide energy for the conversion of carbon dioxide to six-carbon sugars, this process is called carbon fixation (Sello *et al.,* 2019).

There are two stages that occur in photosynthesis, they are in first stage, light dependent reactions or light reaction. In this stage light is captured and use it to make the energy storage molecules ATP and NADPH or converted light into the chemical energy of phosphor anhydride bonds in ATP and stored in the chemical bonds of carbohydrates (Sukhov, 2016). In second stage, the light independent reactions which use this products to capture and reduce CO_2. Therefore, directly or indirectly, Arnon *et. al*., 1959 said that light energy captured by photosynthesis in plants and photosynthetic

bacteria is the ultimate source of chemical energy for almost all cells (Youvan et.al., 1987). Oxygen also formed during photosynthesis. In plants and eukaryotic single celled algae, photosynthesis occurs in chloroplasts. Chloroplasts are the largest and the most characteristic organelles in the cells of plants and green algae. It contain a complex system of thylakoid (Montgomery *et al.,* 2016) membranes in their interiors. These membranes contain the pigments named as chlorophyll and enzymes that absorb light and produce ATP during photosynthesis (Lawson & Vialet-Chabrand, 2019).

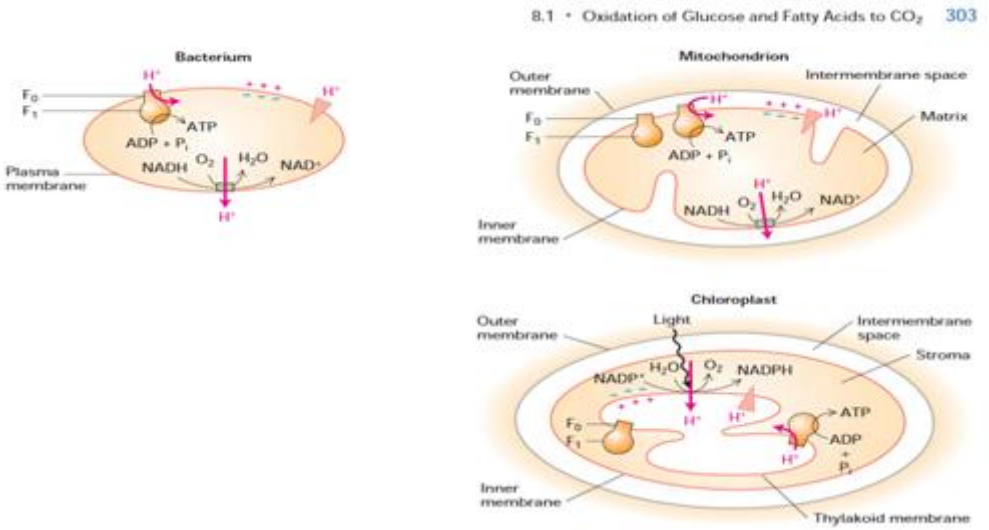

Figure (5): Synthesis of ATP in bacteria, mitochondria and chloroplasts (Lodish *et. al*., 2000)

Mechanism of photosynthetic pathway in plants can be divided into four stages at the area of the chloroplast (Marais *et al.,* 2015), they are as follows: first step in photosynthesis is the absorption of light by chlorophylls attached to protein in membranes, used to remove electron through water molecules. Reaction is as below: $2H_2O \xrightarrow{light} O_2 + 4H^+ + 4e$ Secondly, electron transport leading to formation of O_2 from H_2O, reduction of $NADP^-$ to NADPH and generation of a proton-motive force, electrons move from the quinone primary electron acceptor through a series of electron carriers until they reach the ultimate electron acceptor, usually the oxidized form of nicotinamide adenine dinucleotide phosphate ($NADP^-$), reducing it to NADPH (Sello *et al.,* 2019). Thirdly, synthesis of ATP, protons move down their concentration gradient from the thylakoid lumen to the stroma through the ATP synthase, which couples proton movement to the synthesis of ATP from ADP and Pi and last one is conversion of CO_2 into carbohydrates termed as carbon fixation, the ATP and NADPH generated by the second and third stages of photosynthesis provide the energy and the electrons to drive the synthesis of polymers of six-carbon sugars from CO_2 and H_2O. Thus, photosynthetic organisms convert sunlight to energy compounds like sugars (Heidary *et al.,* 2019).

2.6 Photosystem I and II

The rate of plant photosynthesis was discovered by biophysicist R. Emerson in 1940s found that the reaction in light of wavelength of 700 nm can be greatly enhanced by adding light of shorter wavelength. Photosynthesis in plants involves the interaction of two separate photosystems and is called PSI and PSII. PSI is driven by light of wavelength 700 nm or less and PSII is light of shorter wavelength 680 nm (Lodish *et al.,* 2000). Two photosystems also are distributed differently in thylakoid membranes and PSII splits water to form oxygen, whereas only PSI transfers electron and proton to the final electron acceptor, NADP.

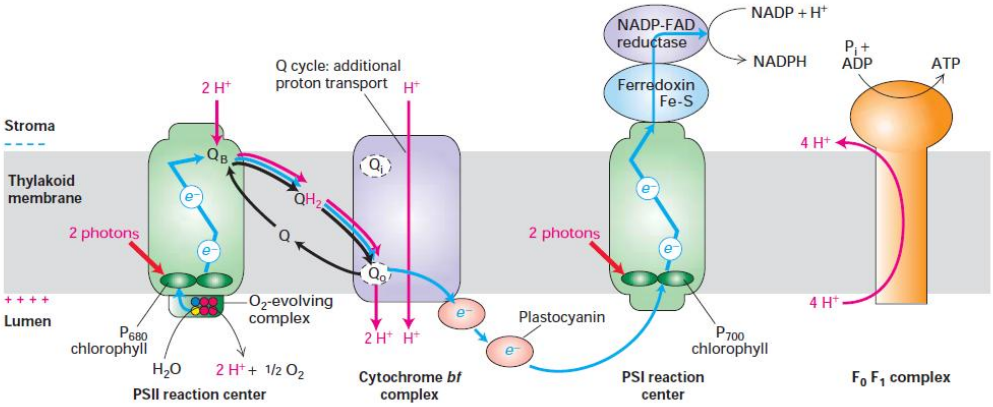

Figure(6): Linear electron flow in plants, photosystems, PSI and PSII (Lodish*et. al*., 2000)

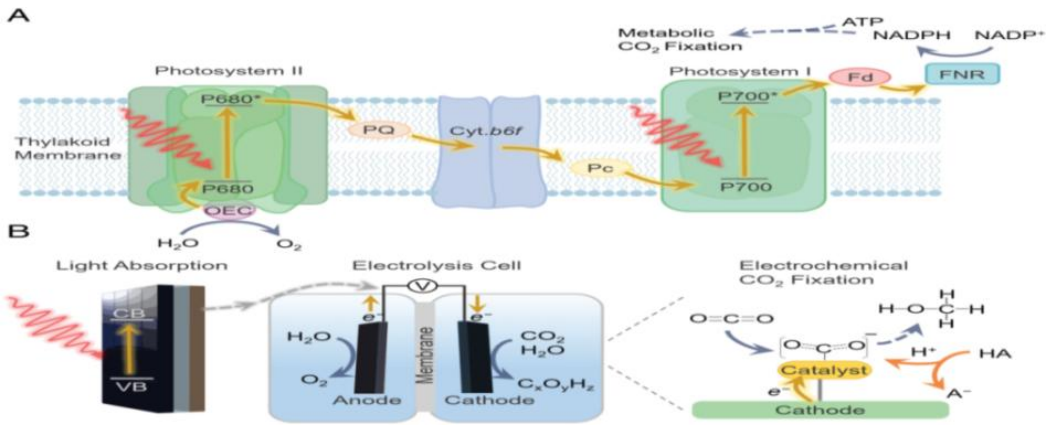

Figure(7): Natural and artificial photosynthesis (Heidary *et al.,* 2019)

The main source of electron in PSII comes from H_2O (Nawrocki *et al.,* 2019) where in PSI comes from PSII through an electron transport chain. Photosystem are found in thyloid membranes of algae, cyanobacteria and mainly in plants. It contains different chlorophyll, proteins and other pigments which get (Danielsson *et. al*., 2004) excited

only after absorbing the photon, and then the electrons is switched to higher energy orbital. Though the two photosystems in the light dependent reactions got discovered. PSII comes first in the path of electron flow and then PSI (Fujita *et. al*., 1987). So, in PSI photons are released by reaction center and that undergoes an electron carriers and finally produced NADPH through $NADP^+$ reductase enzyme from high energy electrons. This NADPH is used in the Calvin cycle. Therefore in PSII, proton and electrons comes from water used to reduce $NADP^+$ and in ATP production(Miyake, 2010). Also the electron flux in PSII exceed the total electron flux required for CO_2 assimilation and photorespiration is in high light conditions whereas the electron flow from water in PSII to water in PSI is termed as the water-water cycle (Makino *et al.,* 2002).

2.7 Photons

The absorption of light energy and its conversion into chemical energy occurs in multiprotein complexes and are called photosystems (Nelson *et. al*., 2006). Photosystems consist of two closely linked components: a reaction center, where the primary events of photosynthesis occur, and an antenna complex consisting of numerous protein complexes, called light-harvesting complexes (LHCs), which capture light energy and transmit it to the reaction center (Panitchayangkoon *et. al*., 2011)**.** So, photons are the best way to transmit information, where they move at the speed of light and do not strongly interact with their environment. Each photon of light has a defined amount of energy and these packets of energy called photons, also known as speed of light. Photons with shorter wavelength have higher energy (Lounis *et. al*., 2005).

Photons travel at the speed of light, $2.997x10^8$ m/s in empty space and Maxwell unveiled this proof in 1864 (ZME physics science, 2017). Photons absorption by an atom occurs due tothe photoelectric effect process in which the photon loses its entire energy to an atomic electron which is in turn liberated from the atom. This process requires the incident photon to have energy greater than the binding energy of an orbital electron.

2.8 Evolution of Cyanobacteria

Before the lives were possible in the earth, there has been adverse situation (BBC, 2015) and CO_2 got reduced and evolved oxygenic environment to make conditions possible for aerobic living organisms. The Kreb Cycle is major energy producers in most of the aerobic organisms (Buchanan & Arnon, 1990) and thus the evolutionary perspective of CO_2 reduction. This could be further substantiated because Euryarcheota such as autotrophic *Archaeoglobales* reduce CO_2 through reductive acetyl CO-A Pathway anaerobically. So this mechanism is energized by inorganic energy sources like oxidation of ammonia, hydrogen sulphide or elemental sulphur and Oxygen or metal ion used as electron acceptor (Barton *et al.,* 2020). On the other hand, Archea use CO_2 in the atmosphere for the fixation of Carbon by involving highly modified metabolic pathway,

3-hydroxypropionate/4-hydroxybutyrate cycle (Berg *et al.,* 2010) or Calvin Cycle, which is important in photosynthetic dark reduction of CO_2. These modes of CO_2 reduction clearly indicate metamorphosis of CO_2 reduction that might have given rise to Calvin cycle through RuBisCo enzyme. There are of two types of phototrophs: one is photoheterotrophs depends on light energy for production of ATP but obtained carbon from environmentally available organic compounds and another one is photoautotrophs, those includes green plant and cyanobacteria.

Cyanobacteria are one of the bacteria that obtain energy through photosynthesis, created the conditions in the planets early atmosphere that directed the evolution of aerobic metabolism and eukaryotic photosynthesis. They have micro compartment called as carboxysomes having RuBisCo enzyme as well as the enzyme carbonic anhydrase used for metabolic channelling to help the local CO_2 concentration to increase RuBisCo enzyme activity. Cyanobacteria are also diazotrops that fix nitrogen as well as carbon fixation through Calvin Cycle (Stal, 2015). The linkage for CO_2 reduction and oxygenic environment evolution could be somewhere linked between archea that reduce CO_2 by using inorganic substrates without sunlight but that system could not have been sufficient thus cyanobacteria evolved with advanced mechanism of CO_2 reduction in oxygenic environment using sunlight available.

However, the nitrogenase enzyme is labile (Robson, 1979) for oxygen and cyanobacteria have two compartments to reduce CO_2 that evolves oxygen and N_2 that works in absence of oxygen (Kerfeld *et al.,* 2010). As diazotrophs are those microorganisms that have the ability to reduce molecular (N_2) gas into ammonium ion with high rate of biological nitrogen fixation in terrestrial environment that can be utilized by microorganisms and plants. Several types of diazotrophs are found from endophytic, symbiotic, free living rhizospheric (Naher *et al.,* 2013) and associative(Santoyo *et al.,* 2016) indicating their critical role in plant growth in natural environment. Moreover, electrotrophs like *Geobacter sulfureducens* have the ability to fix atmospheric nitrogen.

All these organisms are facultative anaerobic (Hallberg *et al.,* 2010) indicating they can survive in poor oxygen conditions. Moreover, some have acetate as preferred reduced carbon source (Widdel, 1987) compared to glucose in several microorganism. This indicates that these organisms have CO_2 fixation ability to through reversible Entner-Doudoroff Pathway for making macromolecules like amino and nucleic acids. Thus, this opens an avenue where bacteria should also have evolved diazotrophic autotrophy in fixing both CO_2 and N_2 for their growth. Some diazotrophs that might have evolved chemoautolithotrophy to autotrophy through Calvin cycle and in *Rhodospirillium rubrum* RuBisCo enzyme is found is also diazotrophic (Tabita *et al.,* 2007). So, its autotrophy or photosynthetic mechanism and diazotrophy is only observed during anaerobic growth.

In present day, RuBisCo system must have evolved from anoxygenic environment. The photosynthetic organisms use sunlight and differ in use of light wave length that plant use 680nm and 700nm whereas photosynthetic bacteria have special pair 760 nm, 840 nm and 870 nm and 960nm (Berg *et al.,* 2002) to generate proton and electron but CO_2 fixation occurs in dark reaction center with RuBisCo that is labile to oxygen (Carmo-silva *et al.,* 2010). Thus, there must have been some evolutionary lineage where CO_2 could have been reduced in dark without any forms of light.

2.9 CO_2 Fixation pathways

Reduction of CO_2 also known as fixation and it is the process of conversion of inorganic carbon into organic carbon by living organisms. There are six natural pathways (Gong *et. al*., 2016) of CO_2 reduction taking place both in aerobic and anaerobic conditions.

2.9.1 Aerobic CO_2 reduction pathways

Calvin-Benson-Bassham cycle

It is one of the most important CO_2 fixation pathways in nature. It exists widely in plants, algae, cyanobacteria and other organisms and most of these are associated with the photon driven water hydrolysis (Krapp *et al.,* 1991). In Calvin cycle, three molecules of CO_2 is converted into one molecule of glyceraldehyde 3-phosphate, with the consumption of nine ATP molecules and six nicotinamide adenine dinucleotide phosphate (NADPH) molecules (Gong *et al.,* 2016). It is the highest energy-consuming pathway among all six natural CO_2 fixation pathways. RuBisCo is the rate-limiting enzyme in this cycle with an average activity of 3.5 µmol min^{-1} mg^{-1}(Bar-even *et al.,* 2010).

3-Hydroxypropionate cycle

This cycle exists in photosynthetic green non-sulfur reducing bacteria and is driven by light, containing 16 enzymatic reaction steps that are catalyzed by 13 enzymes. In contrast to the Calvin cycle, which converts CO_2 to glyceraldehyde 3-phosphate, this cycle converts three molecules of HCO_3^- into one molecule of pyruvate, with the consumption of five ATP and NAD(P)H molecules. There are two CO_2 fixing enzymes in this cycle: acetyl- CoA carboxylase and propionyl- CoA carboxylase, catalyze CO_2 fixation (Ishii, 2004).

3-hydroxypropionate/4-hydroxybutyrate cycle

In this cycle, Archaeal aerobic CO_2 fixation pathway discovered in 2007, is the 3-hydroxypropionate-4-hydroxybutyrate cycle, which is driven by sulfur and hydrogen. This cycle synthesizes one molecule of acetyl coenzyme A from two molecules of HCO_3^-, four molecules of ATP, and four equal molecules of NADPH. The two CO_2 fixing enzymes used are the same as those of the 3-hydroxypropionate cycle (Berg *et al.,* 2010).

2.9.2 Anaerobic CO_2 reductive Pathway

Wood-Ljungdahl pathway

The Wood-Ljungdahl pathway, which exists mainly in acetate-producing anaerobes, was identified in the 1970s by Harland G. Wood and Lars G. Ljungdahl (Ragsdale, 2008) and uses hydrogen as its energy source. It is the only non-cycle CO_2 fixation pathway, contains the fewest reaction steps, and consumes the least amount of energy. This pathway converts two molecules of CO_2 (or one molecule of CO_2 and one molecule of carbon monoxide) into one molecule of acetyl coenzyme A, using one ATP and four NADPH molecules. So it is called the anaerobic acetyl coenzyme A pathway.

Reductive TCA cycle

This cycle exists in photosynthetic green sulfur bacteria and anaerobic bacteria. This cycle generates one molecule of acetyl coenzyme A via two molecules of CO_2, with the consumption of two ATP and four NADPH molecules (New *et al.,* 1966; Kim *et al.,* 1992). The two CO_2 fixing enzymes in this cycle are α-keto glutarate synthase and isocitrate dehydrogenase. The enzyme α-ketoglutarate synthase is strictly anaerobic, with unknown activity. Isocitrate dehydrogenase has the highest activity amongst all CO_2 fixing enzyme (Berg *et al.,* 2010).

Dicarboxylate/4-hydroxybutyratecycle

The archaeal anaerobic CO_2 fixation pathway, the dicarboxylate/4-hydroxybutyrate cycle was discovered in 2008. This cycle uses sulfur and hydrogen as energy sources (Huber *et al.,* 2008). One molecule each of CO_2 and HCO_3^- are used to synthesize one molecule of acetyl coenzymeA consuming three ATP and four NADPH molecules. The CO_2 fixing enzymes in this cycle are pyruvate synthase and phosphoenol pyruvate carboxylase. Pyruvate synthase is strictly anaerobic enzyme whereas phosphoenol pyruvate carboxylase to HCO_3^- is the smallest amongst all carboxylases.

2.10 Rubisco gene in *Azospirillum* sps

Diazotrophs of genus *Azospirillum* are one of the strains which are capable for autotrophic growth alpha proteobacteria (Orlova *et. al*., 2016). While species of *Azospirillum amazonense* contain gene cluster implicated in CO_2 fixation by Calvin cycle. The cluster of main gene, cbbL encode as the large subunit of rubisco and other one is cbbS encode as the small subunit of rubisco enzyme. These above genes are responsible for the biosynthetic pathway (Anna *et al.,* 2011). Additionally, the rubisco phylogenetic reconstruction also indicated the close relationship of *Azospirillum amazonense* enzyme with those from the members of family Brady rhizobiaceae and are the photosynthetic nitrogen fixing bacteria (Kwak & Shin, 2015). So it is said that the horizontal gene

transfer may be important force in the evolution and dispersion of rubisco in proteobacteria (William F Martin et. al., 2018).

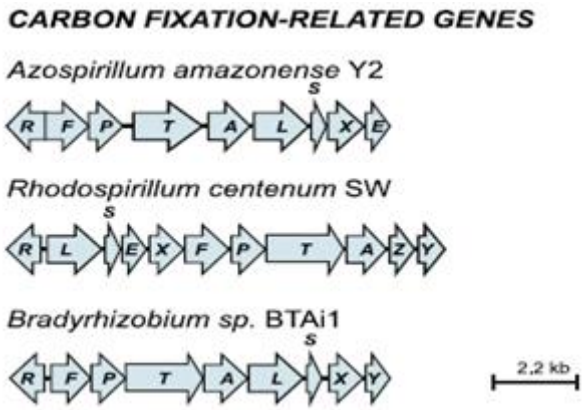

Figure (8): Carbon fixation gene cluster across different species from (Anna *et al.,* 2011)

The operation of the Calvin cycle in *A. thiophilum*, expression of the rbcL gene ended the rubisco large subunit was determined by culturing under auto and heterotrophic condition. The qRT-PCR demonstrated (Kinney *et. al*., 2011) that this gene rbcL-mRNA level under autotrophic condition was approximately eight fold higher than that in heterotrophic condition proved that they can possibly demonstrate autotrophic growth. However, from the *Azospirillum* group, at least *Rhodospirillium centenum* and *Azospirillium lipoferum* are known to be capable of growing autotrophically by means of RuBisCO (Hartmann & Burris, 1987). The genetic organization of the carbon-fixation makes these organisms to be part of the evolutionary process. The diversity between the *Azospirillium* species and RuBisCo gene in them also shows significance of this species in evolution. Among the genus, *A. amazonense* having genes encoding those enzymes for glycolysis likely able to consume carbohydrates via glycolysis but no activity of 6-phosphofructokinase and fructose bisphosphate so most of the gram negative aerobic bacteria glycolysis are inoperative, which follow the Entner-Doudoroff pathway (ED pathway) (Fabiano & Cardona, 1985). But this characteristics gives additional evolutionary prospects that most of the enzymes involved in ED pathway are reversible and if CO_2 is reduced by RuBisCo (Gonçalves *et al.,* 2020) that would ultimately give glyceraldehyde-3-phosphate then this ED pathway can support in taking the sugar molecules to both pathways of TCA and pentose phosphate.

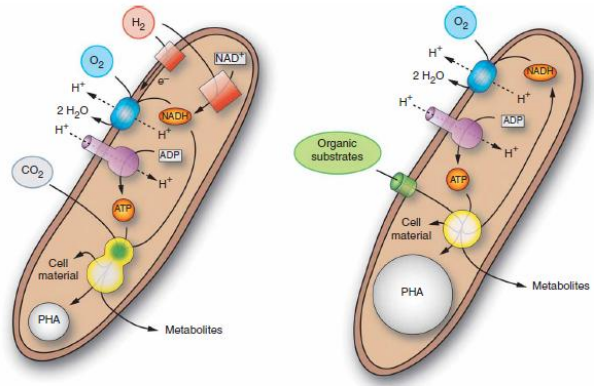

Figure (9): left side; Lithoautotrophic metabolism and right side; heterotrophic metabolism (Pohlmann *et al.,* 2006)

2.11 Water splitting

In the context of chemical reaction, water is broken down into hydrogen and oxygen is named as water splitting (Ni *et al.,* 2007). Thus formed hydrogen is the simplest and most abundant element in the universe (Currao, 2007) whereas the hydrogen is not in the gaseous form but bound by carbon and helps in the reaction of photosynthesis and plants transform water and carbon dioxide in the presence of light into oxygen and carbohydrates (Salas, 2013).

The biological process of photosynthesis could involve the transformation of carbon dioxide into a chemical compound of higher energy content. However, water is photochemically oxidized to dioxygen in photosystem II by the oxygen-evolving complex (OEC), a redox-catalytic center on the lumenal side of PSII and associated with the two electron reductions of two molecules of plastoquinone, which acts as a mobile charge carrier(James Philip Mcevoy *et al.,* 2006). Photoelectrochemical (PEC) water-splitting system was demonstrated in 1972 by Yiyang (Chen *et. al*., 2013). TiO_2-based materials have been widely studied as highly efficient photo catalysts to produce hydrogen from water (Henderson *et al.,* 2008). The generation of H_2 from water requires two catalytic steps: 1) the oxidation of two water molecules into O_2 and protons and 2) the subsequent reduction of protons to molecular H_2. Protons generated through this process could be used by another enzyme found in many green algae and bacteria, hydrogenase, which catalyses the conversion of protons to molecular hydrogen in PSII. Although, the structure of an (FeFe) hydrogenase is also found and the active site of this hydrogenase is a six-iron cluster (Fan *et al.,* 2015) is made up from a classical (4Fe–4S) cubane linked to a di-iron complex that carries uncommon ligands (3CO, $2CN_2$, azadithiolate) that produces hydrogen from excess protons (Rajaambal *et al.,* 2015).

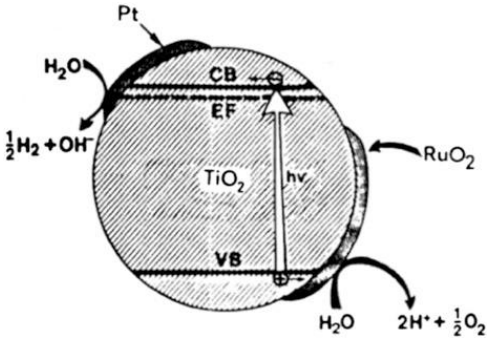

Figure (10): Photoelectrochemical diode (Franks, 2015)

Other types of hydrogenases are also known that harbour a different binuclear metal cluster (NiFe) hydrogenases that converts H_2 into protons and electrons, thereby generating energy for the organisms (Nevin *et al.,* 2010). Nature's water oxidizing catalyst represents a penta- oxygen tetra manganese- calcium cofactor (Mn4O5Ca) where calcium has been correlated with enhanced water splitting activity of manganese oxide water oxidation catalysts (Cox *et al.,* 2015). Nocera's group has reported artificial systems of water splitting requires catalysts that produce oxygen from water without the need for excessive driving potentials (Kanan & Nocera, 2012). Such type of a catalyst that forms upon the oxidative polarization of an inert indium tin oxide electrode in phosphate buffer water containing cobalt (II) ions.

2.12 Microbial fuel cell (MFC)

Microbial fuel cell (MFC) is one of the fascinating bio-electrochemical devices (Khaloufi, 2019) which is used as living bio-catalysts where microorganisms living at the surface of electrodes in the electrolyte and provide electric energy from organic matter naturally present in the environment (Schaetzle, 2008). Water electrolysis could play a key role in sustainable energy conversion and storage infrastructure that releases hydrogen. Hydrogen is an important industrial feedstock for petroleum refining and fertilizer industry (James P Mcevoy *et al.,* 2006) . Electrochemical water splitting is divided into two half-cell redox reactions (Ha *et al.,* 2017). The reduction process at the cathode (hydrogen evolution reaction, HER) proceeds as: $2H^+ + 2e^- \rightarrow H_2$ (Choi & Sang, 2016) while the oxidation process (oxygen evolution reaction, OER) at in the anode (Rosenbaum *et al.,* 2011) of the electrolyzes as: $H_2O \rightarrow 1/2\ O_2 + 2H^+ + 2e^-$ (Franks, 2015). That is:

In oxidative reaction (anode);

$$2H_2O \longrightarrow O_2 + 4H^+ + 4e^-$$

In reductive reaction (cathode); (Zhong & Gamelin, 2010)

$$4H^+ + 4e^- \longrightarrow 2H_2$$

Half reaction of water splitting;

$2H_2O \longrightarrow H_2 + ½\ O_2$

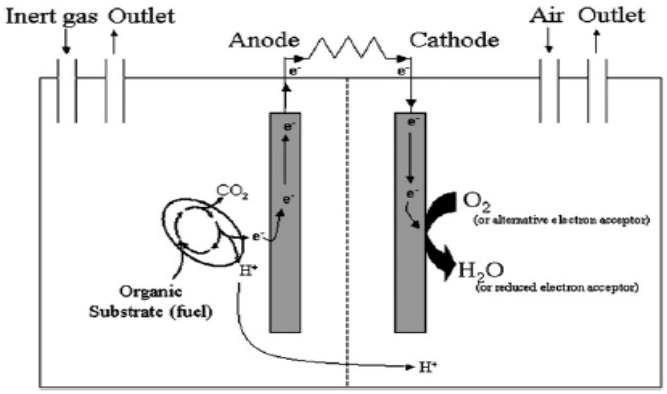

Figure (11): Principle of a MFC (Schaetzle, 2008)

2.12.1 Anodic effect of MFC

Organic substrates serve as electron donors for a complex system of redox reactions that result in the production of an energy carrier molecule (ATP) (Franks, 2015). In here, bacteria are able to substitute an electrode as the terminal electron acceptor in the anodic compartment of MFCs (Choi & Sang, 2016). Among proteo bacteria, some species have the ability to reduce iron or manganese as terminal electron acceptors and thus have the ability to directly transfer their electrons to an electrode and some of them are able to develop thin filaments (pili) involved in extracellular and inter microbial electron transfer, often called nano-bio wires, is one of the best mediator in the process of MFCs (Tremblay & Zhang, 2015). This anodic chamber is filled with substrate, mediator biocatalyst and anode electrode as electron acceptor and conditions are optimized for faster rate of organic matter degradation (Colon *et al.,* 2016). Some modification of anode electrode could be done to improve bacterial adhesion and electron transfer from bacteria to the electrode surface directly in increasing the performance of MFC (Uma Vanitha *et al.,* 2017).

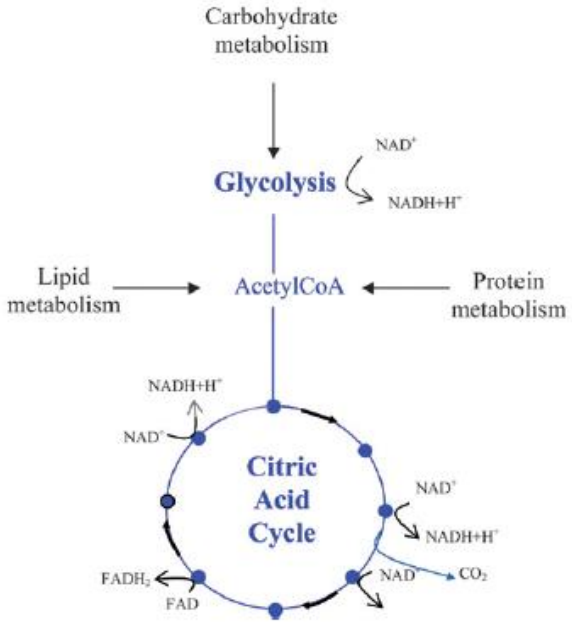

Figure (12): Reduction of NAD and FAD to their electron carrier forms ($NADH_2$ and $FADH_2$) through TCA cycle (Schaetzle, 2008)

2.12.2 Cathodic effect of MFC

MFCs have used oxygen-reducing cathodes and reaction requires expensive catalysts such as platinum. The terminal electron acceptor in the cathode have a great diversity where 50% in the cathode biofilm were beta-proteobacteria with species of the genera *Nitrosomonas* and *Azovibrio restrictus*. In addition, Bacteroidetes was the second most common group of organisms (21.6%). Also, *G. Sulfurreducens* biofilm on stainless steel cathodes was shown to be fully responsible for the reduction of fumarate (Schaetzle, 2008). However, cathodic chamber could be affected by the concentration and species of electron acceptor, proton availability, catalyst performance, electrodes of their catalytic abilities (Oh *et al.,* 2004).

In MFC, the use of proton exchange Nafion membrane which is cation exchange type membrane that can transport the produced proton to cathode and prevent transport of other materials such as substrate or oxygen. This membrane consists of hydrophopic fluoro carbon backbone to which hydrophilic sulphonate group are attached and due to this existence shows high conductivity of different cations (Son & Kasai, 2009). There are other types of membrane found in nature as in the proton exchanger to be used from the sources. They are; natural or synthetic polymer, CMI 7000, Zirfon, Hyflon but high cost, high internal resistance are the greater restriction for MFC performance (Chouler *et al.,* 2017).

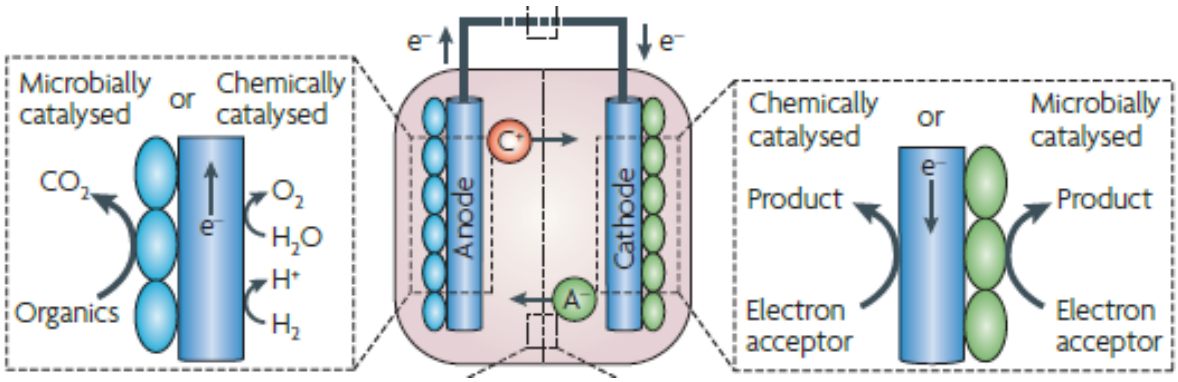

Figure (13): Bioelectrochemical systems both anodic and cathodic chamber (Rabaey & Rozendal, 2010)

2.13 Syntrophic growth

Syntrophy means the obligately mutualistic relationship with co-culture substrate of bacterial metabolism which has a role in the microbial degradation of organic compounds in methanogenic ecosystems (Dolfing, 2013). Reaction occurs in here is to convert it into methane and carbon dioxide. In here hydrogen is the main electron carrier in such syntrophic associations (Kleinsteuber, 2015).

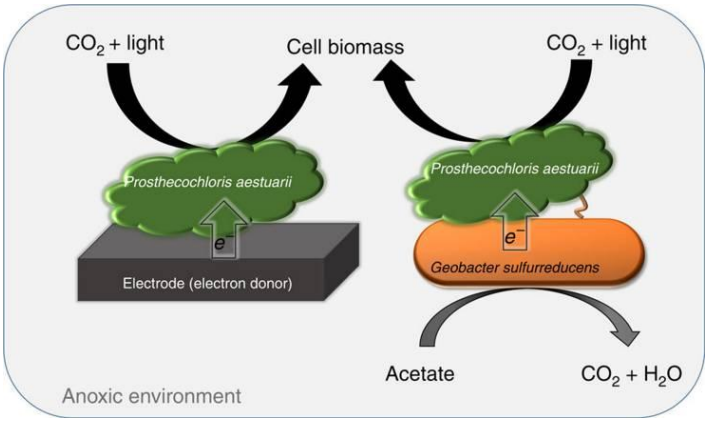

Figure (14): Model of syntrophic anaerobic photosynthesis through direct electron transfer(Ha *et al.,* 2017)

In nature, there all the euphotic and disphotic areas, light are absent but the sediments are rich in reduced carbon and sulfur compounds. There are different types of extracellular electron transfer are possible such as: first one is transfer of electrons by (soluble) chemical compounds from one microbe to another in methanogenic and non-methanogenic environments and another one is transfer of electrons by organic and inorganic mediators to inorganic materials. In addition, electron transfer also occurs by direct cell-cell contact or electro-conductive cellular appendages, the nano wires (Morris *et al.,* 2013).

2.14 Nitrogen fixation

Nitrogen fixation is a process from which nitrogen (N_2) in the atmosphere is converted into ammonia (NH_3). It is essential for agriculture and the manufacture of fertilizer and nitrogen can be fixed by bacteria called diazotrophs (Ho *et al.,* 2014a). Biological nitrogen fixation (BNF) occurs by an enzyme called nitrogenase and this enzymes are used by some organisms to fix atmospheric nitrogen gas. The nitrogenase has 2 components that are Mo-Fe protein (molybdoferredoxin) and Fe-protein (azoferredoxin). Nitrogenases are metallo enzymes, which are proteins that have metalic molecules as subunits. Reaction is: $N_2 + 8\ H^+ + 8\ e^- \rightarrow 2\ NH_3 + H_2$ (Inomura *et al.,* 2018).

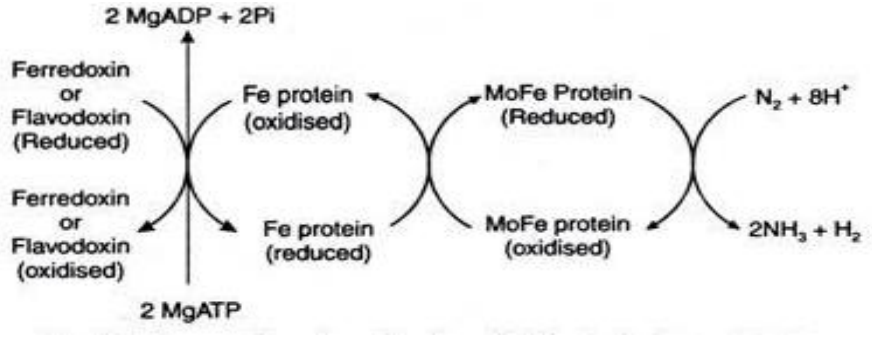

Figure (15): mechanisms of biological nitrogen fixation (Cheng, 2008)

The enzyme nitrogenase can reduce a number of other substrates such as N_2O (nitrous oxide), N_3^- (azide), C_2H_2 (acetylene), protons ($2H^+$) and catalyse hydrolysis of ATP. In some rhizobia, hydrogenase enzyme is found which splits H_2 to electrons and protons (Inomura *et al.,* 2018). The ammonia is the first stable product of nitrogen fixation. Only some prokaryotes like bacteria and cyanobacteria can fix atmosphere nitrogen (Wyss *et. al*., 1941). They fix about 95% of the total global nitrogen fixed annually by natural process.

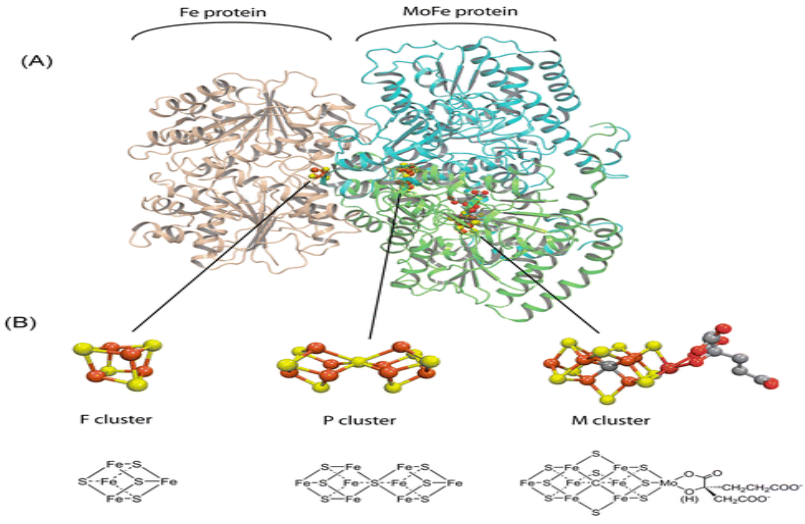

Figure (16): A figure represents as Fe and FeMo proteins and B figure shows the different cluster form of protein structure (Ho *et al.,* 2014b)

The overall biological nitrogen fixation reactions are as follows:

$N_2 + 8H^+ + 8e^- + 16\ ATP \rightarrow 2NH_3 + H_2 + 16\ ADP + 16\ Pi$

2.15 Microbial electrolysis system in MFCs

Microbial electro synthesis is a biotechnology based on microbial energy conversion from electricity to chemical fuels. The utilization of microbial CO_2 fixation activities for the synthesis of chemical fuels has advantages over technologies based on inorganic catalysts because the production of multi-carbon compounds from CO_2 with inorganic catalysts is difficult. The generation of acetate from CO_2 with H_2 as the electron donor, had the ability to convert electrical energy into multi-carbon chemicals under the conditions with poised electrodes as the electron donor. The metabolic engineering of acetogenic bacteria and improvements to cathode materials (Choi & Sang, 2016). Microbes are able to communicate with specific partners for promoting metabolic cooperation. A number of dissimilatory iron-reducing bacteria have to transfer electrons extracellularly and to generate current in microbial fuel cells (Franks, 2015).

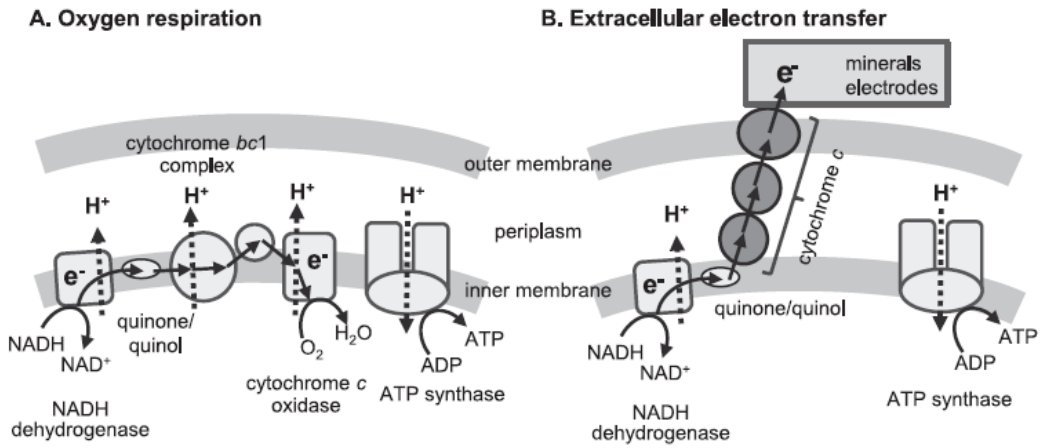

Figure (17): A) shows the oxygen respiration and B) shows the extracellular electron transfer (Kato, 2015)

2.16 Nanoparticle

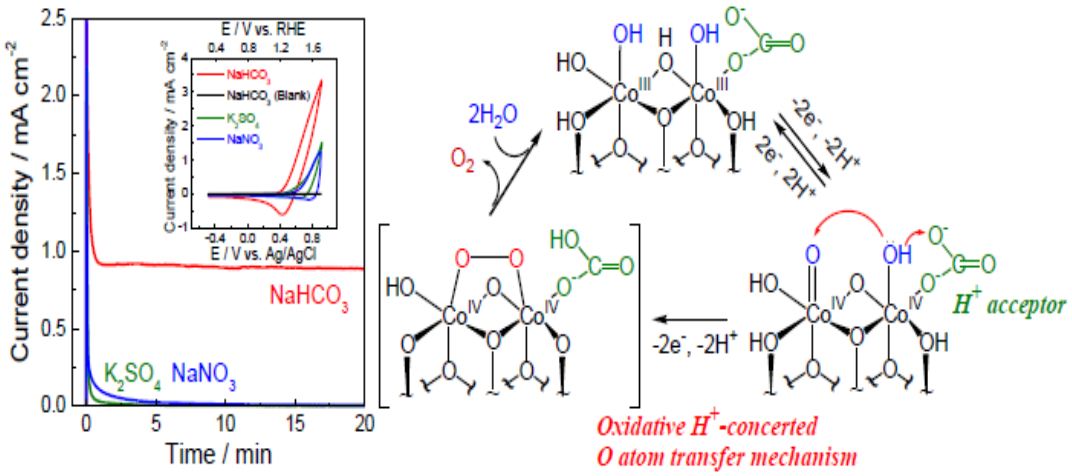

Figure (18): Essential cofactor for carbonate ions for an artificial evolving complex (OEC) model (Aiso *et al.,* 2017)

From the above picture, when water and carbonate combine with cobalt oxy hydroxide then get revesible reaction of oxidized form that is removal of 2 electron and 2 proton and final structure of cobalt IV obtained. Simultaneously, there is the formation of intermediate form and again reduction form occurs and gets back again into that original form cobalt III structure. Cobalt has its catalytic power towards water splitting (Aiso *et al.,* 2017).

Electrochemical water splitting is composed of two half reactions: hydrogen evolution reaction (HER) on the cathode, and oxygen evolution reaction (OER) on the anode (Wang *et al.,* 2016). The oxides of cobalt can acts as catalysts than adsorbents and composite materials and has more oxidation state (Co^{3+}) (Yang *et al.,* 2010). Among these metal oxides and hydroxides, the cobalt oxyhydroxide is a promising electrode material due to its layered structure with large interlayer spacing with defined electrochemical redox activity. Furthermore, the cobalt oxyhydroxide is a better charge storage material due to its innovative properties of high conductivity, morphology control nature of micrometer/nano meter scale (Jagadale *et al.,* 2012). The formation of Co^{IV}=O is a necessary step for cobalt-based molecular complexes to function as a water oxidation catalyst and cobalt centre of the intermediate Co^{III} =OH can go to its higher oxidation state under the application of positive potential and cobalt(II) hexahydrate complex might prove to be electrochemically active towards water oxidation. So electrochemical water oxidation catalysed by these cobalt based materials is one of the technique (Basu *et al.,* 2018). On the other hand chemical oxidants have been employed in combination with dissolved aqua cobalt ions to achieve water oxidation, giving hydrogen peroxide as the initial product. In the presence of Co^{III}, hydrogen peroxide undergoes disproportionate to O_2 and water. However, the kinetics and electrochemical

potential for this process differ substantially from oxygen evolution electrochemical water oxidation mediated by Co catalysts across a broad pH range 0-14 (Gerken *et al.,* 2011).

2.17 Cellulose

Cellulose is a linear-chain homo polymer composed of repeating anhydro-D-glucose monomers (Nevell *et. al*., 1985) with the general formula of $(C_6H_{10}O_5)_n$ linking through a β-(1,4)- glyosidic bond. It's the key component of plant cell walls and the most abundant biopolymer (Nishino *et. al*., 2014). The cellulose molecules organized in the cell walls in the form of micro fibrils have characteristic orientations, which differ as a function of the cell wall layer of plant (Brett, 2000). However, it is a major component of the global carbon cycle and also a representative of microbial extracellular polymers. Cellulose is synthesized by bacteria, where bacterial cellulose belongs to specific products of primary metabolism and is mainly a protective coating. Bacterial synthesis of cellulose occurs at the cytoplasmic side of the (inner) membrane, and elongation of the nascent molecule must be tightly (Ross*et. al*., 1991) linked to its secretion.

Bacterial cellulose is found as in different applications like as: paper, textile, and food industries, and as a biomaterial in cosmetics and medicine (Esa *et. al*., 2014). Thus, it has certain advantages over plant cellulose, including its high purity, high capacity for water retention, and the nano-scale arrangement of the cellulose fibrils. These features make bacterial cellulose an attractive biocompatible material, which is already commercially available as a wound dressing material for complicated wounds such as skin ulcers and use as bone tissue engineering (Pang *et. al*., 2020). Potential applications of bacterial cellulose and its derivatives also include their use as scaffolds for the replacement of small-diameter blood vessels and as drug-delivery systems, as well as membranes and filters (Römling & Galperin, 2015).

2.18 *Azospirillum* species

Azospirillum species is an important procedure when studying their inherent capacity to benefit crops. *Azospirillum* species are commonly found in soils and in association with roots of plants namely rice, maize, wheat and vegetables. Rhizosphere colonization by *Azospirillum* species has been shown to stimulate the growth of a variety of plant species. The success of the *Azospirillum* plant interaction depends on the survival and persistence of these bacteria in soil and the effective colonization of the rhizosphere. Microbial diversity in agricultural is an indicators of soil quality and plant productivity (Senthil K R *et al.,* 2013).

CHAPTER 3

METHOD AND METHODOLOGY

3.1 Isolation of bacteria from soil sample

Soil samples were collected from the Panchase region of the Pokhara valley and stored at Central Department of Biotechnology, Tribhuvan University, Kirtipur. One gram of soil sample was inoculated into the 10 ml water and serially diluted. 100 µl of the soil suspension was taken and poured into the semisolid agar (top agar). Top agar was poured immediately into the plate with basal Nfb(Nitrogen free basal) agar plate (bottom agar). These plates were incubated at 28°C for 24 hours. Then isolated colonies were subculture into specific media of NCF (Nitrogen Carbon free).

3.2 Biochemical identification of bacteria

3.2.1 Gram's staining

A thin layer of bacterial sample was prepared into slide and dried. The material on the slide was heat fixed and allowed to cool before staining. The slide was flooded with crystal violet stain and allowed to remain without drying for 10-30 seconds. The slide was rinsed with tap water, shaking off excess. The slide was flooded with iodine solution and allowed to remain on the surface without drying for twice as long as crystal violet was in contact with the slide surface. The slide was rinsed with tap water, shaking off excess. The slide was flooded with decolorizer for 10 seconds and rinsed immediately with tap water until no further color flowed from the slide with the decolorizer. The slide was flooded with counter stain (safranin) for 30 seconds and washed off with tap water. The slide was dried and examined microscopically under oil immersion at 100 X.

3.2.2 Biochemicals test

3.2.2.1 MR-VP test

The microorganisms were aseptically inoculated into the 2 test tubes labeled as the MR and VP medium. The tubes were incubated at 28°C for 48 hrs. After that, 5-6 drops of MR reagent were added to the test tube labeled as MR and color change of the media was observed. Similarly, for VP, Barrett's reagent A and B in the ratio of 3:1 (α-Naphthol: KOH) were added in the tubes and shaken to provide the oxygen. The changes in color were noticed after 20-30 mins of incubation.

3.2.2.2 Urea broth Base (Urease Test)

For this test the media used was urea broth media. The broth media was inoculated with a loopful of test organisms in the test tubes. The tubes were incubated at 28°C for 24 hrs. A positive urease test was indicated by the change in media color from yellow to pink.

3.2.2.3 Sulphide Indole Motility (SIM) medium

For this test the SIM media was prepared in the test tube and isolated colonies were inoculated with the help of sterile inoculating loop. Inoculation was done by stabbing the colonies at the center of the media at the depth of 1-2 inches. After the inoculation of the organisms the tube was incubated at 28°C for 24 hrs. After incubation the tubes were observed for the production of hydrogen sulfide (H_2S) gas, formation of indole and the motility. After the observation of H_2S production and motility; formation of indole was tested by adding the Kovacs regent (3 drops) at the surface of the media and development of pink to red color was interpreted as positive indole test.

- **Interpretation of the results**
  - A positiveH_2S test was denoted by a blackening of the media along the line of inoculation and a negative H_2S test was denoted by the absence of blackening.
  - A positive motility test was indicated by a diffuse zone of growth flaring from the line of inoculation.
  - A negative motility test was indicated by growth confined to the stab line.
  - A positive test for indole was denoted when a pink to red color band was formed at the top of the media after addition of Kovacs reagent.
  - A negative test for indole was denoted by the yellow color after the addition of the Kovacs reagent.

3.2.2.4 Simmon's Citrate Agar

The media was autoclaved in tubes and the tubes were tilted to form slant. Inoculum was added and incubated for 24 hrs and observed color change in media as slant part.

3.2.2.5 Triple Sugar Iron (TSI) Agar

The autoclaved TSI medium was allowed to set in slope form with a butt about 1 inch of thickness. Inoculum added as in the both part stabbed and stricked, Incubated for 24 hrs and next day observed color changed of that slant and butt region of medium.

3.2.2.6 Oxidation Fermentation Test

For this test the media was hugh-leifson media. The media was prepared in separated in different test tubes and labelled as “O” for oxidative and “F” for fermentative. Microorganisms were inoculated using sterile wire by stabbing straight. In order to maintain the anaerobic condition in the tube labeled as “F” small drop of heavy paraffin oil was added after the inoculation of microorganisms. Tubes were incubated at 28°C and change in media color from green to yellow was interpreted as positive test

3.2.2.7 Nitrate reduction Test

Nitrate broth was prepared and the microorganisms were inoculated into the respective labeled tubes. The tubes were incubated at 28°C for 48 hrs. After incubation, reagent A i.e. Sulfanilic acid and reagent B i.e. Naphthylamine; 5 drops each were added. Color changed were observed which indicated that the nitrate was reduced resulting in the pink-red color. To the tubes which were colorless even after the addition of the reagents, a small amount of Zinc powder was added and shaken vigorously and allowed to stand at room temperature for 10-15 mins. And for the medium which remained colorless even after the addition of Zinc powder the result was positive and the media which turned pink after the addition of the Zinc powder, the result was negative.

3.3 Molecular characterization of the Bacteria

The screened and the identified bacteria based on their morphology and the biochemical characterization were further subjected to the molecular characterization to confirm the specific isolates. So, the genomic DNA extraction and PCR amplification were performed to confirm the specific bacteria.

3.3.1 Genomic DNA (gDNA) extraction

The DNA of the useful bacterial colonies was extracted using various chemicals and enzymes. Cells were streaked on the LB agar plate and incubated overnight at 37°C.The single colony was isolated and inoculated in 2 ml of LB medium for 12 hours. From the overnight culture (1.5 ml) was transferred into the sterile eppendorf (EP) tube. Tube was centrifuged at 5000 rpm for 5 minutes at 4°C. Immediately, the supernatant was discarded by aspiration and remaining overnight culture (0.5 ml) was also added to the same tube containing the cell pellet and centrifuged again at 5,000 rpm for 5 minutes 4°C. Then supernatant was removed as much as possible without disturbing the pellet. Cell pellet was re-suspended in 450 µl of TE1 buffer (pH 7.5) by gentle pipetting. The solution was spitted into 2 fresh sterilized E.P tubes by transferring 225 µl of the above suspension to each tube. To each tube 180 µl of lysozyme (1mg/ml) was added. Both the tubes were incubated at 37°C for 30 minutes gently mixing the solution by inverting the tube every 5 minutes for proper cell lysis. Then, 45 µl of STEP solution was added in both tubes. Tubes were incubated for 45 minutes or until the solution became clean due to the cell lysis with gentle inversion in between the ice incubation period. Equal volume of chilled phenol (450 µl) was added and mixed by votexing. The mixture was centrifuged at 13,000 rpm for 10 minutes. The upper aqueous layer containing DNA was transferred to the fresh sterilized E.P tubes without carrying of lower organic phase. Again, equal volume of chilled phenol: chloroform: Isoamyl alcohol (25:24:1) was added to the above aqueous solution mixed by vortexing. The tubes were centrifuged at 13,000 rpm for 10 minutes at 4°C. After collection of aqueous layers in a fresh tube, equal volume of

chloroform was added and vortexed. The mixture was then centrifuged at 13,000 rpm for 2 minutes and aqueous phase was collected in a fresh E.P tube. To the aqueous solution (450 µl) containing genomic DNA, 100 µl of 3 M chilled sodium acetate (pH 5.2) and double volume of 95% ethanol (i.e. 1,100 µl) was added. Tubes were incubated at -20°C for 30 minutes. The mixture was centrifuged at 13,000 rpm for 20 minutes at 4°C. The supernatant was poured off and pellet was washed with 250 µl of 70% ethanol without disturbing the pellet. The tubes were centrifuged at 13,000 rpm for 10 minutes at 4°C. After draining the supernatant, remaining ethanol was removed by keeping the tubes open in room temperature for 5-10 minutes. Care was taken so as not to over-dry the DNA pellet. The genomic DNA was re-suspended in 100 µl of autoclaved MilliQ water or TE buffer (pH 8.0) and stored at -20°C until use or gel run.

3.3.2 Polymerase Chain Reaction (PCR)

Polymerase Chain Reaction (PCR) is a method of exponential amplification of single copy of specific segment of DNA to generate thousands to millions of more copies of that particular DNA segment. In PCR, the reaction is repeatedly cycled through a series of temperature changes, which allow many copies of target region to be produced. The thermal cycling exposes reactants to repeated cycles of heating and cooling to permit different temperature-dependent reactions- specifically DNA melting and enzyme-driven DNA replication. PCR relies on a thermostable DNA polymerase, and requires DNA primers which serve as the starting point for DNA synthesis.

The first step is the DNA denaturation. During this step the hydrogen bond holding the two stands of DNA is denatured. This provides single-stranded template for the next step i.e. annealing. In the second step (annealing) the reaction temperature is lowered and the primers bind to the complementary sequences on the single-stranded DNA template for thermo-stable DNA polymerase to amplify from the 3'-end of the primer. Since two primers are used; one is forward and another is the reverse primer which binds the sense strand and antisense strand respectively. The two strands of DNA become template for DNA polymerase to enzymatically assemble a new DNA strand. The final step is the extension where the temperature is raised to optimize extension by the polymerase. And the continuous cycle of heating and cooling take place until sufficient amount of DNA is synthesized.

3.4 Cobalt oxy hydroxide (CoOOH) nanoparticle synthesis

Cobalt nanoparticle was synthesized by chemical method. For this; 100 ml of 0.05 mol/L $Co(NO_3)2.6H_2O$ (cobalt nitrate hexahydrate) was made and warmed at 45^oC. NaOH solution (50 ml) of 0.1 mol/L prepared and warmed at 45^oC .Then 80 ml of above cobalt solution was added dropwise into NaOH solution. It was allowed to react and see pink precipitate being formed by stirring with magnetic stirrer. After that the solution was

filtered without disturbing the pellet and filtrate residue was taken for further work. Then this residue was washed several times with deionized water and checked the pH of the solution. The volume of the solution was made to 20 ml by adding deionized water and warmed at 45^{o}c. Then 5 ml of 8 mol/L NaOH along with 2ml of 30% H_2O_2 was added dropwise while the pink precipitate was stirred with magnetic stirrer for 18 hours. And then it was dried at 65^{o}c in oven for two days. Finally the quantity of dried cobalt nanoparticles formed was obtained by measuring in the weighing machine. Then all the dried CoO(OH) was stored in the eppendroff tube and characterized by FTIR and XRD (Yang *et al.,* 2010).

3.5 Revive of bacteria

All the bacterial samples *Azospirillum* sps*, Pseudomonas* sps, *Azotobacter* sps and *Geobacter* sps were cultured in LB broth, which was isolated and screened by my seniors and incubated it in 28°C for 2 days. Later on, these were confirmed from streaked into different specific media with specific bacteria.

3.6 Preparation of specific media

Firstly NCF media was prepared added NCF media and agar and made plates and then this inoculated culture was streaked into NCF plates and again incubated at 28°C for 3 days. Then seen small creamy colonies with isolates and then it can be further streaked in NCF plates for pure colonies.

3.7 Water splitting concept and mechanism developed

Firstly modified Nfb media with added cobalt nano-particle was autoclaved and then this media divided into 10 different culture tubes. Then overnight culture in all 4 bacterial suspensions, each bacterial combination was mixed. Then this was incubated at 28°C for 1 days and next day, measured absorbance at 600 nm. A result of cell density was observed from that absorbance. Similarly, nitrogen reduction test also done of that each sample and their absorbance also interpreted. Different types of bacterial growth with added cobalt nano particle with Nfb media and potassium carbonate as carbon source was done. The growth of bacterial cell density was measured from there and also measured the carbon and nitrogen reduction test. In here we removed bromothymol and added only KOH.

3.8 Glucose and ammonia standard curve

Standard curve of glucose and ammonia were obtained by dissolving various concentrations of glucose and ammonium hydroxide respectively in water. From this

standard curve; the amount of carbon and nitrogen reduced of that syntrophic growth was noticed.

3.9 Precipitate treated procedure

Pellet was separated from Nfb media with carbon source sodium carbonate; it was centrifugation at 3000 rpm for 10 min. Then this was washed several times by deionized distilled water. Then pellet was treated with 3 ml of 1 N NaOH and was heat shocked in waterbath at 100°C for 1 hour. NaOH insoluble fraction was separated and further treated with 2ml of 0.66N HCl, waterbath at 100°C for 2 hours. From this treatment, insoluble crystal like component was completely hydrolysis by 6N HCl treatment. Finally, treated this pellet was ready to use further confirm that whether this pellet produce any glucose or not. Here were some lists of test for preliminary test. They were as follows:

3.9.1 Microscopic examination test

Firstly grease free slide was taken and already treated precipited sample was placed, covered with cover slip and examined under the 40X microscope. This is very important for our research and observed.

3.9.2 Preliminary test for cellulose

3.9.2.1 Molisch's test

Firstly two test tubes were cleaned and labelled them as one as positive control and another for sample test. Then 2ml of sample was taken in dry test tube as labelled as sample test and 2ml mixture of glucose with distilled water was added in another tube labelled as positive control. And then 2 drops of Molish's reagent was added into the solution and 1ml of conc. H_2SO_4 was also pipette into it. Finally the junction of two layers with color changes was observed in both test tubes.

3.9.2.2 Benedict's test

In this test, first of all two test tubes were cleaned and dried .Then 1ml of sample was taken in the test tube labelled as sample. For the test tube labelled as positive control; 1 ml of glucose solution was taken. Then 2ml of Benedict's reagent was added into that both of tubes and was kept it in waterbath for 5 minutes. Then finally change in color was observed.

3.9.2.3 Iodine test

In this test; two test tubes were cleaned and dried. Then 2ml of sample was taken and poured into the test tube labelled as sample. While 2 ml of starch solution was kept in the test tube labelled as positive control. Iodine solution (4 drops) was added into that both tubes and observed for color change.

3.10 Single vessel syntrophic growth

First step: Nfb media composition containing Calcium Carbonate as sole carbon source.

All 4 bacterial culture putative (*Azospirillum*, *Azotobacter*, *Geobacter* and *Pseudomonas*) to each 625 µl of was used in Nfb media. Then 24 hours inoculated culture was prepared as in the LB broth and then after next day total 2.5 ml of bacterial culture were used as in the syntrophic growth of respective media and were incubated at 28°C for some days.

Second step: Nfb media composition containing Sodium carbonate as sole carbon source. Nfb media was prepared that contained sodium carbonate as a carbon source and this was autoclaved. Culture were prepared in LB and incubated for 24 hours. Then overnight culture 625 µl of each bacterial culture was added into that media to make it 2.5 ml total bacterial load in media. Then incubated at 28°C for 7 days and ammonium and carbon fixation test was performed using Nessler's test and Anthrone test respectively. Bacterial cell density was also measured from Spectrophometer and all of the data were noted.

Third step: Nfb media composition containing Sodium carbonate as sole carbon source along with KOH (BTB replaced by KOH). 24 hours inoculated innoculum was prepared as in the LB broth and then after next day total 2.5 ml of bacterial culture were used as in the syntrophic growth of respective media. Here, carbon source used in the media was sodium carbonate, BTB was removed which was replaced by the KOH. This media was called the modified media. All the four organisms were incubated at 28°C for 1 week and Spectrophotometric data were collected for the growth, carbon and nitrogen.

Fourth step: Nfb media composition containing potassium carbonate as sole carbon source along with KOH (BTB replaced by KOH) 24 hours inoculated innoculum was prepared as in the LB broth and then after next day total 2.5 ml of bacterial culture were used as in the syntrophic growth of respective media. All the four organisms were incubated at 28°C for some weeks. Spectrophotometric readings were noted for the growth, carbon and nitrogen test.

3.11 Qualitative test for presence of carbohydrate in bacterial culture media

3.11.1 Carbon reduction test

The detection of capability of CO_2 reduction by syntrophic growth was also done by culturing bacteria in modified Nfb broth media. For this, single vessel co-culture method was applied; 2.5 ml of bacterial culture were transferred into the 250 ml of the modified broth and incubated at 28°C for 10 days. After next days, growth rate was observed from spectrophotometer at 600nm. Then cell from broth media was separated by

centrifugation at 5000 rpm and supernatant was used to detect carbohydrate in the modified media following different two tests methods.

3.11.2 Molisch's test

This test is a general test for all carbohydrates, in this test, carbohydrates when react with conc. H_2SO_4 get to from furfural and its derivatives. These products react with sulphonated α-naphthol to give a purple complex. For this test, 1ml of supernatant sample was taken in test tube and one drop of 5% α-naphthol was added then, about 1 ml of conc. H_2SO_4 was added from the wall of the test tube, then purple color development was observed.

3.11.3 Anthrone test

It was also another general test for all carbohydrates. In this test, carbohydrate gets dehydrated when react with conc. H_2SO_4 to form furfural. This furfural reacts with anthrone to give bluish green colored complex. For this, 1ml of sample was taken and 2ml of anthrone reagent was added. Then it was mixed well and observed color development.

3.12 Microbial Electrochemical synthesis by MFCs

Though, the syntrophic culture helps each other for the growth and other metabolic activities. However, providing external electron and proton in the media aid for the better growth, carbon and nitrogen fixation. Which was done via Microbial Fuel cell (MFC) but before MFC set up, membrane and some graphite electrodes were pre-treated to clean following given protocol:

3.12.1 Nafian membrane cleaning protocol

Correctly, 200ml of 3% H_2O_2 was added and boiled that membrane for 2 hours at 100°C and then it was further boiled with distilled water for 2 hours at 100°C. Again it was boiled for 2 hours at 100°C through 0.5M H_2SO_4 then finally it was again boiled with distilled water for 2 hours at 100°C.

3.12.2 Graphite electrodes cleaning protocol

Graphite was dipped into 70% methanol for 15 min inside the ultra sonication machine and then it was kept in 70% acetone for 15 min then after in distilled water it was sonicated for 15 min and finally exposed in UV for 15 min.

All the MFC apparatus were sterilized using 70% ethanol. Then MFC was set up by joining two MFC apparatus and keeping the proton exchange membrane between them. 200 ml of phosphate buffer (pH7) was prepared and poured in anodic chamber of MFC, along with 250 ml of NCF media was also prepared and poured in cathodic chamber of MFC. Similarly, 250 ml of NCF media was prepared in the conical flask for normal culture

of bacterial mixture. These were subjected to autoclave for the sterilization. After sterilization, overnight culture of four bacteria were inoculated aseptically (inoculums diluted 100 times in media) in cathodic chamber MFC and conical flask containing NCF media. The graphite electrodes were used in anodic chamber and steel in cathodic chamber and electricity was supplied for the dissociation phosphate buffer. And another technique was applied without give any electricity that is measure the electricity produced by microorganism in that mfc media in both cathodic and anodic chamber. This setup was incubated at room temperature for 5 days and daily growth rate and electricity was observed by reading spectrophotometer respectively.

3.13 Extracellular electrochemical method through MFC

The MFC was set up by joining the two sterile glass MFC each having capacity of 250ml via a glass tube with help of sterilized by autoclave. Nafion117 was used as a permeable membrane. The graphite felt was used as anode at anodic chamber where culture of one of the putative *Geobacter* was kept. At the cathodic chamber, 250 ml of 0.1 M pH 7.6 phosphate buffers was kept where steel wire was inserted as an electron acceptor, the wires arising from the anode and cathode compartment were connected to the multimeter and open circuit voltage was observed. Voltage production was observed for 7 days at the interval of each day at same time.

In this experiment, we have developed water splitting mechanism for the proton and electron generation under ambient condition and without need of excessive energy source. For this, phosphate buffer (pH 7) was prepared with 0.5mM cobalt nitrate and poured into anodic chamber of MFC. Steel electrode was used in place of graphite electrode to avoid carbon contamination in NCF media in cathodic culture. Remaining MFC setting procedure and culturing condition was same as already done. While doing the MFC; different concentration of nitrogen and carbon produced from media containing chamber, cells growth and electricity produce by bacterial combination were measured through spectrophotometer. There were different steps changed at that NCF media as in modified with added different carbon sources and protocol was changed while doing this research. They were as follows:

First experiment: Nitrogen and Carbon free media with KPi buffer and mix of two bacteria that is *Geobacter* and *Azospirillum* (1250 µl each) were used in anodic chamber. While in cathodic chamber there were only added each of 625 µl among 4 bacterial growths in that of 200 ml media. Then this was incubated at dark room temperature for overnight and after that day electricity growth cells, nesseler's and anthrone test was measured and plotted the graph. This was done for some weeks, each day same work was repeated and noted down all above test.

Second experiment: Modified GS media, KPi buffer along with cobalt nano particle in anodic chamber while Cathodic chamber only contained media. Both chambers had sytrophic growth and measure electricity. Growth was observed in both of the chambers .Comparatively growth was seen higher in cathodic chamber. **Composition of KPi buffer**: K_2HPO_4 and K_2HPO_4 were measured in appropriate amount and make it as its final pH at 7 and was used for as KPi buffer in MFCs chamber.

Third experiment: NCF media with syntrophic culture in cathodic chamber and syntrophic anodic chambers only contained KPi buffer with pH 7. Externally 3V voltage was supplied to that MFC setting. Spectrophotometric reading of growth, carbon and nitrogen fixed by culture was taken on regular basis.

Fourth experiment: Syntrophic culture was placed in cathodic chamber, 1.3V voltage was supplied externally. While anodic chamber contained Nocera's cobalt with KPi buffer. Preparation of **Nocera's cobalt buffer** was as follows: first of all 0.5mM solution of $CoNO_3$ added into that KPi buffer and made its 7 pH through pH meter and was used as in this buffer for MFCs special purpose.

Fifth experiment: Both of the chamber contained syntrophic culture while NCF media was there in the cathodic chamber. And anodic chamber containing Nocera's buffer and modified GS media buffer. Electricity generated by the syntrophic culture, the growth of the culture, carbon and nitrogen fixed were measured spectrophotometrically.

Sixth experiment: NCF media containing syntrophic culture in cathodic chamber and anodic chamber containing **Yagi's buffer**. Finally the electricity generated was noted and growth of cathodic chambers was measured. **Yagi's buffer composition**: 0.1M of $NaHCO_3$ with pH 10, 30mM of K_2SO_4 and 1/1 ml of vitamin and minerals were mixed.

3.14 Bacterial cellulose production by genetic engineering

Chemicals and Restriction Enzymes: Restriction enzymes used were *Nde*I, *EcoR*I, *BamH*I of NEB Company. Master mix used was PCR Master Mix (2X) of Zymogen company whereas, T4 -DNA ligase and *Spe*I were obtained from TakaRa CloneTech, China. The primers amplifying the DNA were purchased from Macrogen, Korea. All the chemicals and reagents were obtained from Hi-media and Thermo-fischer Company.

Bacterial strain and plasmid: *Escherichia coli* DH5α were used as host for transformation and genomic DNA extraction for the preparation of genes of interest. Plasmid pET28a+ was used as expression vector, the expression region of the coding strand transcribed by T7 RNA polymerase under this vector.

3.14.1 Genomic DNA extraction

All the genes of interest are present in the DH5α *E.coli;* therefore, genomic DNA was extracted from this bacteria. And TIANGEN Kit was used for the extraction of genomic DNA. The materials used were GD buffer, PW buffer, GA buffer, GB buffer, absolute ethanol, RNase A, Proteinase k.

3.14.1.1 Cell preparation

E. coli DH5α strain streaked on LB agar plate was taken and single isolated colony was inoculated in 50 ml of LB broth and incubated overnight at 37°C. Then, 1.5 ml of the overnight culture was transferred to sterilize Eppendorf tube and cell was harvested by centrifuging at 13,000 rpm for 3 minutes. Then supernatant was poured off and again 1.5 ml culture was added to same tube with cell pellet and centrifuged again at 13,000 rpm for 3 minutes to collect more cells. This process was repeated at for two times then supernatant was removed as much as possible without disturbing cell pellet.

3.14.1.2 Cell lysis: TIANGEN kit protocol

Bacterial DNA was extracted from the TIANGEN DNA secure kit protocol but slight modification was done. 200 µl GA buffer was added to the cell pellet and mix by vortexing for 5 seconds. After that 6 µl of RNase A was added to it followed by vortexing for 15 seconds and incubated for 5 minutes at RT (room temperature). To it 2 µl proteinase K was added and mixed thoroughly by vortexing. Then, it was again incubated at 37°C in incubator for 20 minutes. After 220µl GB buffer was added followed by vortexing for 15 seconds. White precipitation was seen after addition of GB buffer and then, it was incubated at 70°C in water bath. To it 200 µl of absolute ethanol was added resulting in formation of white precipitate, followed by vortexing for 15 seconds. Then, it was processed to recovery and purification.

3.14.1.3 DNA recovery and purification

The solution was transferred to spin column, allowed to hold it for some 2-3 minutes and centrifuged 13,000 rpm for 30 seconds. To it 500µl GD buffer was added, hold for 2 minutes and centrifuged it at 13,000rpm for 30 seconds, then, flow through was discarded and the spin column was placed into the collection tube. 600 µl PW buffer was added to spin column and centrifuged at 12,000 rpm for 30 seconds, flow through was discarded and the spin column was placed into the collection tube. This step was repeated again. It was then centrifuged at 12,000 rpm for 2 minutes to dry the membrane completely. Supernatant was discarded and spin column was placed in new eppendorf tubes. 50 µl NFW was then added to the centre of membrane. Then, it was centrifuged at 12,000 rpm for 3 minutes to get the DNA in eppendorf tube. Finally, gel electrophoresis was done to visualize DNA.

3.14.1.4 Gel electrophoresis

The 1% agarose gel was prepared with 2 µl EtBr was added in gel. The gel was casted in casting tray and allowed to solidify. Then, it was placed in gel tank containing 1X TAE buffer. Genomic DNA sample and loading dye was loaded into the well, 1.5 µl and 3µl respectively. Gel was initially run for 60 minutes at 60 Volt to collect all the disperse DNA sample in the well. After completion of gel electrophoresis band was visualized in UV transilluminator and then for clear picture used gel documentation.

3.14.2 Isolation of pET28a+ plasmid

The pET28a+ expression vector was extracted from transformed DH5α *E. coli* which is provided from NAST. It was done by alkaline lysis method using the solution prepared in lab manually. The solutions used in plasmid extraction were STE, solution I, solution II, solution III, RNase, ice cold isopropanol, 70% ethanol and finally NFW.

3.14.2.1 Bacterial culture and cell harvest

Transformed E. coli DH5α strain streaked on LB/kanamycin agar plate was taken and single isolated colony was inoculated in 50ml of LB broth with 100 µg/ml kanamycin concentration medium and incubated 2 days at 37°C. Then, 1.5ml of the overnight culture was transferred into the sterilized eppendorf tube and centrifuged at 13,000 rpm for 4 minutes. The supernatant was poured off, this process was repeated for two times to harvest required cell. At final supernatant was removed and the cell was resuspended into 500 µl of ice cold STE solution to remove excess salt present in the cell pallet. After adding 500 µl ice cold STE solution it was immediately processed for pipetting followed by vortexing for 15 seconds and then centrifuged at 13,000 rpm for 1 minute. Supernatant was discarded.

3.14.2.2 Cell lysis: Alkaline lysis method

Obtain pellet was resuspended in 200 µl of alkaline lysis solution I, and mixed well by pipetting and vortexing. To this 200 µl of freshly prepared alkaline lysis solution II was added and mixed by gentle inversion of tubes for five times. And then immediately, 200µl of ice cold alkaline solution III was added to this mixture and mixed by inverting the tubes gently for several times. The mixture was then centrifuged at 13,000 rpm for 8 minutes. The supernatant solution consisting plasmid DNA was transferred to new Eppendorf tube and centrifuged at 13,000 rpm for 5 minutes to be sure about any contamination. Then it was separated in new tube followed by the addition of 3 µl RNase A (20 mg/ml) and incubated at 37°C in incubator for an hour.

3.14.2.3 Plasmid DNA Recovery

After an hour of incubation 500µl of ice cold isopropanol was added and again incubated in ice for half an hour. Then, it was centrifuged at 13,000 rpm for 20 minutes and

supernatant was discarded. Then, 70% of ethanol was added to eppendorf tube where pellet was emerged and it was processed for centrifugation at 13,000rpm for 5 minutes. Supernatant was poured off and eppendorf tube was left for 40 minutes for air drying. After completion of air drying pellet was dissolved in 25 µl of NFW. Then it was subjected to gel electrophoresis for visualization in gel documentation system.

3.14.3 Inserts Preparation

3.14.3.1 PCR amplification of *bcsA* gene and *adrA* gene

The chromosomal DNA isolated from *E. coli* DH5α was used as template DNA for amplification of *bcs*A and *adr*A using specially designed primer under following condition and mixture. Then this PCR product was subjected to gel electrophoresis with comparision with 1kb ladder.

Table (1): PCR mixture for *bcsA* and *adrA*

Component	Volume
Master Mix(2X)	12.5 µl (1X)
Template (100ng)	2 µl
Forward primer	1.5 µl (1 µM)
Reverse primer	1.5 µl (1 µM)
DMSO	0.4 µl (3%)
NFW	2.1 µl
Total	20 µl

Table (2): PCR condition of bcsA gene amplification

Steps	Temperature	Time	Cycle
Initial denaturation	95°C	5 min	1
Denaturation	95°C	1 min	10
Annealing	**42°C**	1.30 min	
Extension	72°C	**2.42 min**	

Denaturation	95°C	1 min	
Annealing	**69°C**	1.30 min	
Extension	72°C	**2.42 min**	20
Final extension	72°C	10 min	1
Hold	4°C	Infinite	

Table (3): PCR condition of adrA gene amplification

Steps	Temperature	Time	Cycle
Initial denaturation	95°C	5 min	1
Denaturation	95°C	1 min	
Annealing	**42°C**	1.30 min	10
Extension	72°C	**1.06 min**	
Denaturation	95°C	1 min	
Annealing	**69°C**	1.30 min	20
Extension	72°C	**1.06 min**	
Final extension	72°C	10 min	1
Hold	4°C	Infinite	

3.14.3.2 PCR product purification

After confirmation of correct amplicon size from gel electrophoresis, PCR product was purified by using Foregene Kit with slight modification. First, four times the buffer BD (corresponding volume of isopropanol was added) of the PCR product volume and one volume of buffer BD-S was added. The solution was then transferred to the spin column, hold for 1 minute and centrifuged at 12,000 rpm for 1 minute. After flow through was discarded from the collection tube, 700 µl of buffer WB1 was added to the spin column, held for 1 minute and centrifuged at 12,000 rpm for 1 minute. Flow through was discarded and step was repeated. Spin column was placed back into the collection tube.

It was centrifuged at 12,000 rpm for 2 minutes and residue was discarded from collection tube. Spin column was moved to a new 1.5 ml centrifuge tube and 20 µl of NFW was added to the middle of the silica gel membrane. It was incubated at room temperature (RT) for 5 minutes and centrifuged for 1 minute at 12,000 rpm. The final eluted supernatant was taken as purified PCR product and used for restriction digestion.

3.14.3.3 Restriction digestion

Obtain purified PCR product was now subjected in restriction digestion with *Nde*I and *EcoR*I for *bcsA* and *Nde*I and *BamH*I for *adrA* to create site for cloning and mixture was prepared as follows:

Table (4): Restriction digestion with *Nde*I and *BamH*Ifor adrA gene

Purified *adr*A gene	10µl
NdeI	0.5µl
EcoRI	0.5µl
NEB buffer 4(10X)	1.5µl
NFW	2.5µl
Total	15 µl

Table (5): Restriction digestion with *Nde*I and *EcoR*I for *bcsA* gene

Purified *bcs*A gene	10 µl
NdeI	0.5 µl
EcoRI	0.5 µl
NEB buffer 4(10X)	1.5 µl
NFW	2.5 µl
Total	15 µl

The reaction mixture was incubated for 3 hours at 37°C in water bath and then to 65°C for an hour in order to inactivate the enzyme and stored at -20°C.

3.14.4 Restriction digestion of vector pET28a+

Plasmid pET28a+ was used as a vector to clone the *bcs*A gene and *adr*A gene. The plasmid was digested with *Nde*I and *EcoR*I for *bcsA* and *Nde*I and *BamH*I for *adrA*. Two

step digestion protocol was performed to avoid enzyme activity inhibition due to short distance restriction site of two enzyme. The reaction mixture was prepared as following:

Table (6): First step restriction digestion of pET28a+ with *Nde*I

Plasmid pET28a+	20µl
NdeI	1µl
NEB buffer 4(10X)	3µl
NFW	6µl
Total	30 µl

Then the reaction mixture was incubated on water bath for overnight at 37°C and 2µl of sample was subjected to the gel for the confirmation of digestion. And then inactivated enzyme at 65°C for an hour. Second step restriction digestion of pET28a+ with *EcoR*I was done by adding 1µl enzyme *EcoRI* and 1µl of NFW to first step digested product. And then incubated on water bath for overnight at 37°C and inactivated enzyme at 65°C for an hour. After the digested plasmid and inactivation of enzyme, product was subjected to electrophoresis.

3.14.5 Gel Electrophoresis for quantification of insert and vector

Eluted gene insert and vector was then visualized in 1% agarose gel along with 1kb DNA ladder for calibration and quantification. Quantification is based on the intensity of the band with respect to the ladder bands.

3.14.6 Ligation

For the preparation of both insert and vector, they were subjected to ligation and the reaction mixture was prepared as following:

Table (7): Ligation mixture

Vector	1 µl
Insert	6 µl
DNA ligase	0.5 µl
DNA ligase buffer (10X)	1.5 µl

NFW	6 µl
Total	15 µl

This ligation mixture was incubated overnight at 16°C in PCR machine. This ligation mixture was used for transformation of E coli DH5αcompetent cell.

3.14.7 Preparation of competent cells by Calcium chloride method

A loopful of *E.coli* DH5α from glycerol stock was inoculated overnight in 5ml of LB broth. After overnight incubation at 37°C (200 rpm), 1 ml of this culture was inoculated in 50ml of LB broth in 250 ml conical flask and shaking incubated at 37°C till the OD600 reached 0.4. Culture was then aliquot into 2 chilled falcon tubes and chilled in ice for 10 minutes. Then centrifugation was done at 4000 rpm for 10 minutes to harvest the cells and supernatant was discarded. Pellet was washed with autoclaved chilled distilled water. Pellet was re-suspended in 30 ml solution of mixture of chilled 80mM Magnesium chloride and 20 mM Calcium chloride. Suspension was again centrifuged at 4000 rpm for 10 minutes and pellet was re-suspended in 1 ml 100 mM Calcium chloride Suspension was aliquoted 200 µl each in fresh ice chilled and was directly used for transformation by heat shock.

3.14.8 Transformation by Heat shock method

200 µl of competent cell was taken in a fresh ice chilled eppendorf tube and 7µl ligation product was mixed with it (for duplicate). The mixture was chilled in ice for 30 minutes. The tubes were then placed in pre-heated water bath for heat shock at 42°C for 90 seconds. Immediately after heat shock, tubes were kept in ice bath for 5 min and 1 ml of LB media was added in tube and incubated at 37°C for an hour. After incubation, tube was centrifuged at 8000 rpm for 1 minute and supernatant was discarded. Pellet was suspended in 100 µl of fresh LB medium and plated on LB Agar supplemented with 100µg/ml kanamycin. The plates were then incubated at 37°C overnight.

3.14.9 Confirmation of Transformants

3.14.9.1 Plasmid Extraction

Kanamycin resistant transformed colonies grown on plate were selected and inoculated to 10 ml of LB with kanamycin (100 µg/ml) broth and incubated at 37°C with shaking at 200 rpm. The plasmid was isolated as described previously by alkaline lysis method.

3.14.9.2 Restriction digestion

Isolated possible kanamycin resistance plasmid DNA was digested with restriction enzyme *Spe*I to confirm colonies with vector with *bcs*A gene and *adr*A gene. The

restriction digestion mixture was prepared as follows and incubated at 37°C for three hours to allow digestion. Reaction mixture was subjected for 1% agarose gel electrophoresis and required size was compared with 1 kb ladder and control run on the adjacent well.

3.14.9.3 Restriction digestion of transformed vector with gene with *Spe*I

Table (8): Restriction digestion

Plasmid	10µl
*Spe*I	0.3µl
Buffer 4 (10X)	2µl
NFW	7.7µl
Total	20µl

CHAPTER 4

RESULT AND DISCUSSION

4.1 Isolation, screening and identification of Bacteria

Soil samples collected earlier from Panchase region of Pokhara valley and stored at Central Department of Biotechnology, Tribhuvan University, Kirtipur were used to isolate the bacteria. Bacterial were isolated on the basis of the carbon catabolite repression metabolisms (CCR). Enriched soil sample in nutrient broth media were poured in the nitrogen free basal (Nfb) media and isolated colonies were observed in the Nfb media plate indicating isolates had ability to fix atmospheric nitrogen for their survival. Further selection was done by culturing bacteria in nitrogen carbon free (NCF) media plate to isolate diazotrophic autotrophs from the mixed culture. Some of the isolates were able to grow in NCF media. The result suggested that isolates might have the functional enzyme RuBisCo which reduce atmospheric CO_2 for their cell growth and development.

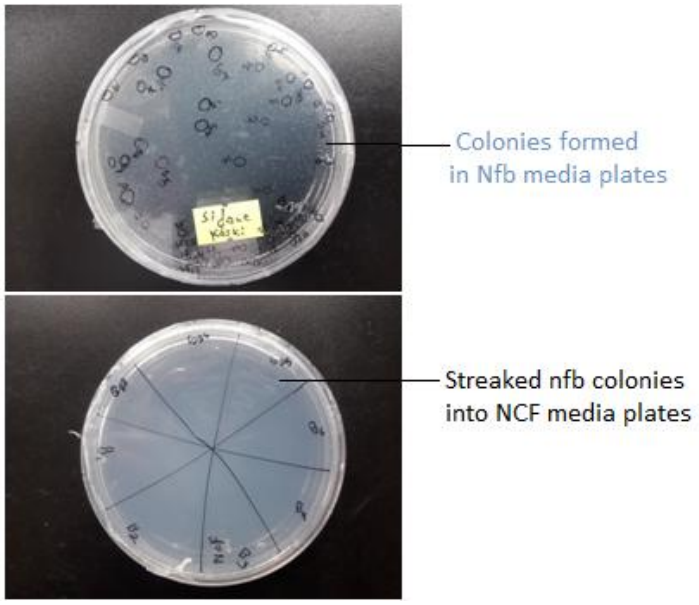

Figure (20): Colonies of bacteria in Nfb and NCF media

4.2 Morphological characteristics of isolated bacteria by the use of selected media

Small size of mucoid colonies inside the media and some above the media with round and oval shaped, creamy white colour were observed. Morphological analysis was done through Gram's staining and microscopic analysis. Gram staining is one of the most common, important, and most used differential staining techniques mostly used in microbiology. It allows the differentiation of bacterial species into two large groups: Gram's-positive and Gram's-negative bacteria on the basis of differential staining with a crystal violet-iodine complex and a safranin counter stain (Coico, 2005). The 31 isolates

were subjected to Gram's staining and 3 isolates were found to be Gram's positive and were rods (Figure). Some mix and positive rod bacterial sample were discarded as *Azospirillum* is known to be Gram's negative and rod.

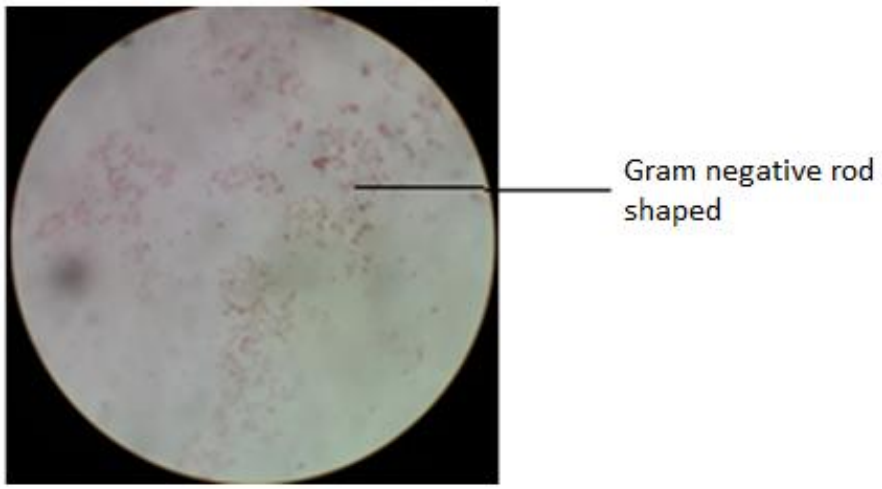

Figure (21): Microscopic examination of *Azospirillum* sps

For those bacteria that exhibited Gram's negative nature in staining were selected for further screening through different biochemical tests and those which were found to be gram positive were discarded. The six isolates showing best atmospheric nitrogen fixing ability were further subjected to 9 different biochemical tests and the isolates having the same biochemical tests to the preferred bacteria were further subjected to molecular tests.

Table (9): Results of different biochemical tests for putative *Azospirillum* sps.

S.N.	Tests	AS19	AS21	ASc	S1	S9	AS14	B3
1	Indole	Negative	Negative	Positive	Positive	Negative	Negative	Negative
2	MR	Positive	Positive	Negative	Positive	Negative	Negative	Negative
3	VP	Negative	Negative	Positive	Negative	Positive	Positive	Negative
4	Citrate	Positive	Positive	Negative	Positive	Positive	Positive	Positive
5	TSIA	Y/Y	Y/Y	R/R	Y/Y	Y/Y	Y/R	Y/R
6	Urease	Negative	Positive	Positive	Positive	Negative	Positive	Positive
7	SIM	motile but no sulfide	motile but no sulfide	motile but no sulfide	motile but no sulfide	motile but no sulfide	motile but no sulfide	motile but no sulfide
8	Nitrate	Positive	Positive	Positive	Positive	Positive	Positive	Positive
9	Oxidative-Fermentative	Positive	Positive	Negative	Positive	Negative	Negative	Positive

Note: Y/Y-yellow/yellow, R/R-red/red, Y/R-yellow/red

4.3 Molecular characterization of isolated *Azospirillum* sps

For the molecular characterization of the putative *Azospirillum* sps genomic DNA (gDNA) was extracted and subjected to PCR.

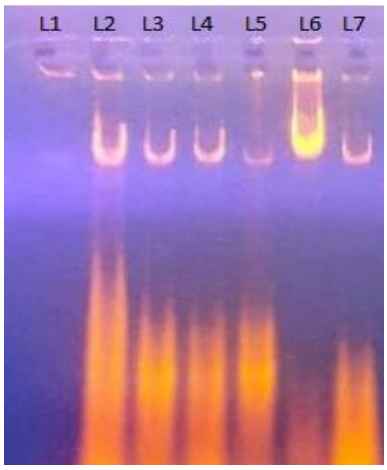

L1=Amplicon from B3
L2= Amplicon from AS14
L3= Amplicon from AS21
L4= Amplicon from ASc
L5= Amplicon from S9;
L6= Amplicon from AS19
L7= Amplicon from S1

Figure (22): Gel electrophoresis picture of isolated genomic DNA of selected 7 samples.

Thus, isolated strains that showed to be putative *Azospirillum* sps were subjected to molecular characterization to validate the isolates were *Azospirillum* sps. Molecular characterization and identification of isolates were done using polymerase chain reaction (PCR) amplification of specific gene and sequencing. Two samples (As19 and S9) that performed the best result in previous assessments were selected for the further confirmation as isolates are *Azospirillum* sps. Genomic DNA was isolated from the bacterial cell using phenol chloroform method for the molecular characterization. Then PCR amplification and sequenced by my senior (Pun M; 2019).

4.4 Quantification of reduced nitrogen by Nessler's Test in culture media

Nitrogen is the most important nutrient for the plant growth and development because it is main constitute of nucleic acid (DNA/RNA), protein. So its availability for the crops plant directly affects the crops productivity. So this test was performed to quantify amount of reduce nitrogen source in Nfb culture media after 48 hrs of incubation.

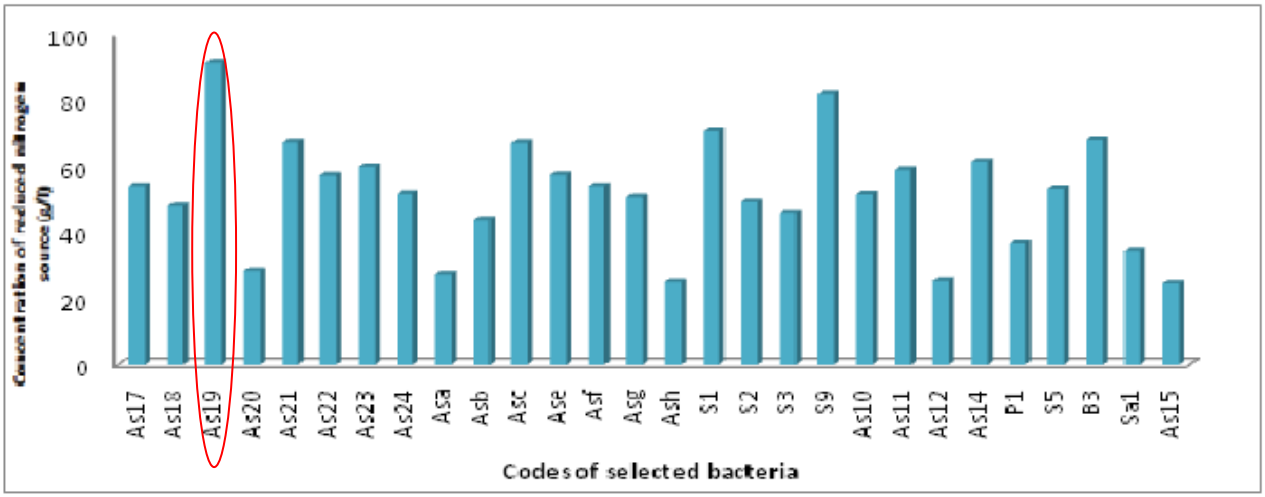

Figure (23): Quantification of atmospheric nitrogen reduced by the isolates.

Among 28 sample, isolate As19 showed best result followed by S9 indicating these isolates could be use as nitrogen fertilizer to substitute chemical fertilizer urea for the development of sustainable and environment friendly agriculture system.

4.5 Revival of bacteria from cryostock stock

Apart from the *Azospirillum* sps other 4 non pathogenic bacteria such as putative *Azospirillum* sps, putative *Azotobacter* sps, putative *Pseudomonas* sps and putative *Geobacter* sps were revived in 10ml of LB broth in sterile culture tubes (available in Central Department of Biotechnology) and these were again grown in specific media to reproduce the protocol and to validate and their reproduction, based on CCR (Pun, M. 2019 and references there in).

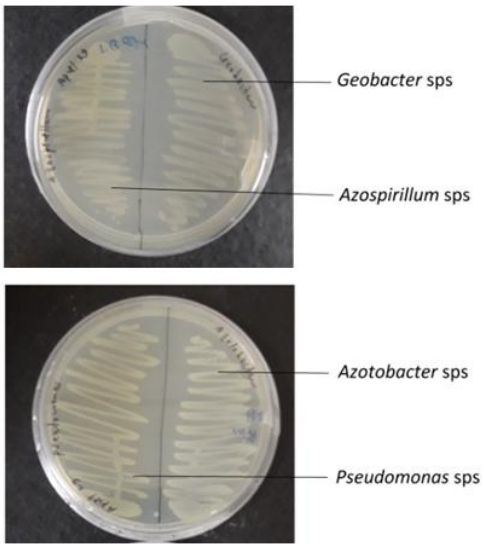

Figure (24): Streaking of all 4 putative isolates.

For the reproduction of all four bacteria in respective specific media, the putative *Pseudomonas* sps (sample P8) was streaked on NCF media containing toluene as sole carbon source and whereas putative *Azotobacter* sps (sample A17) also streaked in same media but carbon source was used as ethylene glycol. Different reduced carbon sources were used because some paper reported that the bacteria like *Pseudomonas* sps can survive in toluene containing media (Volkers *et al.,* 2015) due to presence of genes which are responsible for degradation of toluene (Kahraman & Geckil, 2005) from the media and it import and efflux mechanisms (Worsey & Williams, 1975). Likewise, *Azotobacter* sps has ability to utilize ethylene glycol as carbon source and energy source (Shi *et al.,* 1996). Similarly, putative *Geobacter* sps (sample S4) was streaked in same media as above mentioned but aniline used as a sole source of carbon (Young, 1995). It has been described that this species can breakdown aniline and utilizes it as carbon source to rule out other diazotrophs that cannot utilize aniline. The putative *Azospirillum* sps (sample AS19) was streaked as in the NCF media which is very much specific for this bacteria, in this media only the carbon and nitrogen fixing bacteria can grow without

giving any nitrogen and carbon sources. Obtaining single colonies of above bacteria in specific media were used for further application.

4.6 Synthesis of Cobalt oxy hydroxide nanoparticles

Cobalt nanoparticle was synthesized by chemical method; drying at 65° for 2 days (detail description in method and methodology section). Cobalt nanoparticle thus synthesized was characterized by FTIR (for functional group identification) and XRD (crystalline phase determination and chemical composition information).

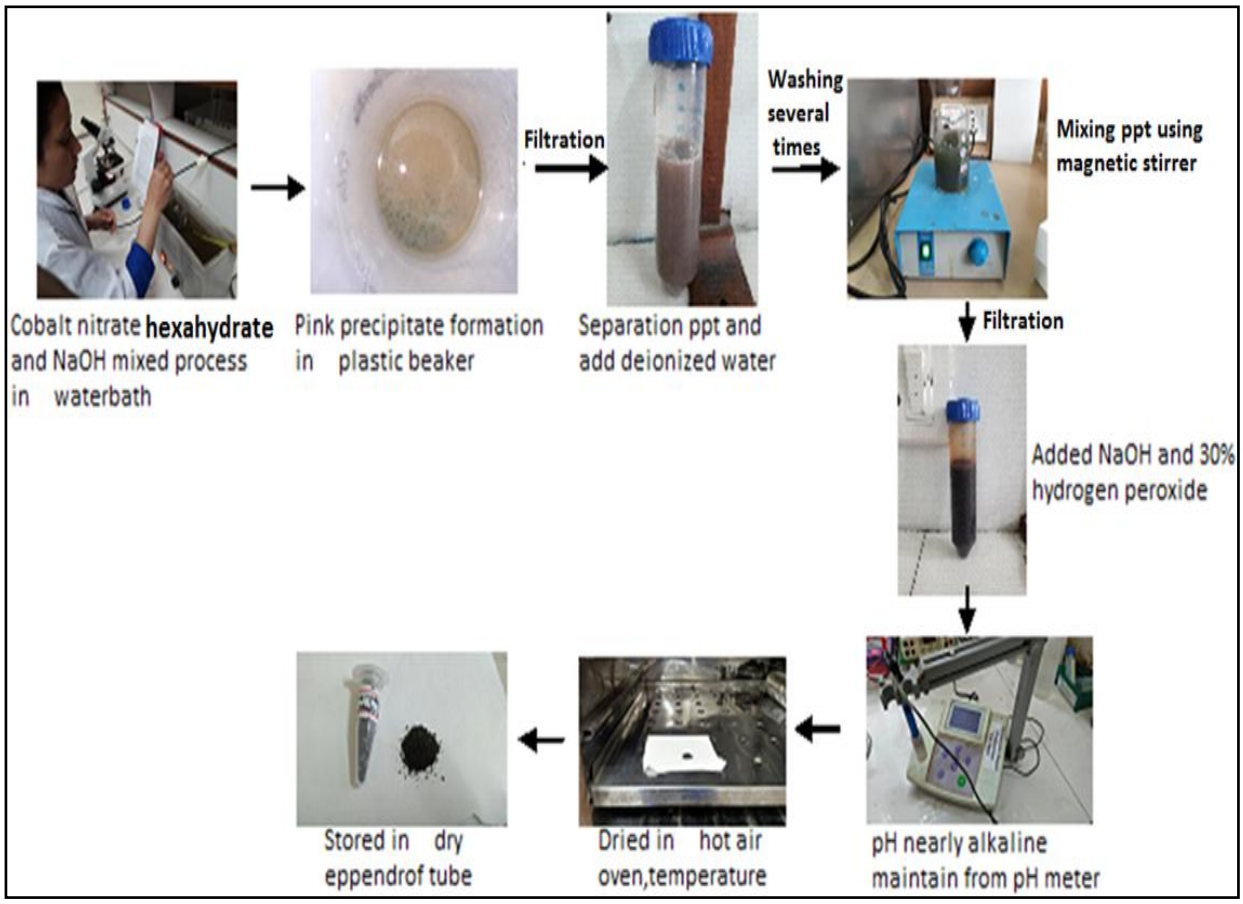

Figure (25): Diagramatic figure of synthesis of cobalt nano particle

4.6.1 Synthesis of Cobalt oxy hydroxide nano-particles

As described in material methods, alkali treatment of cobalt nitrate hexahydrate at 45°C gradually gives pink precipitate of cobalt hydroxide (Yang et. al., 2010). Then upon oxidation with hydrogen peroxide (caution has to be taken for explosiveness and carefully drop wise added and stirred) at 45°C the pink precipitate gradually changes to brownish particles giving rise to cobalt oxyhydroxy nano-particle. Thus, prepared cobalt nano-particle was completely dried at 65° for 2 days (detail description in method and methodology section) and was characterized by FTIR (for functional group identification) and XRD (crystalline phase's determination and chemical composition information). As X-ray diffraction is a tool for determining the atomic and molecular structure of a crystal which follow the Bragg's law (Hummel, 2011). $2d\sin\theta=n\lambda$ where n is a positive integers, λ

is the wavelength of incident wave, θ is scattering angle, d is path difference between two waves.

A crystal is a composition of periodically arranged in a 3D space while amorphous do not show periodicity and atoms are randomly distributed in 3D space so scattering of X-rays by atoms is the point to be considered. When there is periodic arrangement of atoms the X-rays will be scattered only in certain directions when they hit the formal lattice planes, which will cause high intensity peaks. Moreover, in amorphous phase, X-rays are scattered at many directions leading to a large bump distributed in a wide range that is 2θ instead of high intensity narrower peaks (Ladd *et. al.,* 1985).

4.6.2 XRD characterization of Cobalt nano-particle

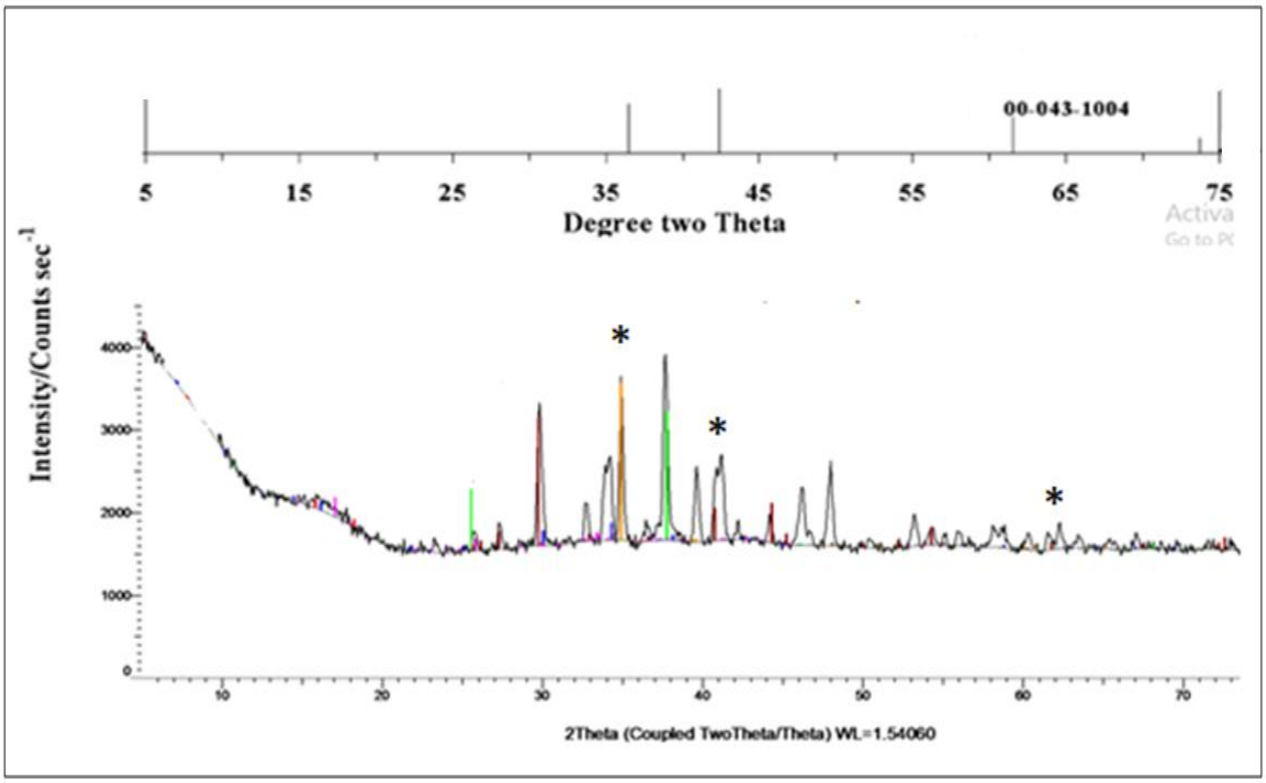

Figure (26): XRD patterns of cobalt oxy hydroxide sample compared with Joint Committee on Powder Diffraction Standards (JCPDS; upper) peak range of Cobalt nano-particle.

The XRD diffraction at 2° theta gave diffraction peaks of 36, 42 and 62 as observed in the (Yang et. al., 2020) JCPDS standard (upper). This suggested that there is also presence of cobalt oxyhydroxy nano-particle. Furthermore, the sample was analysed in FTIR.

4.6.3 Fourier Transfer Infra-Red (FTIR) characterization of Cobalt-nanoparticle

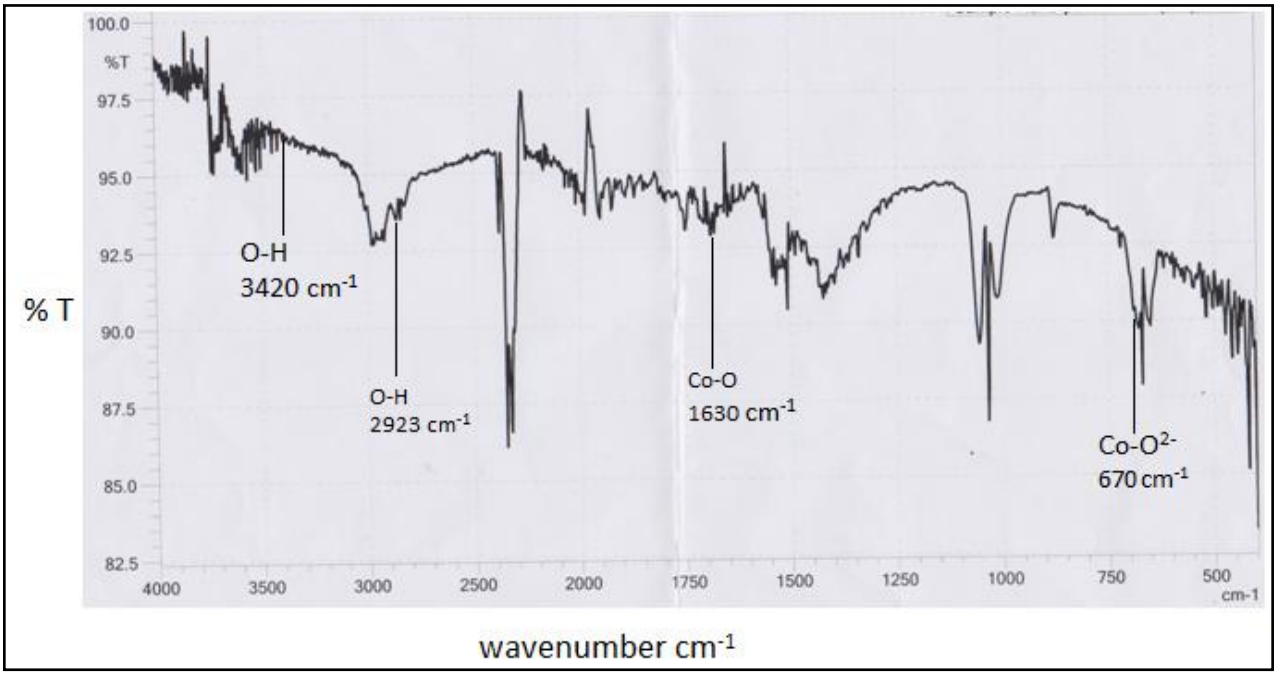

Figure (27): FTIR of cobalt sample with reference paper with transmittance (%T) via wavenumber (cm^{-1})

FTIR result showed that the synthesized CoOOH nano-particle was found to have 1630 wave number cm^{-1}corresponding to Co-O bond and O-H bond at 3420 and 2923 wave number cm^{-1}. Similarly, presence of $Co\text{-}O^{-2}$ at 670 wave number cm^{-1} was seen. Presence of band at around 2400 cm^{-1}could not be explained. Furthermore, occurrence of this band could be due to the presence of interfering ions and impurities during the nano-particle synthesis. While comparing the FTIR data of our sample with the standard FTIR data of Co nano-particle we found presence of majority (Jagadale et. al., 2012) of functional groups thus confirming the synthesis of nano-particles. For eliminating presence of extra bands in the spectrum, we have modified the protocol for nano-particle synthesis and preliminary works were done but the experimental works could not be completed due to time limitations (works are being pursued by other team members).

4.7 Single chamber syntrophic growth checked in modified nitrogen free media

In order to study the effect of cobalt hydroxyoxy nano-particle in water splitting and the carbon dioxide reduction in our system without the use of light energy or electrical energy a syntrophic growth of consortium of bacteria was performed in single vessel with modified media that was nitrogen free and sodium carbonate as a source of carbon. In order to estimate the nitrogen and inorganic carbon reduction Nessler's and

Anthrone tests, respectively were performed and for quantification a calibration curve for both experiments were made.

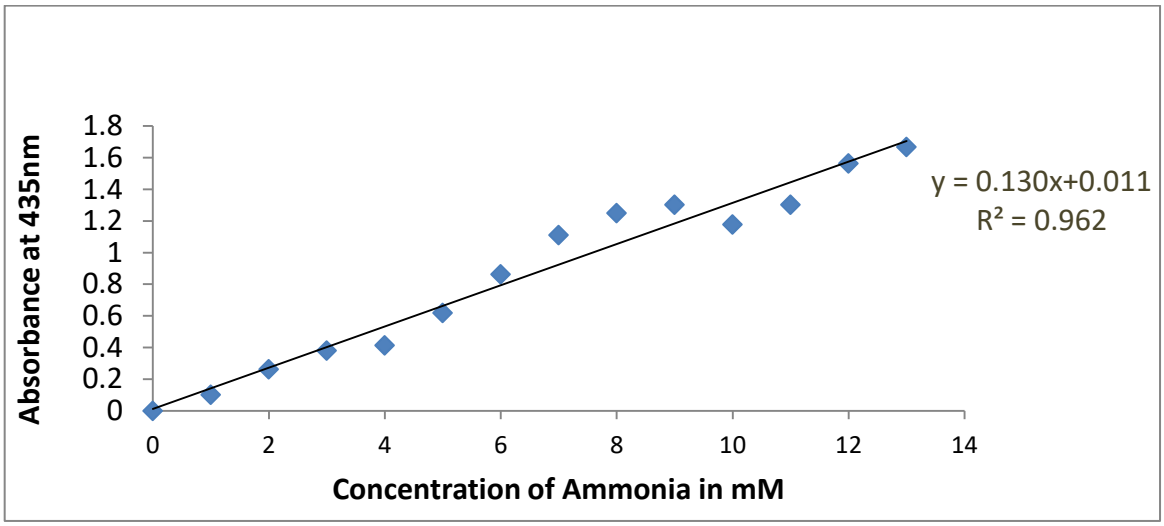

Figure (28): Standard calibration curve of ammonium hydroxide for reduced nitrogen quantification

Using different concentration of ammonium hydroxide, the standard calibration curve was developed to calculate the amount of reduced nitrogen and showed linear line in correspondence to absorbance at 435 nm by Nessler's reagent. The R^2 value was found to be 0.962 indicating the graph was reasonably accurate as standard calibration curve. Thus, the value of constant for equation Y= ax+b was found to be 0.130 for 'a' and 0.011 for 'b' was taken for subsequent calculation of amount nitrogen reduced by consortium of bacteria in Nfb media.

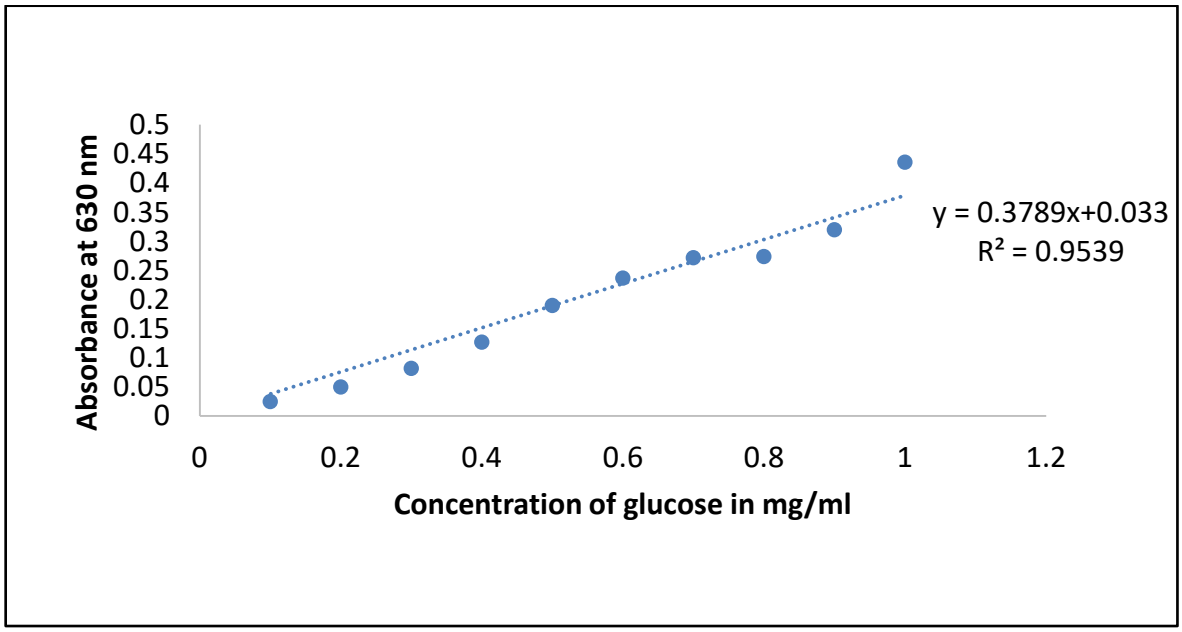

Figure (29): Standard calibration curve of glucose for carbon fixation quantification

Similarly, using different concentration of glucose, the standard calibration curve was developed to calculate the amount of carbon fixed by the syntrophic culture by Anthrone reagent showed linear line in correspondence to absorbance at 630 nm. The R^2 value was found to be 0.953 indicating the graph was reasonably accurate as standard calibration curve. Thus, for equation Y=ax+b the value of constant 'a' was found to be 0.378 and 0.033 for 'b' were taken for subsequent calculation of amount of reduced sugar fixed in culture media by consortium of bacteria.

4.8 Single chamber syntrophic growth checked in modified nitrogen free media

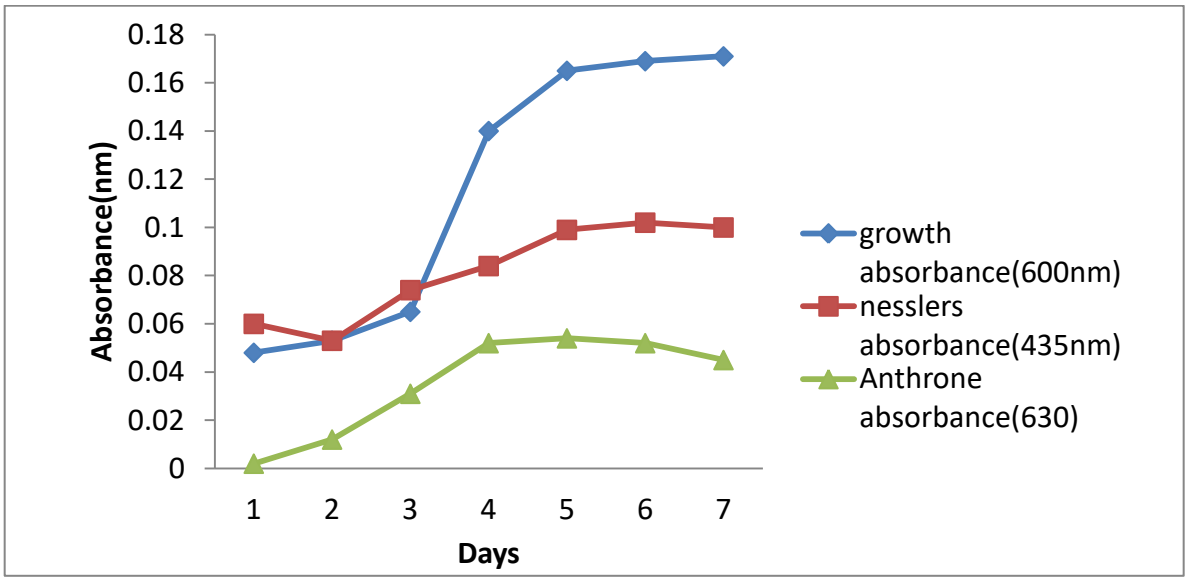

Figure (30): Absorbance of different parameter versus incubation time (days)

Then, the syntrophic culture was incubated for a successive period of 7 days at 28°C with the regular measurement of growth. The graph (Figure 28) showed that bacterial culture were live (OD_{600}) even incubating for 7 days despite the media was devoid of nitrogen source and organic carbon suggesting that the atmospheric nitrogen dissolved in media and the available inorganic carbon as carbonate were reduced to function biologically available forms. Upon Nessler's test (Geo et. al., 2018) for presence of reduced nitrogen as ammonia and Anthrone test for reduced organic carbon, the amount of reduced forms of nitrogen (Steenhoudt & Vanderleyden, 2000) and carbon were found to increase in response to the cell growth and plateaued on 5 days. Based on the standard calibration curve of ammonium hydroxide and glucose, respectively for the reduced nitrogen and carbon in syntrophic culture were quantified. The maximum amount of nitrogen reduce was found to be on the 6^{th} day and for carbon it was found to be higher on the 5^{th} day of incubation (Table 10). Since the bacteria were cultured in nitrogen free media but supplied with Sodium carbonate as a carbon source.

Table (10): Quantification of reduced nitrogen and carbon in syntrophic growth

Days	Number of cells Per ml	Concentration of Reduced nitrogen test (mM/ml)	Amount of reduced Nitrogen(g/l)	Amount of reduced Carbon(g/l)
1	3.84×10^7	0.462	16.19	0.005
2	4.24×10^7	0.408	14.29	0.032
3	5.20×10^7	0.569	19.94	0.082
4	1.12×10^8	0.646	26.14	0.137
5	1.32×10^8	0.762	26.70	**0.142**
6	1.35×10^8	**0.785**	**27.51**	0.137
7	1.37×10^8	0.769	26.95	0.119

4.9 Prospect of microbial cellulose biosynthesis

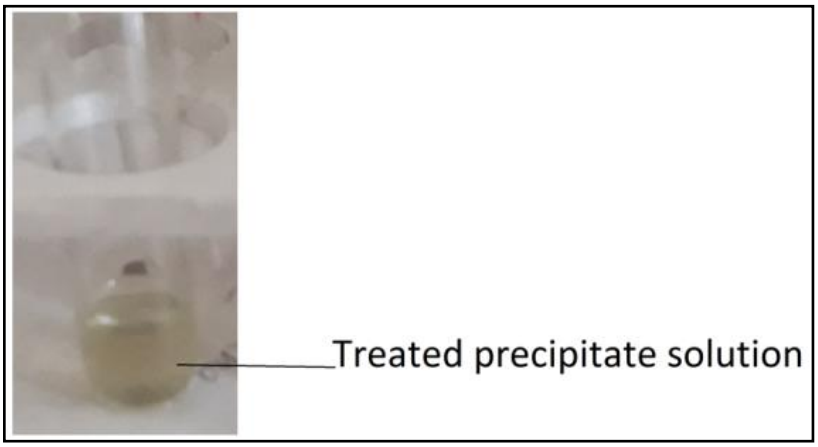

Figure (31): Test tube with teated precipitate without using any dye

Since isolated *Azospirillum* sps. (Pun, M., 2019) was included in the consortium and some of the *Azospirillum* sps. have been reported to make microbial cellulose and in earlier works similar precipitate was observed when incubated without carbonate but with higher electrical energy, the precipitate observed in the culture medium was thought to be probably microbial cellulose since the constituents of the media (water soluble sodium carbonate was used as carbon source instead of calcium carbonate since

this is insoluble in water) which was viewed microscopically (Figure 32). We wanted to confirm that the precipitate is organic carbon or not and whether it carries reducing sugar equivalent and to confirm whether it is starch or cellulose.

4.9.1 Microscopic examination of precipitate of cellulose

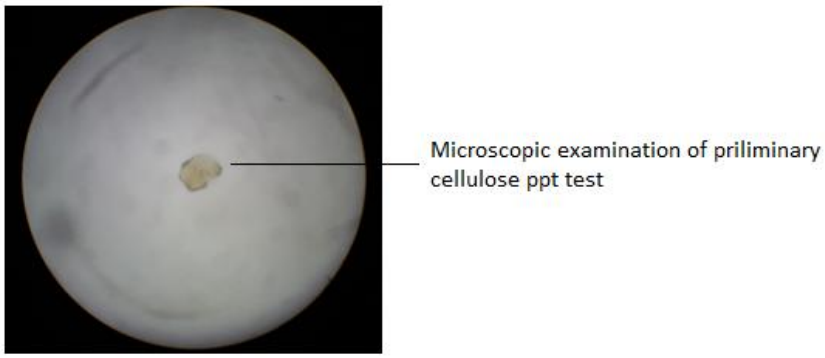

Figure (32): (40X) Micrograph taken from microscopic examination

4.9.2 Reducing sugar test

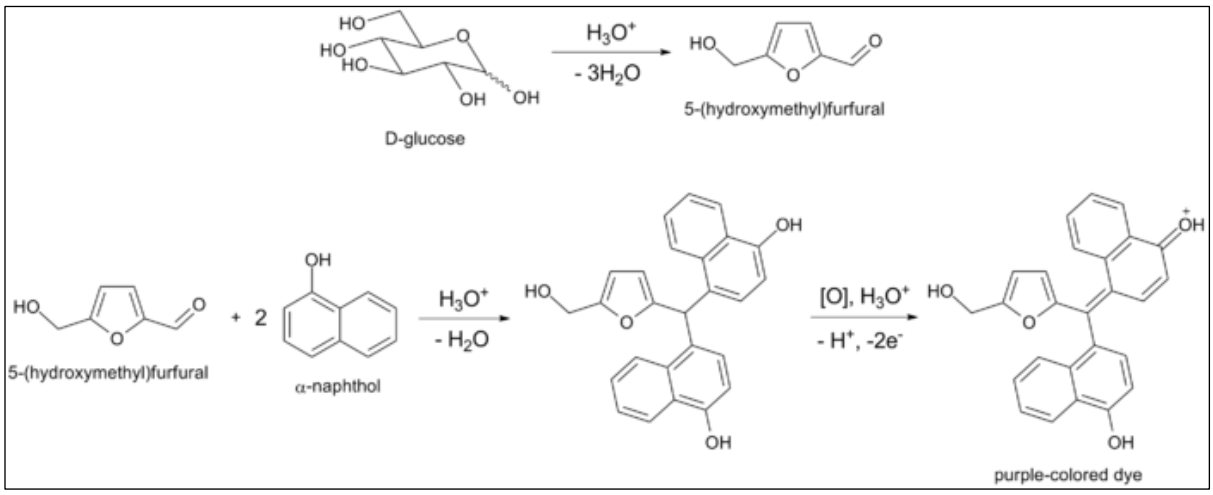

Figure (33): Schematic representation of Molisch's test (courtesy: Wikipedia).

Whether the precipitate is organic carbon or not and we wanted to test for availability of reducing sugar equivalent and Molish test (Levine 1930) was chosen since it uses sulphuric acid that can easily break the polymer bond of starch or cellulose and the reaction with the reducing equivalent of the monomer it will give furfural and its derivatives (Lüning et. al., 1980). This furfural reacts with sulphonated alpha naphthol to give a purple complex (Figure 31). In both positive and test samples purple color was observed (Figure 32) indicating that the precipitate is polymer of organic carbon with reducing equivalent suggesting that the precipitate can be used for making different useful compounds.

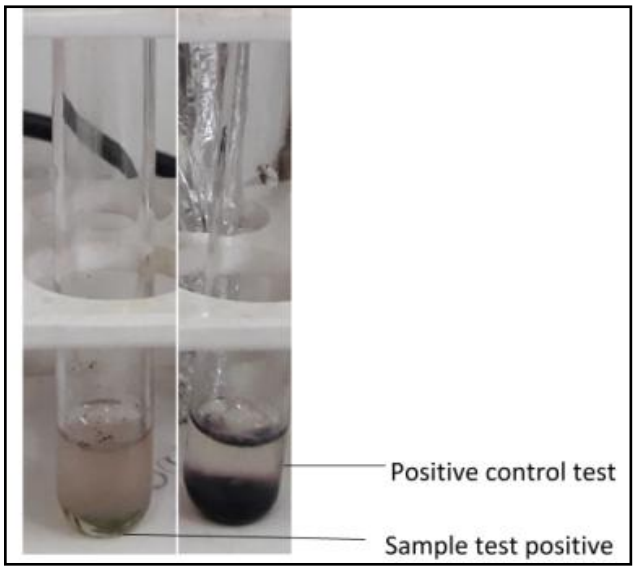

Figure (34): Reaction mechanisms for carbohydrates test through Molisch's reagents

Further to validate that the crystals are polymer of reducing sugar, the alkaline method of detecting, Benedict's test (Simoni et. al., 2002), where the mild alkaline treatment will not break the polymer bond even in thermal energy to release reducing sugar as in acid treatment. In this reaction the reducing sugar is converted to powerful reducing agents, enediols, that can reduce cupric ions (blue colored $CuSO_4$. $5H_2O$) to the cuprous ions (cuprous hydroxide) where sodium citrate increases solubility and thermal energy changes this to red brick colored cuprous oxide. The precipitated crystal showed negative results (Figure 33) indicating that the polymers end molecule has not reducing equivalents suggesting that it could not be starch but structure like cellulose where the additional hydrogen bonds mask all the side chain moieties.

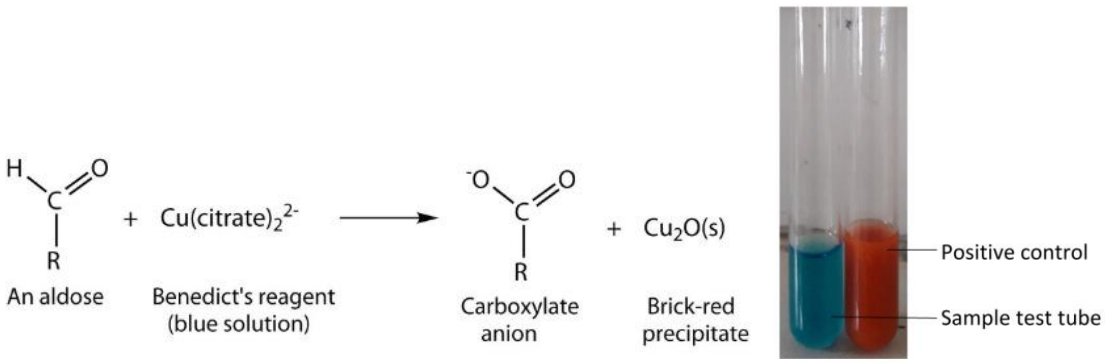

Figure (35): Reaction mechanisms and principle of Benedict's reagent test (Seager & Slabaugh, Michael R, Boudreaux, 2005)

4.9.3 Iodine test

In earlier works the precipitated crystals were tested for whether it was lignin or not and was found to be negative suggesting that the polymer could be of hexose sugar (data not shown). Now we wanted to confirm whether this is glucose or other reducing sugar polymer. In general starch like amylose show α-acetyl linkage with bond angle to form a

spiral like a coil spring structure because of α-acetyl linkage between C1 and C4 of two α-D-glucose molecules. This can be detected through Iodine test where the color are caused by charge transfer complex. In general, the molecular iodine (I_2) that is sparingly soluble in water when mixed with soluble potassium iodide (KI) and the iodine ion (I^-) reacts with the free iodine (I_2) to form a water soluble triiodide ion (I_3^-) and form polyiodide ions (I_n^-) which acts as charge donor with the neutral iodide as charge acceptor in making charge transfer complex where the electrons easily excite to high energy level by light and the light is absorbed to give brownish color in aqueous solution. Moreover, upon addition of starch like amylose it acts as charge donor and the polyiodide as the charge acceptor absorbing light of different wavelength to give dark blue color (Seager & Slabaugh, Michael R, Boudreaux, 2005). The precipitated crystal solution did not change in to dark blue color but retained brownish color (Figure 34) suggesting that it is not the starch.

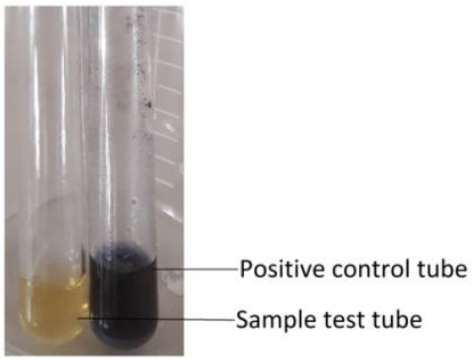

Figure (36): Iodine test

4.10 Monoculture and co-culture of bacteria in specific media

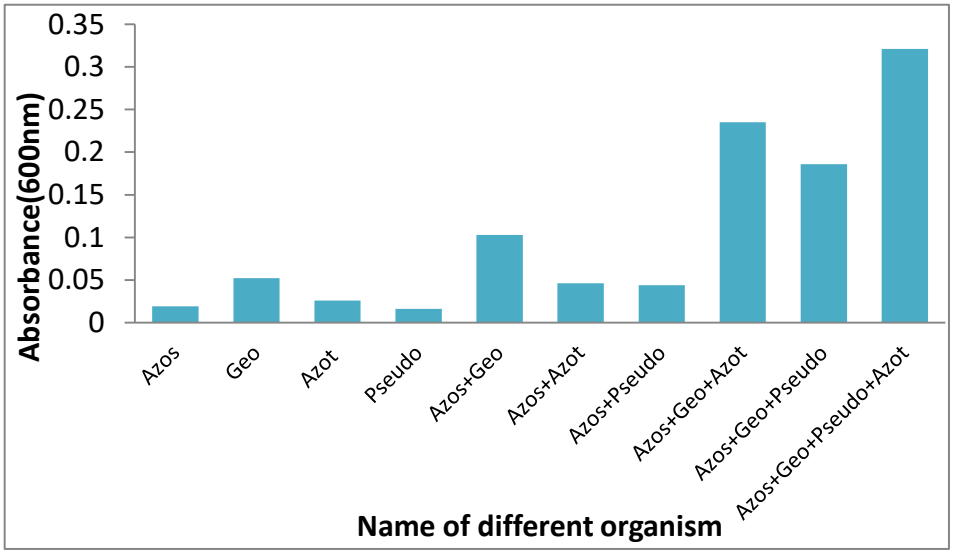

S.N.	Number of cells per ml
1	1.52 x10^7
2	4.16 x10^7
3	2.08 x10^7
4	1.28 x10^7
5	8.24 x10^7
6	3.68 x10^7
7	3.52 x10^7
8	**1.88 x10^8**
9	1.49 x10^8
10	**2.57 x10^8**

Notes: Azos-*Azospsirillum*; Geo-*Geobacter*; Azot-*Azotobacter*; Pseudo-*Pseudomonas*

Figure (37): Graph Mono culture and syntrophic culture of bacteria in specific media and absorbance measured at 600 nm in left side and in right side of table shown the cells per ml

Growth of Mono and syntrophic culture of bacteria were checked in the media containing cobalt nanoparticle and sodium carbonate as a sole carbon source. From above graph it was concluded that bacterial growth was found higher in syntrophic culture than monoculture. Furthermore, growth was enhanced in co-culture where *Geobacter* was present. Because *Geobacter* is the master regulator which donate the electron and proton. Whereas cobalt nanoparticle acts as an electrocatalyst for transfer of electrons. Corresponding to the absorbance at 600 nm for growth; number of cell/ml has been counted and presented in the table and found higher in co-culture of *Azospirillum* sps., *Geobacter* sps., *Pseudomonas* sps. and *Azotobacter* sps. From the above table best one growth was found to be as 2.57 $x10^8$ cells per ml.

4.11 Syntrophic culture in Nfb media with varied carbon source

Table (11): Number of cells per ml

Days	Number of cells Per ml	Amount of reduced Carbon(mg/l)
1	2.46 $x10^8$	4.85
2	3.29$x10^8$	5.93
3	4.25 $x10^8$	8.36
4	4.31 $x10^8$	9.43
5	4.37 $x10^8$	11.32
6	4.43 $x10^8$	15.90
7	4.47 $x10^8$	19.95
8	4.50 $x10^8$	22.91
9	**4.62 $x10^8$**	**23.72**
10	**4.62 $x10^8$**	**25.61**
11	4.34 $x10^8$	17.25
12	4.37 $x10^8$	11.59
13	4.26 $x10^8$	9.43

Nfb media was modified by varying the carbon source provided to the syntrophic culture. The media contained sodium carbonate and potassium hydroxide (here BTB used in the media was replaced by KOH). The best growth was observed during the 10th day of incubation with the colony forming unit 4.62*10^8 per ml and high carbon fixation on 10^{th} day as calculated by anthrone test (26.61 mg/l). In the anodic chamber the bacteria would survive by consuming carbonate as carbon source to reduce it. The hole created in anodic chamber will allow the splitting of water molecule and release electron and proton some of which would be used to reduce the carbonate for cell growth. In the anodic chamber *Geobacter* would facilitate the transfer of electron in anode electrode while in cathodic chamber would act to trap the electron from cathodic chamber and transfer to other bacteria also. With this nano-bio wiring the electrons coming from

water splitting in anodic chamber to cathodic chamber would be trapped before it reacts with proton to give hydrogen molecule. Even if the hydrogen molecule is made it would be converted to proton and electron by all these four bacteria. Similarly, when the media was replaced by potassium carbonate instead of Sodium carbonate as a sole carbon source and maximum growth was observed at the 9th day of incubation with the colony number 21*10^{6} cells per ml of media.

4.12 Syntrophic culture in Microbial fuel cell (MFC)

Syntrophic culture was maintained in the microbial fuel cell where the anodic and cathodic chamber was separted by transmembrane. Anodic chamber contained phosphate (KPi) buffer and cathodic chamber contained NCF media.

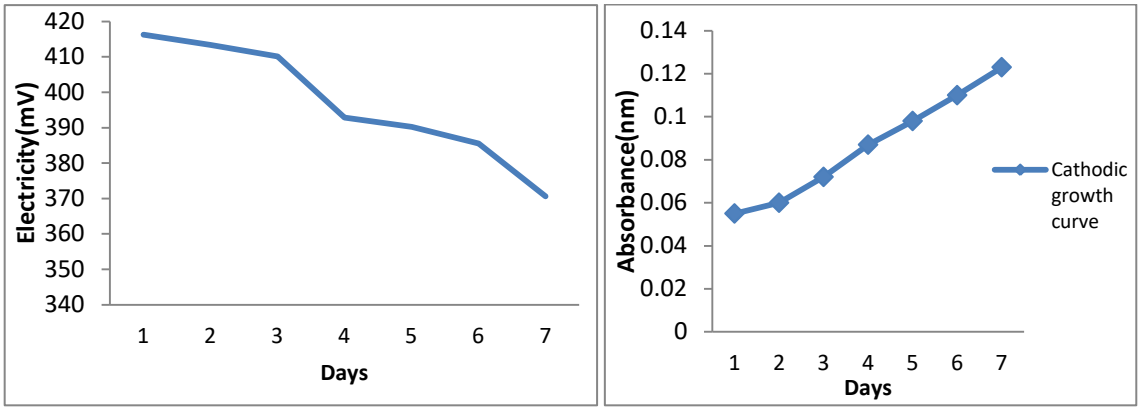

Figure (38): Electricity supplied Vs incubation time (days) graph in left side and growth Vs incubation time (days) in right side

Table (12): Number of syntrophic culture per ml

Days	Number of cells Per ml in cathode
1	4.40 x10^{7}
2	4.80 x10^{7}
3	5.76 x10^{7}
4	6.96 x10^{7}
5	7.84 x10^{7}
6	8.80 x10^{7}
7	**9.84 x10^{7}**

Incubating the syntrophic culture for some days in MFC without providing external power supply; bacterial growth reached maximum during 7th day of incubation. While the electricity generated was found to decrease with the increase in incubation time. This might be because the syntrophic culture has utilized the electricity generated for nitrogen fixation and other metabolism.In addition to this, at anodic chamber Noceras

buffer was added which also contained and Kpi buffer (as former) and cathodic chamber contained syntrophic culture with NCF media. While comparing the result of growth using Kpi only and in combination with Nocera's buffer no any contrasting result was found with $7.84*10^7$ bacterial cells per ml in cathodic chamber.

Certain modification in MFC was made; which contained NCF media and syntrophic culture in cathodic chamber and anodic chamber contained Nocera's buffer, GS modified media and syntrophic growth. So as to compare the growth in both chamber.

4.12.1 Syntrophic culture

NCF media and syntrophic growth in cathodic chamber whereas, Noceras buffer, GS modified media and syntrophic growth in anodic chamber.

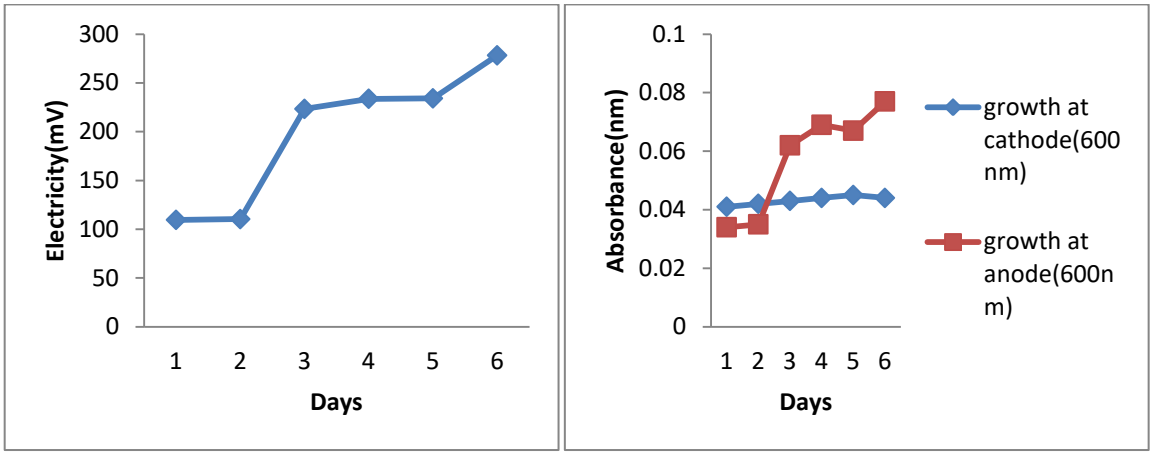

Figure (39): In cathodic chamber added NCF media and syntrophic growth and in anodic chamber added Noceras buffer and GS modified media and syntrophic growth in left side and another one the electricity measured graph.

Table (13): Number of syntrophic culture per ml

Days	Number of cells Per ml in anode	Number of cells Per ml in cathode
1	2.7×10^7	3.3×10^7
2	2.8×10^7	3.4×10^7
3	4.9×10^7	3.4×10^7
4	5.5×10^7	3.5×10^7
5	5.4×10^7	**3.6×10^7**
6	**6.2×10^7**	3.5×10^7

In both of the chamber syntrophic culture was added distinguished by the media composition, which contain NCF in cathodic chamber and GS modified media, Nocera buffer in anodic chamber. Electricity generated was found higher with the increase in incubation time reaching maximum during 6 days. While observing the growth pattern; growth found higher in anodic chamber. This might be aided by the GS modified media

containing required nutrient for bacterial culture and Nocera buffer as well. While in cathodic chamber; media deprived both nitrogen and carbon source.

4.13 Syntrophic culture with Yagi's buffer

Another experiment was conducted using Yagi's buffer which is the mixture of 0.1M $NaHCO_3$ and 0.03M K_2SO_4 and pH maintained 10 at anodic chamber of MFC; while cathodic chamber contained NCF media and syntrophic culture. The electricity generated was found higher with the increasing incubation time.

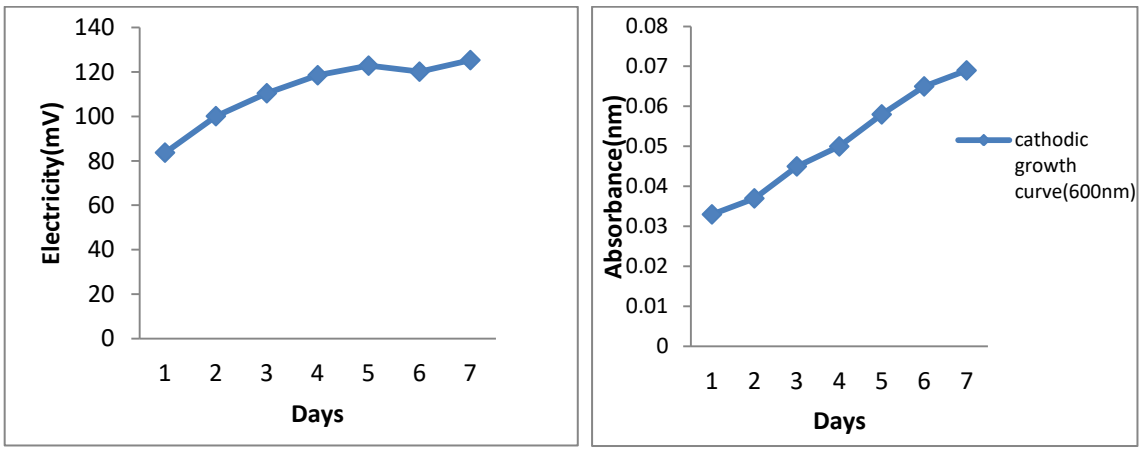

Figure (40): Electricity generated (mV) Vs culture incubation time (days) in left side and another one the growth via days graph

Table (14): Number of syntrophic culture per ml

Days	Number of cells Per ml in cathode
1	2.64×10^7
2	2.96×10^7
3	3.28×10^7
4	3.60×10^7
5	3.36×10^7
6	3.20×10^7
7	**4.64×10^7**

Incubating the syntrophic culture for 7 days it was found that the growth reached maximum during the 7^{th} days in NCF media. Electricity generated was found highest during the 5 days and decreased after that.

4.14 Syntrophic culture using cobalt nano-particle

Using GS media and KPi buffer along with Co nano particle in anodic chamber and GS media and syntrophic culture in cathodic chamber another experiment was conducted to see if the growth and the electricity generated in MFC was enhanced by the Co nanoparticle. Although some fluctuation was observed but then also growth was higher

in anodic chamber indicating Co nanoparticle facilitate in cell density increment. Electricity generation found proportion with the incubation time.

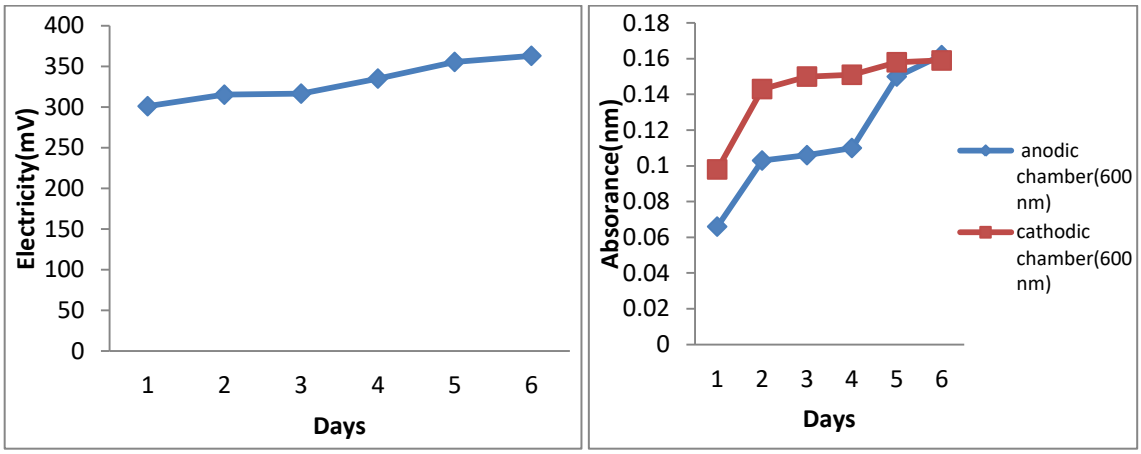

Figure (41): Electricity generation (mV) Vs culture incubation time in left side and another right side graph shown the growth vs days

Table (15): Numer of cells per ml

Days	Number of cells Per ml in anode	Number of cells Per ml in cathode
1	5.3×10^7	7.8×10^7
2	8.2×10^7	1.1×10^8
3	8.5×10^7	1.2×10^8
4	8.8×10^7	1.2×10^8
5	**1.2×10^8**	**1.3×10^8**

The reduced carbon source in modified NCF media derived from dissolved carbondioxide in the media would be utilized by *Geobacter* and release extracellular electron and proton. The electron could act as power supply to tin oxide in the buffer and that would react with Co present in the media. Co changes into Co(O)OH nano-particals. Co(O)OH acts as water splitting catalyst in conjuction with carbonate. The electron generated would probably pass to cathodic chamber since *Geobacter* can act both as electron donor and acceptor. Thus creating power gradient across anode and cathode chamber. This power gradient will allow proton transfer to cathodic chamber and support additional growth. Therefore, including the buffer in the MFC with *Geobacter* sps and *Azospirillum* sps can create additional oxygen in the water. The hydrogen will be used by hydrogenase of diazotroph for additional growth.

4.15 Hydrogen gas evolving test in MFC

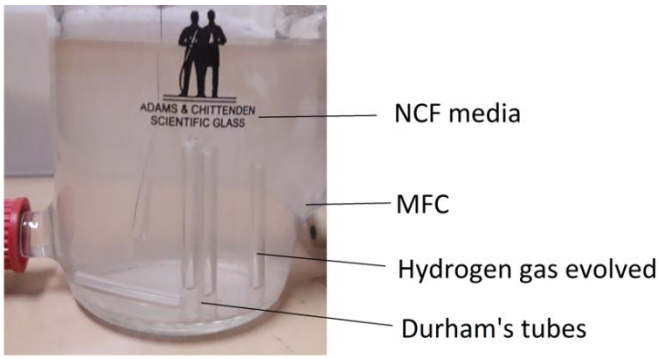

Figure (42): Hydrogen gas evolved in MFC

The hydrogen gas evolved inside the Durham's tubes suggested that the syntrophic growth with that *Geobacter* sps. produced proton and electron into that media. This helped to make further more proton and make final product as gas form and only proton form acts as their respective mechanisms and transformed through membrane at that another chamber.

4.16 Cloning for strain development

Bacterial cellulose is very important biocompatible component which has huge industrial application including paper industry, food industry along with medical importance for wound healing, tissue generation. Moreover cellulose production from plant has various environmental impacts such as deforestation, strong solvent management problems. Primer of different four genes that is *adr*A, *bcs*A, pgm and *gal*U were already designed. Primer for PCR amplification of *adr*A, *bcs*A, *gal*U and *pgm* gene were designed based on nucleotide sequence of *E. coli* deposited in NCBI using different freely available web based tools including Oligocalc, Oligo analyzer, m-fold and BLAST. Different parameters of primers like length, GC%, Tm, homodimer, heterodimer, secondary structure, sequence specificity were optimized to the optimal range.

Designed primer sequences are given below.
1. AdrA
Forward: GGTGTGCCGCCTCATATGTTCCCAAAAATAATGAATGATGAAAAC
Reverse: ATTATTGGATCCTTATTTGTAGTCACTAGTTTAGGCCGCCACTTC

2. BcsA
Forward: GAATTTGTATCTAGAAGTCGGGAGTGCCATATGAGTATCCTG
Reverse: GTTTCCGAATTCTTCCGATGAGATACTAGTTTATTGTTGAGCCAAAG

3. pgm
Forward: GGTATCCGCAAGTCTAGATTAAAGGACAAACATATGGCAATC
Reverse: GACTTTGAATTCCCTGCATGAACAACTAGTTTACGCGTTTTTC

4. galU

Forward: CCACACAGGTCCGTCATATGGCTGCCATTAATAC
Reverse: ACACACGAATTCCCTTGATCCTTTACTAGTTTACTTCTTAATGCC

Where restriction sites are:

GAATTC-*Eco*RI, CATATG- *Nde*I, GGATTC- *BamH*I, ACTAGT- *Spe*I, TCTAGA- *Xba*I

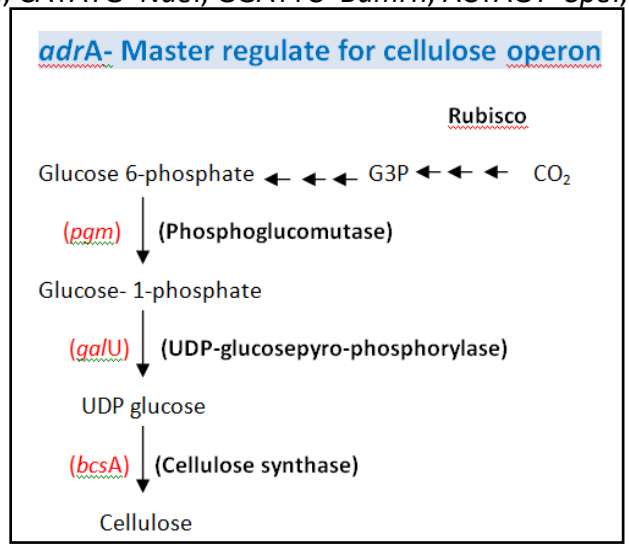

Figure: Flow chart of Microbial Cellulose Synthesis

4.16.1 PCR amplification of *bcs*A and *adr*A gene

Genomic DNA was extracted from *E.coli* DH5α strain because *bcs*A gene is also found in *E.coli* and it was confirmed by blast of *bcs*A gene sequence with whole genome sequence of *E.coli.* Therefore, whole genome of *E. coli* was used as template for the target gene amplification using the specifically designed primers of *bcs*A forward and reverses. In amplification 3% Dimethyl sulfoxide (DMSO) was used in PCR mixture because it is an organosulfur compound with a high polarity and high dielectric constant which help to disrupt secondary structure formation in the DNA template as well as primer.

Similarly, annealing temperature was also optimized, it is necessary because when the annealing temperature is too low, it may result multiple bands due to non-specific primer binding. Whereas when the annealing temperature is too high, primer may be unable to bind with template (Rychlik *et al.,* 1990). Thus, two step reaction conditions were used for PCR amplification. For the first 10 PCR cycles with low (42°C) annealing temperature targeted to initially amplify the genomic region by binding of only primer region that has complimentary sequence of respective gene and for the rest 20 cycles with high (69°C) annealing temperature (Tm-5°C) was determined because the amplicon that have been produced from 10 cycles would have complimentary region to the entire primer sequences and non-specific binding of primer could be avoided to amplify the respective gene (Pun M;2019).

The PCR product gave clear band corresponding to around 2.6kb DNA fragment comparing with 1kb ladder in another well after electrophoretic run in 1% agarose gel with ethidium bromide (Figure). It was assumed that *bcs*A gene has been successfully amplified because the target gene size is 2.678kb long.

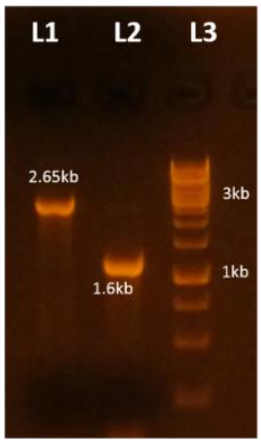

Figure: PCR product of L1-*Bcs*A, L2-*Adr*A L3- 1kb ladder of Gene ladder thermo scientific

Figure (43): PCR product of *adrA* gene and *bcsA* gene

4.16.2 Restriction digestion of *bcs*A gene

The PCR product that gave 2.6kb DNA fragment size and presumed to be *bcs*A gene was purified by using Foregene Kit with slight modification. After purification, the amplified DNA was completely digested with *Nde*I and *Eco*RI for subsequent cloning in pET28a+ vector digested with *Nde*I and *Eco*RI. Then, enzymes present in mixture were inactivated in order to prevent any star activity of *Eco*RI enzymes (Robinson and Sligar, 1993) and store at -20°C.

4.17 Plasmid isolation

The cloning vector pET28a+ vector was chosen for the cloning because it is high copy number plasmid (Mirkalantari *et al.,* 2012) and has high expression property under constitutive T7 promoter that does not require any inducer to express gene thus as a suitable vector. The target is stable as well as over production of the enzyme to enhance nanocellulose production in industrial application from the reduced carbon source obtained from CO_2 reduction by isolated bacteria would be facilitated with this constitutive expression promoter system. The rationale of this works was that If the vector with the respective gene would be constructed for cellulose synthesis genes then the *E. coli* harboring this plasmid could be co-culture with CO_2 reducing isolates or transformed into this CO_2 reducing isolates for the nano-cellulose production continuously proceeding simultaneous CO_2 reduction and conversion to reduced sugar

by CO_2 reducing isolated autotroph. Therefore, pET28a+ vector was extracted (Figure 44) from transformed DH5α *E. coli* provided from NAST using alkaline lysis method.

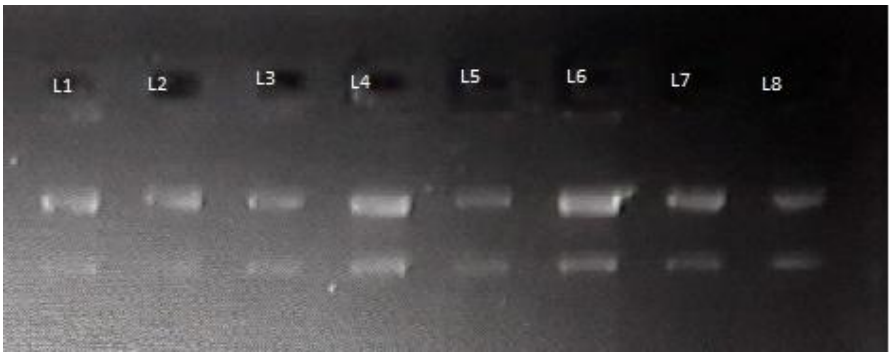

Figure (44): Gel electrophoresis band shown in all lane of isolated plasmid

4.17.1 Restriction digestion of vector

The expression vector pET28a+ was prepared for cloning of *bcs*A gene by two step double digestion with *Nde*I and *Eco*RI. Two step digestions were performed to avoid enzyme activity inhibition due to short distance restriction site of two enzymes in vector. It may also protect from star activity of enzyme *EcoR*I because enzyme *Eco*RI is fast digester as compared to enzyme *Nde*I. The digestion mixture was inactivated at 65℃.

4.18 DNA purification for ligation

The whole reaction mixture of digested vector and insert were subjected to gel electrophoresis in 1% agarose gel in order to obtain proper size of digested vector and insert without the small fragment of DNA that are released after the restriction digestion which otherwise could hinder during ligation. This can also help to be assuring that there is no re-ligation of vector because small bp cut size DNA fragment separate easily during gel electrophoresis due to its small size, move faster than large size insert or vector. After visualization, both bands were excised from gel separately and purified by low melting agarose gel extraction kit. Then 1/1µl of purified product was subjected to the 1% agarose gel for the empirical quantification of the insert and vector comparing with DNA band intensity of the DNA ladder to optimize the amount of DNA of both insert and vector required for efficient ligation.

4.19 Restriction Digestion of plasmid and insert

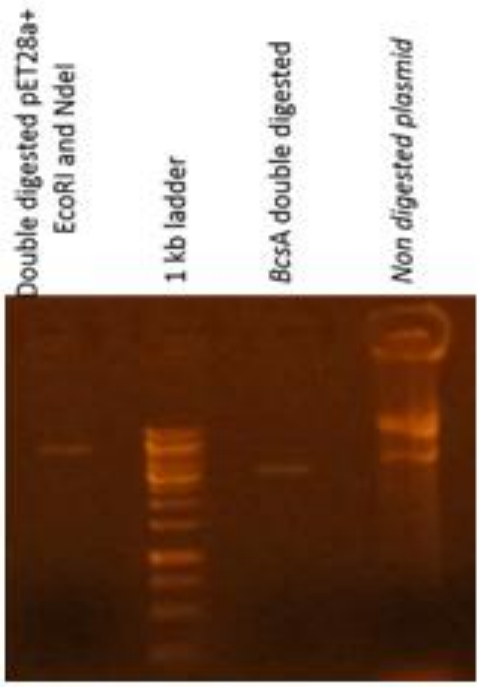

Figure (45): Gel electrophoresis of purified product of digested insert (2.6kb) and vector (5.3kb) with 1kb ladder.

4.20 Ligation and transformation

The ligation reaction was carried out with purified insert (*bcs*A) and vector (pET28a+) by using T4 DNA ligase enzyme. The ligation mixture contained approximately 3:1 molar ratio of insert and vector (the insert length of 2.6kb and vector length 5.3kb thus giving stoichiometric molar equilibrium of the respective DNA). The DNA ligase enzyme is found to have optimal activity at 25°C but overnight incubation was done at 16 °C to be assured about ligation. After ligation, the ligation mixture was used to transform freshly prepared competent *E. coli* DH5α cell by using heat shock method as described in method and methodology. The kanamycin resistant transformants that grew in LBA with kanamycin (100µg/ml) media plates were presumed to be *bcs*A sub-cloned transformants shown as this strain is sensitive to this antibiotic.

This result tentatively said that the isolated colonies which were able to grow on kanamycin antibiotic containing media plates are transformed cells with antibiotics resistant marker gene and the sub-cloning site does not interrupt this marker gene even upon cloning of insert into the vector. However, there could be only vector containing cells due to re-ligation of vector that was not completely digested by any one of the enzymes but specially *Nde*I that has poor digestion rate than the *Eco*RI as mentioned above. Therefore, some colonies were selected randomly for the further confirmation through restriction enzyme digestion map. After digestion, digested product and

inserted product was purified them using purification kit. Then upon ligation, transformation was done by following heat shock method.

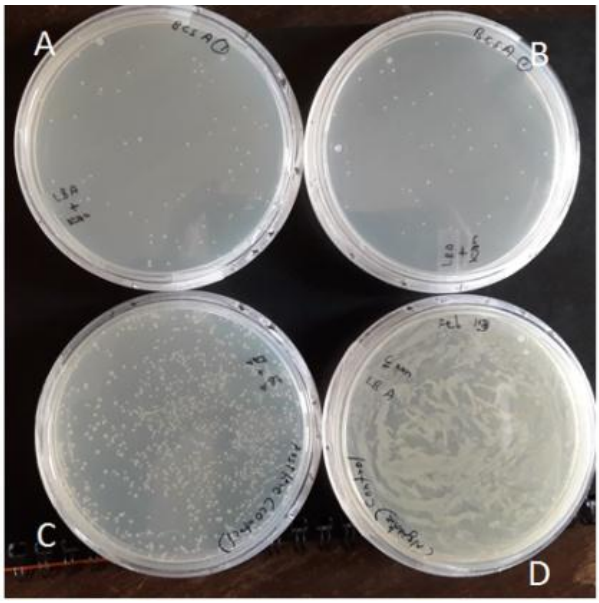

Figure (46): Transformed colonies of *E. coli* DH5α competent cells A and B are trasnformation of ligated *bcs*A and vector, C- positive control and D-viability test

4.21 Confirmation of transformants by restriction digestion map

For the confirmation of transformants, colonies were picked up from plates and cultured in LB with kanamycin and plasmid was extracted from each transformant. Then, plasmids were subjected to single restriction digestion with *EcoR*I. One of the plasmids (Figure 45) showed expected result with band size around 8kb that would be due to ligation of vector (5.396 kb) and insert (2.678kb).

After transformation, transformant was confirmed by single restriction digestion. The enzyme used in this method was *EcoR*I.

Figure (47): Single digested bands comparision with control

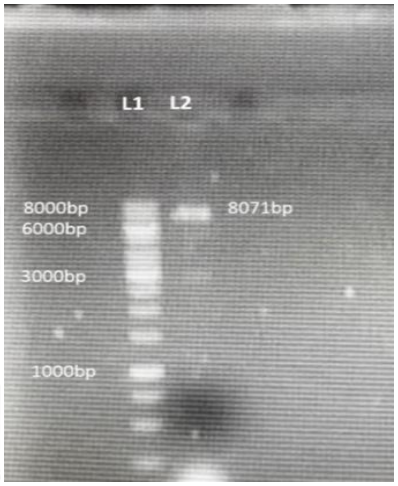

Figure (48): Transform plasmid digested with *Spe*I

One of the positive transformant of *bcs*A was further confirmed by using enzyme *Spe*I because restriction site of this enzyme was created in primer for the second clone. But the *adr*A transformant were showed negative result. This result indicates presence of clone (*bcs*A and Vector pET28a+) in DH5α *E. coli.* Thus, it is concluded that the protocol for the gene cloning was optimize. So it would be easier for the further cloning of other genes in respective vector as further biconstruct or engineering part. Furthermore, the plasmid showing band size around 8,000 kb was further validated by digesting the plasmid with enzyme *Spe*I because this restriction site is not present in the vector plasmid but was created in the reverse primer of *bcs*A gene thus creating recognition site if the insert has been cloned. Single band with size about 8 kb was observed under UV transilluminator indicating the gene of interest *bcs*A has been inserted into the pET28a+ vector and sub-cloned. In similar way, the gene *adr*A gene was also amplified and sub-cloned in the same vector. Further validation is required. The main purpose of this cloning is optimization of all the protocol including PCR amplification, restriction digestion, and ligation, transformation for the further cloning to make monocistronic and bi-construct for the development of new strain with ability to stably synthesize cellulose from atmospheric carbon dioxide. Additionally, role of single *bcs*A gene in cellulose synthesis could also be observed by culturing DH5α *E. coli* with pET28a+ and *bcs*A gene in the media with required composition. Thus, it can be concluded that the cloning strategy has been devised to over express genes for higher microbial nanocellulose production from reduced carbon source obtained from atmospheric carbon dioxide reduction.

RECOMMENDATION

- All respective four genes have to be cloned and transformed into *Azospirillum sps* for enhanced production of microbial cellulose.
- Produced putative cellulose has to be characterized as cellulose.
- Sustained alkaline reaction has to be done while preparing cobalt oxy hydroxide nano-particles in removing the impurities.

CHAPTER 5

SUMMARY

Diazotrophs bacteria are found in a wide variety of habitats with free living in soil and water and assist in managing the soil fertility and soil physical properties. Beneficial microbes as a biofertilizer have become very importance in agriculture sector for their potential role in food safety and sustainable crop production. In agriculture, soil fertilization on organic inputs to improve nutrient supply and conserve the field management. Nitrogen is fixed biologically by free-living and associative nitrogen fixers. Nitrogen fixing soil bacteria like *Azospirillum* are the impotant biofertilizer which encourages the plant growth. Members of the genus *Azospirillum* fix nitrogen under micro aerophillic conditions and frequently associated with root and rhizosphere, and thus termed as diazotrophs. This bacterium was isolated from soil sample, screened in specific medium; which was carbon and nitrogen free. The nitrogenase enzyme present in bacteria reduces the atmospheric nitrogen into the ammonia. The ammonia present in the media was estimated by the Nessler's regent.

The additional advantages of bio-fertilizers include longer shelf life causing no adverse effects to ecosystem and organic farming and food consumption helps all living things. Bio-fertilizers keep the soil environment rich in all kinds of micro and macronutrients through nitrogen fixation, release of plant growth regulating substances, production of antibiotics and biodegradation of organic matter in the soil. Bio-fertilizers can help solve the problem of feeding an increasing global population at a time when agriculture is facing various environmental stresses. The new technology developed using the powerful tool of molecular biotechnology can enhance the biological pathways of products.

Water and fixed nitrogen are the most common limiting factors for plant growth with that molecular hydrogen is a specific and competitive inhibitor of biological N_2 fixation and it is an essential component of life for all living beings. Nitrogen is an essential macronutrient for plant species. Ammonia is used in the synthesis of essential elements, which is a process known as biological nitrogen fixation. Symbiotic N_2 fixation is one of the biological processes important for development of sustainable agriculture by which the atmospheric N_2 is converted to ammonia with the aid of a key enzyme called nitrogenase. In this research we can found that the amount of ammonium fixed by nitrogen fixation bacteria and also calculate the amount of carbon with specific modified medium by doing Nessler's and anthrone test respectively. Rubisco is an important rate-limiting enzyme and key enzyme, its activity determines the overall rate of a metabolic pathway. In our experiment this mechanism follows the Calvin cycle in dark reaction under single and MFC chamber with co-culture growth. In photosynthetic bacteria, Rubisco is usually a dimer of proteins homologous. The light reactions result in the formation of the high energy compounds ATP and NADPH which are for the carbon

fixation. CO_2 was reduced to carbohydrate and test for the carbohydrate was done by anthrone test.

Mono and co culture of bacteria in the media showed better result in the media incubating with the putative *Geobacter* sps. *Geobacter* being the master regulator, produced the electron and proton itself in the media and was also enhanced by the Calvin cycle going on in the media. Electricity generated was measured and found increased with the increase in the incubation time of bacteria. Nano bio electrode cobalt nano-particle was used as a catalyst to enhance the reaction going on into the MFC and water splitting mechanism has been employed during this process.

Furthermore, the cellulose production has been uplifted by the genetic engineering mechanism by integrating the cellulose producing gene viz. *adrA*, *bcsA, pgm* and *galU* into the *E.coli* DH5 alpha strain using pET28a+ vector. In this research work only the monocistronic construct of *adrA* and *bcsA* were performed rather than the bicistronic because of time limitation and resources. This research emphasised on the easiest and rapid production of cellulose by the microorganisms in contrary to the plant based cellulose production; minimizing the global warming problem. In addition, these microorganisms were implemented as bio-fertilizer that has direct positive effect on the plant by various mechanisms.

CONCLUSION

Putative *Azospirillum sps* was isolated from the soil on the basis of carbon catabolite repression method. Isolates were able to fix atmospheric nitrogen and carbondioxide. Then these isolates were biochemically characterized and molecularly confirmed. Syntrophically cultured into different media with the regular measure of growth, electricity generated, carbon fixation and nitrogen reduction were done with measured different parameters. Cobalt nano-particle was chemically synthesized and characterized by XRD and FTIR. Additionally, water splitting mechanism was also performed by adding different carbon source with different buffer changed into it. The *bcs*A gene which is responsible for cellulose production was cloned into the expression vector pET28a+ and another *adr*A gene was also transformed into same vector.

REFERENCES

Alam, S., & Kumar Seth, R. (2012). Comparative study on effect of chemical and bio- fertilizer on growth, development and yield production of paddy crop (Oryza sativa). International Journal of Science and Research (IJSR), 3(9), 2319–7064.

Analysis, N. (2017). On the evolutionary origin of CAM photosynthesis. 49(0). https://doi.org/10.1104/pp.17.00195

Andersson, I. (2008). Catalysis and regulation in Rubisco. 59(7), 1555–1568. https://doi.org/10.1093/jxb/ern091

Andersson, I., & Backlund, A. (2008). Structure and function of Rubisco. 46. https://doi.org/10.1016/j.plaphy.2008.01.001

Anna, F. H. S., Almeida, L. G. P., Cecagno, R., Reolon, L. A., Siqueira, F. M., Machado, M. R. S., Vasconcelos, A. T. R., & Schrank, I. S. (2011). Genomic insights into the versatility of the plant growth-promoting bacterium *Azospirillum amazonense*.

Aiso, K., Takeuchi, R., Masaki, T., Chandra, D., Saito, K., Yui, T., & Yagi, M. (2017). Carbonate ions induce highly efficient electrocatalytic water oxidation by cobalt oxyhydroxide nanoparticles. ChemSusChem, 10(4), 687-692.

Arnon, D. I. (1959). Conversion of light into chemical energy in photosynthesis. Nature, 184(4679), 10-21.

Agbodjato, N. A., Amogou, O. E., Noumavo, P. A., Dagb&enonbakin, G., Salami, H. A., Karimou, R., ... & Baba-Moussa, L. S. (2018). Biofertilising, plant-stimulating and biocontrol potentials of maize plant growth promoting rhizobacteria isolated in central and northern Benin. African Journal of Microbiology Research, 12(28), 664-672.

Bankura, A., & Chandra, A. (2015). Proton transfer through hydrogen bonds in two-dimensional water layers: A theoretical study based on ab initio and quantum-classical simulations. Journal of Chemical Physics, 142(4), 0–13. https://doi.org/10.1063/1.4905495

Bar-even, A., Noor, E., Lewis, N. E., & Milo, R. (2010). Design and analysis of synthetic carbon fi xation pathways. 107(19). https://doi.org/10.1073/pnas.0907176107

Barton, L. L., Fardeau, M., & Fauque, G. D. (2020). Hydrogen Sulfide : A Toxic Gas Produced by Dissimilatory Sulfate and Sulfur Reduction and Consumed by Microbial Oxidation. https://doi.org/10.1007/978-94-017-9269-1

Basu, O., Mukhopadhyay, S., & Das, S. K. (2018). Cobalt based functional inorganic materials : Electrocatalytic.

Bathellier, C., Tcherkez, G., Lorimer, G. H., Farquhar, G. D., & Bathellier, C. (2014). Rubisco isn ’ t really so bad. https://doi.org/10.1111/pce.13149

Berg, I. A., Kockelkorn, D., Vera, W. H. R., Say, R. F., Zarzycki, J., Hügler, M., Alber, B. E., & Fuchs, G. (2010). Autotrophic carbon fixation in archaea. Nature Publishing Group, 8(6), 447–460. https://doi.org/10.1038/nrmicro2365

Borland, A. M., Hartwell, J., Weston, D. J., Schlauch, K. A., Tschaplinski, T. J., Tuskan, G. A., Yang, X., & Cushman, J. C. (2014). Engineering crassulacean acid metabolism to improve water-use efficiency. Trends in Plant Science, 19(5), 327–338. https://doi.org/10.1016/j.tplants.2014.01.006

Buchanan, B. B., & Arnon, D. I. (1990). A reverse KREBS cycle in photosynthesis : consensus at last. 47–53.

Blankenship, R. E. (2014). Molecular mechanisms of photosynthesis. John Wiley & Sons.

Bathellier, C., Tcherkez, G., Lorimer, G. H., & Farquhar, G. D. (2018). Rubisco is not really so bad. Plant, cell & environment, 41(4), 705-716.

Bräutigam, A., Schlüter, U., Eisenhut, M., & Gowik, U. (2017). On the evolutionary origin of CAM photosynthesis. Plant physiology, 174(2), 473-477.

Brett, C. T. (2000). Cellulose microfibrils in plants: biosynthesis, deposition, and integration into the cell wall.

Berg JM, Tymoczko JL, Stryer L. Biochemistry. 5th edition. New York: W H Freeman; 2002. Chapter 19, The Light Reactions of Photosynthesis. Available from: https://www.ncbi.nlm.nih.gov/books/NBK21191/

Carmo-silva, A. E., Keys, A. J., Andralojc, P. J., Powers, S. J., Arrabac, M. C., & Parry, M. A. J. (2010). Rubisco activities , properties , and regulation in three different C 4 grasses under drought. 61(9), 2355–2366. https://doi.org/10.1093/jxb/erq071

Choi, O., & Sang, B. I. (2016). Biotechnology for Biofuels Extracellular electron transfer from cathode to microbes : application for biofuel production. Biotechnology for Biofuels, 1–14. https://doi.org/10.1186/s13068-016-0426-0

Chouler, J., Bentley, I., Vaz, F., O’Fee, A., Cameron, P. J., & Di Lorenzo, M. (2017). Exploring the use of cost-effective membrane materials for Microbial Fuel Cell based sensors. Electrochimica Acta, 231, 319–326. https://doi.org/10.1016/j.electacta.2017.01.195

Chrispeels, M. J., & Maurel, C. (1994). Aquaporins : The Molecular Basis of Facilitated Water Movement Through Living Plant Cells ?’. 9–13.

Coico, R. (2005). Gram Staining BASIC PROTOCOL Commonly Used Techniques. Current Protocols in Microbiology, 3–4.

Colombo, M., Suorsa, M., Rossi, F., Ferrari, R., Tadini, L., Barbato, R., & Pesaresi, P. (2016). Photosynthesis control: An underrated short-term regulatory mechanism essential for plant viability. Plant Signaling and Behavior, 11(4).

Chen, Z., Dinh, H., & Miller, E. Photoelectrochemical Water Splitting: Standards, Experimental Methods, and Protocols, 2013.

Cousins, A. B., Mullendore, D. L., & Sonawane, B. V. (2020). Recent developments in mesophyll conductance in C3, C4, and crassulacean acid metabolism plants. The Plant Journal, 101(4), 816-830.

https://doi.org/10.1080/15592324.2016.1165382

Colon, B. C., Ziesack, M., & Silver, P. A. (2016). Water splitting-biosynthetic system with CO_2 reduction efficiencies exceeding photosynthesis.

https://doi.org/10.1126/science.aaf5039

Cosgrove, W. J., & Loucks, D. P. (2015). Water Resources Research. 4823–4839. https://doi.org/10.1002/2014WR016869.Received

Cox, N., Pantazis, D. A., Neese, F., Lubitz, W., Cox, N., & Lubitz, W. (2015). Artificial photosynthesis : understanding water splitting in nature. figure 1. https://doi.org/10.1126/science.1254910

Currao, A. (2007). Photoelectrochemical Water Splitting. 61(12), 815–819. https://doi.org/10.2533/chimia.2007.815

Dau, H., Limberg, C., Reier, T., Risch, M., & Roggan, S. (2010). The Mechanism of Water Oxidation : From Electrolysis via Homogeneous to Biological Catalysis. 724–761. https://doi.org/10.1002/cctc.201000126

Deng, Y. (2004). Hydration of Amino Acid Side Chains: Nonpolar and Electrostatic Contributions Calculated from Staged Molecular Dynamics Free Energy Simulations with Explicit Water Molecules. 17, 16567–16576.

Dolfing, J. (2013). Syntrophy in microbial fuel cells. 8(1), 4–5. https://doi.org/10.1038/ismej.2013.198

Chemical Biology, 16(3–4), 337–344. https://doi.org/10.1016/j.cbpa.2012.05.002

Danielsson, R., Albertsson, P. Å., Mamedov, F., & Styring, S. (2004). Quantification of photosystem I and II in different parts of the thylakoid membrane from spinach. Biochimica et Biophysica Acta (BBA)-Bioenergetics, 1608(1), 53-61.

Drennan, P. M., & Nobel, P. S. (1997). Frequencies of major C3, C4, and CAM perennials on different slopes in the northwestern Sonoran Desert. Flora, 192(3), 297-304.

Esa, F., Tasirin, S. M., & Abd Rahman, N. (2014). Overview of bacterial cellulose production and application. Agriculture and Agricultural Science Procedia, 2, 113-119.

Fabiano, E., & Cardona, A. (1985). Carbohydrate Catabolism in *Azospirillum*. 50(1), 183–185.

Fan, Y., Li, D., Deng, M., Luo, Y., & Meng, Q. (2015). An overview on water splitting photocatalysts. March. https://doi.org/10.1007/s11458-009-0100-1

Fnca, B., Project, B., Forum, G., & Cooperation, N. (2006). Biofertilizer Manual. https://doi.org/ISBN4-88911-301-0 C0550

Franks, A. E. (2015). Microbial electron transport and energy conservation – the foundation for optimizing bioelectrochemical systems. 6(June), 1–18.

https://doi.org/10.3389/fmicb.2015.00575

Frequencies, C., Drennan, P. M., & Nobel, P. S. (1997). Frequencies of major C3, C4, and CAM perennials on different slopes in the northwestern Sonoran Desert. Flora - Morphology - Geobotany - Ecophysiology, 192(3), 297–304.

https://doi.org/10.1016/S0367-2530(17)30795-8

Fukami, J., Cerezini, P., & Hungria, M. (2018). *Azospirillum*: benefits that go far beyond biological nitrogen fixation. AMB Express, 8(1), 1–12. https://doi.org/10.1186/s13568-018-0608-1

Fujita, Y., & Murakami, A. (1987). Regulation of electron transport composition in cyanobacterial photosynthetic system: stoichiometry among photosystem I and II complexes and their light-harvesting antennae and cytochrome b 6/f complex. Plant and cell physiology, 28(8), 1547-1553.

Geissler, P. L., Dellago, C., Chandler, D., Hutter, J., & Parrinello, M. (2001). Autoionization in liquid water. Science, 291(5511), 2121–2124. https://doi.org/10.1126/science.1056991

Gerken, J. B., Mcalpin, J. G., Chen, J. Y. C., Rigsby, M. L., Casey, W. H., Britt, R. D., & Stahl, S. S. (2011). Electrochemical Water Oxidation with Cobalt-Based Electrocatalysts from pH 0 À 14 : The Thermodynamic Basis for Catalyst Structure , Stability , and Activity. 14431–14442.

Gonçalves, A. Z., Latansio, S., Detmann, K. C., Marabesi, M. A., Neto, A. A. C., Aidar, M. P. M., Damatta, F. M., & Mercier, H. (2020). Plant Physiology and Biochemistry What does the RuBisCO activity tell us about a C 3 -CAM plant ? Plant Physiology and Biochemistry, 147(December 2019), 172–180. https://doi.org/10.1016/j.plaphy.2019.12.020

Gong, F., Cai, Z., & Li, Y. (2016). Synthetic biology for CO 2 fixation. 59(11), 1106–1114. https://doi.org/10.1007/s11427-016-0304-2

Guralnick, L. J., Cline, A., Smith, M., & Sage, R. F. (2008). Evolutionary physiology : the extent

of C 4 and CAM photosynthesis in the genera Anacampseros and Grahamia of the Portulacaceae. 59(7), 1735–1742. https://doi.org/10.1093/jxb/ern081

Gong, F., Cai, Z., & Li, Y. (2016). Synthetic biology for CO 2 fixation. Science China Life Sciences, 59(11), 1106-1114.

Gao, X., Wen, Y., Qu, D., An, L., Luan, S., Jiang, W., ... & Sun, Z. (2018). Interference effect of alcohol on Nessler's reagent in photocatalytic nitrogen fixation. ACS Sustainable Chemistry & Engineering, 6(4), 5342-5348.

Ha, P. T., Lindemann, S. R., Shi, L., Dohnalkova, A. C., Fredrickson, J. K., Madigan, M. T., & Beyenal, H. (2017). interspecies electron transfer. Nature Communications, 8, 1–7. https://doi.org/10.1038/ncomms13924

Hallberg, K. B., Gonza, E., & Johnson, D. B. (2010). Acidithiobacillus ferrivorans , sp . nov .; facultatively anaerobic , psychrotolerant iron- , and sulfur-oxidizing acidophiles isolated from metal mine-impacted environments. 9–19. https://doi.org/10.1007/s00792-009-0282-y

Hartmann, A., & Burris, R. H. (1987). Regulation of nitrogenase activity by oxygen in *Azospirillum* brasilense and *Azospirillum* lipoferum. Journal of Bacteriology, 169(3), 944–948. https://doi.org/10.1128/jb.169.3.944-948.1987

Heidary, N., Harris, T. G. A. A., Ly, K. H., & Kornienko, N. (2019). Artificial photosynthesis with metal and covalent organic frameworks (MOFs and COFs): challenges and prospects in fuel-forming electrocatalysis. Physiologia Plantarum, 166(1), 460–471. https://doi.org/10.1111/ppl.12935

Henderson, M. A., Box, P. O., & K-, M. (2008). II . K . 10 Fundamental Investigations of Water Splitting on Model TiO 2 Photocatalysts Doped for Visible Light Absorption. 303–305.

Hermida-carrera, C., Fares, M. A., Font-carrascosa, M., Kapralov, M. V, Koch, M. A., Mir, A., Molins, A., Ribas-carbó, M., Rocha, J., & Galmés, J. (2020). Exploring molecular evolution of Rubisco in C 3 and CAM Orchidaceae and Bromeliaceae. 8, 1–17.

Ho, B. M., Lukoyanov, D., Yang, Z., Dean, D. R., & Seefeldt, L. C. (2014a). Mechanism of Nitrogen Fixation by Nitrogenase : The Next Stage.

Ho, B. M., Lukoyanov, D., Yang, Z., Dean, D. R., & Seefeldt, L. C. (2014b). Mechanism of Nitrogen Fixation by Nitrogenase : The Next Stage. https://doi.org/10.1021/cr400641x

Huber, H., Gallenberger, M., Jahn, U., Eylert, E., Berg, I. A., Kockelkorn, D., Eisenreich, W., & Fuchs, G. (2008). A dicarboxylate / 4-hydroxybutyrate autotrophic carbon assimilation cycle in the hyperthermophilic Archaeum Ignicoccus hospitalis. 105(22), 7851–7856.

https://www.zmescience.com/science/what-is-photon-definition-

04322/https://www.sciencedirect.com/topics/physics-and-astronomy/photon-absorption

http://www.bbc.com/earth/story/20150701-the-origin-of-the-air-we-breathe

HW, H. (2005). Photosynthesis is an electron transport process. Plant Biochemistry.(Eds.: Hans-Walter Heldt in cooperation with Fiona Heldt) Elsevier. San Diego, USA. p, 67-114.

https://www.universetoday.com/65588/what-percent-of-earth-is-water/

Ishii, M. M. (2004). Occurrence , biochemistry and possible biotechnological application of the 3-hydroxypropionate cycle. 605–610. https://doi.org/10.1007/s00253-003-1540-z

Iñiguez, C., Capó-Bauçà, S., Niinemets, Ü., Stoll, H., Aguiló-Nicolau, P., & Galmés, J. (2020). Evolutionary trends in Rubisco kinetics and their co-evolution with CO_2 concentrating mechanisms. The Plant Journal, 101(4), 897-918.

Jagadale, A. D., Dubal, D. P., & Lokhande, C. D. (2012). Electrochemical behavior of potentiodynamically deposited cobalt oxyhydroxide (CoOOH) thin films for supercapacitor application. Materials Research Bulletin, 47(3), 672–676. https://doi.org/10.1016/j.materresbull.2011.12.029

Journal, I. (2014). Evolution of CAM and C4 Carbon - Concentrating Mechanisms Author (s): Jon E . Keeley and Philip W . Rundel Source : International Journal of Plant Sciences , Vol . 164 , No . S3 , Evolution of Functional Traits in Plants (May 2003), pp . S55-S77 Publi. 164(May 2003).

K, S. (2015). Biotechnological Aspects of Microbial Extracellular Electron Transfer. 30(2), 133–139. https://doi.org/10.1264/jsme2.ME15028

Kahraman, H., & Geckil, H. (2005). Degradation of benzene, toluene and xylene by Pseudomonas aeruginosa engineered with the Vitreoscilla hemoglobin gene. Engineering in Life Sciences, 5(4), 363–368. https://doi.org/10.1002/elsc.200520088

Kanan, M. W., & Nocera, D. G. (2012). In Situ Formation of an Water Containing Phosphate and Co 2 +. 1072(2008). https://doi.org/10.1126/science.1162018

Kerfeld, C. A., Heinhorst, S., & Cannon, G. C. (2010). Bacterial Microcompartments. https://doi.org/10.1146/annurev.micro.112408.134211

Khaloufi, Y. El. (2019). MICROBIAL FUEL CELLS FOR ELECTRICITY GENERATION. April.

Kim, B. W., Chang, H. N., Kim, I. K., & Leet, K. S. (1992). Growth Kinetics of the Photosynthetic. 40, 583–592.

Kleinsteuber, S. (2015). Microbial interspecies interactions : recent findings in syntrophic consortia. 6(May), 1–8. https://doi.org/10.3389/fmicb.2015.00477

Krapp, A., Quick, W. P., & Stitt, M. (1991). other Calvin-cycle enzymes , and chlorophyll decrease when glucose is supplied to mature spinach leaves via the transpiration stream. 58–69.

Kwak, Y., & Shin, J. (2015). Marine Genomics First *Azospirillum* genome from aquatic environments : Whole-genome sequence of *Azospirillum* thiophilum BV-S T , a novel diazotroph harboring a capacity of sulfur-chemolithotrophy from a sul fi de spring. Marine Genomics, 1–4. https://doi.org/10.1016/j.margen.2015.11.001

Karnaukhov I. (1965). O mekhanizme biologicheskoĭ fiksatsii molekuliarnogo azota [On the mechanism of the biological fixation of molecular nitrogen]. Izvestiia Akademii nauk SSSR. Seriia biologicheskaia, 5, 714–730.

Kinney, J. N., Axen, S. D., & Kerfeld, C. A. (2011). Comparative analysis of carboxysome shell proteins. Photosynthesis Research, 109(1-3), 21-32.

Keeley, J. E., & Rundel, P. W. (2003). Evolution of CAM and C4 carbon-concentrating mechanisms. International Journal of Plant Sciences, 164(S3), S55-S77.

Kazarian, A., Dadson, A. E., Paull, B., Nesterenko, P. N., & Linford, M. R. (2015). A1. 1. Auto-Ionization of Water. Chuan-Hsi Hung, 2015, 134.

Kato, S. (2015). Biotechnological aspects of microbial extracellular electron transfer. Microbes and environments, ME15028.

Latner, A. L. (1970). Principles of Biochemistry. In Bmj (Vol. 4, Issue 5733). https://doi.org/10.1136/bmj.4.5733.481-a

Lawson, T., & Vialet-Chabrand, S. (2019). Speedy stomata, photosynthesis and plant water use efficiency. New Phytologist, 221(1), 93–98. https://doi.org/10.1111/nph.15330

Lei, L. (1983). Stomatal mechanism as the basis of the evolution of CAM and C4 photosynthesis. 275–279.

Lentz, J., & Garofalini, S. H. (2018). Structural aspects of the topological model of the hydrogen bond in water on auto-dissociation: Via proton transfer. Physical Chemistry Chemical Physics, 20(24), 16414–16427. https://doi.org/10.1039/c8cp02592d

Lodish, H., Berk, A., Zipursky, S. L., Matsudaira, P., Baltimore, D., & Darnell, J. (2000).

Lenton, R., Lewis, K., & Wright, A. M. (2008). Water, sanitation and the millennium development goals. Journal of International affairs, 247-258.

Lounis, B., & Orrit, M. (2005). Single-photon sources. Reports on Progress in Physics, 68(5), 1129.

Lodish, H., & Zipursky, S. L. (2001). Molecular cell biology. Biochem Mol Biol Educ, 29, 126-133.

Lodish, H., Berk, A., Kaiser, C. A., Krieger, M., Scott, M. P., Bretscher, A., ... & Matsudaira, P. (2008). Molecular cell biology. Macmillan.

Levine, V. E. (1930). A General Test for Carbohydrates. Proceedings of the Society for Experimental Biology and Medicine, 27(8), 830-831.

Lüning, B., Wiklund, B., Redelius, P., & Björklund, B. (1980). Biochemical properties of tissue polypeptide antigen. Biochimica et Biophysica Acta (BBA)-Protein Structure, 624(1), 90-101.

Makino, A., Miyake, C., & Yokota, A. (2002). Physiological Functions of the Water – Water Cycle (Mehler Reaction) and the Cyclic Electron Flow around PSI in Rice Leaves. 43(9), 1017–1026.

Marais, A., Sinayskiy, I., Petruccione, F., & Van Grondelle, R. (2015). A quantum protective mechanism in photosynthesis. Scientific Reports, 5, 1–8.

https://doi.org/10.1038/srep08720

Matassa, S., Boon, N., & Verstraete, W. (2015). Resource recovery from used water: The manufacturing abilities of hydrogen-oxidizing bacteria. Water Research, 68, 467–478. https://doi.org/10.1016/j.watres.2014.10.028

Mcevoy, James P, Gascon, J. A., Batista, V. S., & Brudvig, G. W. (2006). The mechanism of photosynthetic water splitting †. 940–949.

Mcevoy, James Philip, Holloway, R., & Batista, V. (2006). The mechanism of photosynthetic water splitting. January. https://doi.org/10.1039/b506755c

McNamara, J. T., Morgan, J. L. W., & Zimmer, J. (2015). A Molecular Description of Cellulose Biosynthesis. Annual Review of Biochemistry, 84(1), 895–921. https://doi.org/10.1146/annurev-biochem-060614-033930

Mechanism, T. H. E., & Biological, O. F. (1941). appreciated difficulty. 41–73.

Microbiology, F., & Advance, E. (2016). FEMS Microbiology Ecology Advance Access published September 21, 2016.

Miyake, C. (2010). Alternative Electron Flows (Water – Water Cycle and Cyclic Electron Flow Around PSI) in Photosynthesis : Molecular. 51(12), 1951–1963.

https://doi.org/10.1093/pcp/pcq173

Montgomery, B. L., Lechno-Yossef, S., & Kerfeld, C. A. (2016). Interrelated modules in cyanobacterial photosynthesis: The carbon-concentrating mechanism, photorespiration,

and light perception. Journal of Experimental Botany, 67(10), 2931–2940. https://doi.org/10.1093/jxb/erw162

Moqadam, M., Lervik, A., Riccardi, E., Venkatraman, V., Alsberg, B. K., & Van Erp, T. S. (2018). Local initiation conditions for water autoionization. Proceedings of the National Academy of Sciences of the United States of America, 115(20), E4569–E4576. https://doi.org/10.1073/pnas.1714070115

Morris, B. E. L., Henneberger, R., Huber, H., Moissl-eichinger, C., & Dynamics, P. (2013). Microbial syntrophy: interaction for the common good. https://doi.org/10.1111/1574-6976.12019

Mueller-Cajar, O. (2017). The diverse AAA+ machines that repair inhibited Rubisco active sites. Frontiers in molecular biosciences, 4, 31.

Molecular analysis of photosystems. In Molecular Cell Biology. 4th edition. WH Freeman.

Youvan, D. C., & Marrs, B. L. (1987). Molecular mechanisms of photosynthesis. Scientific American, 256(6), 42-49.

Naher, U. A., Othman, R., & Latif, M. A. (2013). Biomolecular Characterization of Diazotrophs Isolated from the Tropical Soil in Malaysia. 17812–17829. https://doi.org/10.3390/ijms140917812

Nawrocki, W. J., Bailleul, B., Picot, D., Cardol, P., Rappaport, F., Wollman, F., & Joliot, P. (2019). BBA - Bioenergetics The mechanism of cyclic electron fl ow. 1860(August 2018), 433–438. https://doi.org/10.1016/j.bbabio.2018.12.005

Neupane, D., Pandey, A., Pandey, A., Shreevastava, N., & Neupane, D. (2015). Qualitative Tests for Carbohydrates. Biochemistry Laboratory Manual, 11–11. https://doi.org/10.5005/jp/books/12493_4

Nevin, K. P., Woodard, T. L., & Franks, A. E. (2010). Microbial Electrosynthesis : Feeding Microbial Electrosynthesis : Feeding Microbes Electricity To Convert Carbon Dioxide and Water to Multicarbon Extracellular Organic. https://doi.org/10.1128/mBio.00103-10.Editor

New, A., Reduction, C., In, C., Bacterium, A. P., Evans, B. Y. M. C. W., & Buchanan, B. O. B. B. (1966). trophic cells. 928–934.

Ni, M., Ã, M. K. H. L., Leung, D. Y. C., & Sumathy, K. (2007). A review and recent developments in photocatalytic water-splitting using TiO 2 for hydrogen production. 11, 401–425. https://doi.org/10.1016/j.rser.2005.01.009

Nelson, N., & Yocum, C. F. (2006). Structure and function of photosystems I and II. Annu. Rev. Plant Biol., 57, 521-565.

Nishino, T., & Peijs, T. (2014). All-cellulose composites. In HANDBOOK OF GREEN MATERIALS: 2 Bionanocomposites: processing, characterization and properties (pp. 201-216).

Nevell, T. P., & Zeronian, S. H. (1985). Cellulose chemistry and its applications.

Oh, S., Min, B., & Logan, B. E. (2004). Cathode performance as a factor in electricity generation in microbial fuel cells. Environmental Science and Technology, 38(18), 4900–4904. https://doi.org/10.1021/es049422p

Orr, L. (2007). Photosynthesis and the Web: 2008. Photosynthesis Research, 91(2-3), 107-131.

Orlova, M. V., Tarlachkov, S. V., Dubinina, G. A., Belousova, E. V., Tutukina, M. N., & Grabovich, M. Y. (2016). Genomic insights into metabolic versatility of a lithotrophic sulfur-oxidizing diazotrophic Alphaproteobacterium *Azospirillum* thiophilum. FEMS microbiology ecology, 92(12), fiw199.

Onyeze, R. C., Onah, G. T., & Igbonekwu, C. C. (2013). Isolation and characterization of nitrogen-fixing bacteria in the soil. International Journal of Life Sciences Biotechnology and Pharma Research, 2(3), 438-445.

Pate, J. (2001). Chapter 2 Carbon Isotope Discrimination and Plant Water-Use Efficiency. 19–36.

Perdomo, J. A., Capó-bauçà, S., Carmo-silva, E., & Galmés, J. (2017). Rubisco and Rubisco Activase Play an Important Role in the Biochemical Limitations of Photosynthesis in Rice , Wheat , and Maize under High Temperature and Water Deficit. 8(April), 1–15. https://doi.org/10.3389/fpls.2017.00490

Pinto, H., Sharwood, R. E., Tissue, D. T., & Ghannoum, O. (2014). Photosynthesis of C 3 , C 3 – C 4 , and C 4 grasses at glacial CO 2. 65(13), 3669–3681.

https://doi.org/10.1093/jxb/eru155

Pohlmann, A., Fricke, W. F., Reinecke, F., Kusian, B., Liesegang, H., Cramm, R., Eitinger, T., Ewering, C., Pötter, M., Schwartz, E., Strittmatter, A., Voß, I., Gottschalk, G., Steinbüchel, A., Friedrich, B., & Bowien, B. (2006). Genome sequence of the bioplastic-producing “Knallgas” bacterium Ralstonia eutropha H16. Nature Biotechnology, 24(10), 1257–1262. https://doi.org/10.1038/nbt1244

Pederson, T. (1986). Molecular cell biology: By J. Darnell, H. Lodish, and D. Baltimore. New York: WH Freeman and Company.(1986). 1187 pp. $42.95.

Panitchayangkoon, G., Voronine, D. V., Abramavicius, D., Caram, J. R., Lewis, N. H., Mukamel, S., & Engel, G. S. (2011). Direct evidence of quantum transport in photosynthetic light-harvesting complexes. Proceedings of the National Academy of Sciences, 108(52), 20908-20912.

Pate, J. S. (2001). Carbon isotope discrimination and plant water-use efficiency. In Stable isotope techniques in the study of biological processes and functioning of ecosystems (pp. 19-36). Springer, Dordrecht.

Pohorille, A., & Pratt, L. R. (2012). Is water the universal solvent for life?. Origins of Life and Evolution of Biospheres, 42(5), 405-409.

Pang, M., Huang, Y., Meng, F., Zhuang, Y., Liu, H., Du, M., ... & Cai, T. (2020). Application of bacterial cellulose in skin and bone tissue engineering. European Polymer Journal, 122, 109365.

Rabaey, K., & Rozendal, R. A. (2010). Microbial electrosynthesis — revisiting the electrical route for microbial production. 8. https://doi.org/10.1038/nrmicro2422

Rajaambal, S., Sivaranjani, K., & Gopinath, C. S. (2015). Recent developments in solar H 2 generation from water splitting. 127(1), 33–47. https://doi.org/10.1007/s12039-014-0747-0

Rajasekaran, S., Sundaramoorthy, P., & Ganesh, K. S. (2015). Effect of FYM, N, P Fertilizers and Biofertilizers on Germination and Growth of Paddy (Oryza sativa. L). International Lettersof Natural Sciences, 35, 59–65.

https://doi.org/10.18052/www.scipress.com/ilns.35.59

Robson, B. R. L. (1979). Characterization of an Oxygen-Stable Nitrogenase Complex Isolated from Azotobacter chroococcum. 569–575.

Römling, U., & Galperin, M. Y. (2015). Bacterial cellulose biosynthesis: Diversity of operons, subunits, products, and functions. Trends in Microbiology, 23(9), 545–557. https://doi.org/10.1016/j.tim.2015.05.005

Rosenbaum, M., Aulenta, F., Villano, M., & Angenent, L. T. (2011). Bioresource Technology Cathodes as electron donors for microbial metabolism : Which extracellular electron transfer mechanisms are involved ? Bioresource Technology, 102(1), 324–333. https://doi.org/10.1016/j.biortech.2010.07.008

Rosiak, J. M. (1999). Hydrogels and their medical applications. 151, 56–64.

Rubisco, C., Atpase, A. A. A., Tsai, Y. C., Ye, F., Liew, L., Liu, D., Bhushan, S., & Gao, Y. (2019). Insights into the mechanism and regulation of the. 1–7. https://doi.org/10.1073/pnas.1911123117

Ross, P., Mayer, R., & Benziman, M. (1991). Cellulose biosynthesis and function in bacteria. Microbiology and Molecular Biology Reviews, 55(1), 35-58.

Sack, L. (2012). Evolution of C 4 plants : a new hypothesis for an interaction of CO 2 and water relations mediated by plant hydraulics.583–600. https://doi.org/10.1098/rstb.2011.0261

Salas, S. E. (2013). Scholarship @ Western Photocatalytic Water Splitting using a Modified Pt-TiO2 . Kinetic Modeling and Hydrogen Production Efficiency Salvador Escobedo Salas.

Santoyo, G., Moreno-hagelsieb, G., Orozco-mosqueda, C., & Glick, B. R. (2016). Plant growth-promoting bacterial endophytes. Microbiological Research, 183, 92–99. https://doi.org/10.1016/j.micres.2015.11.008

Schaetzle, O. (2008). Bacteria and yeasts as catalysts in microbial fuel cells : electron transfer from micro-organisms to electrodes for green electricity. 607–620. https://doi.org/10.1039/b810642h

http://montessorimuddle.org/2013/10/23/testing-for-sugars-and-starch/

Seager, S. L., & Slabaugh, Michael R, Boudreaux, K. A. (2005). Carbohydrates and Biochemistry.

Sello, S., Meneghesso, A., Alboresi, A., Baldan, B., & Morosinotto, T. (2019). Plant biodiversity and regulation of photosynthesis in the natural environment. Planta, 249(4), 1217–1228. https://doi.org/10.1007/s00425-018-03077-z

Sharwood, R. E., Ghannoum, O., & Whitney, S. M. (2016). ScienceDirect Prospects for improving CO 2 fixation in C 3 -crops through understanding C 4 -Rubisco biogenesis and catalytic diversity. Current Opinion in Plant Biology, 31, 135–142. https://doi.org/10.1016/j.pbi.2016.04.002

Shi, F., Ashby, R., & Gross, R. A. (1996). Use of poly(ethylene glycol)s to regulate poly(3-hydroxybutyrate) molecular weight during Alcaligenes eutrophus cultivations. Macromolecules, 29(24), 7753–7758. https://doi.org/10.1021/ma960805k

Slesak, I., & Slesak, H. (2017). RubisCO Early Oxygenase Activity : A Kinetic and Evolutionary Perspective. 1700071, 1–8. https://doi.org/10.1002/bies.201700071

Son, D. N., & Kasai, H. (2009). Proton transport through aqueous Nafion membrane. European Physical Journal E, 29(4), 351–361. https://doi.org/10.1140/epje/i2009-10500-1

Stal,L.J.(2015).Cyanobacteria. 1–9. https://doi.org/10.1002/9780470015902.a0021159.pub2

Steenhoudt, O., & Vanderleyden, J. (2000). *Azospirillum*, a free-living nitrogen-fixing bacterium closely associated with grasses: Genetic, biochemical and ecological aspects. FEMS Microbiology Reviews, 24(4), 487–506. https://doi.org/10.1016/S0168-6445(00)00036-X

Stikker, A. (1998). WATER TODAY AND. 30(1), 43–62.

Sukhov, V. (2016). Electrical signals as mechanism of photosynthesis regulation in plants. Photosynthesis Research, 130(1–3), 373–387. https://doi.org/10.1007/s11120-016-

0270-x

Spreitzer, R. J., & Salvucci, M. E. (2002). Rubisco: structure, regulatory interactions, and possibilities for a better enzyme. Annual review of plant biology, 53.

Simoni, R. D., Hill, R. L., & Vaughan, M. (2002). Benedict's solution, a reagent for measuring reducing sugars: the clinical chemistry of stanley R. Benedict. Journal of Biological Chemistry, 277(16), e5-e5.

Tabita, F. R., Hanson, T. E., Li, H., Satagopan, S., Singh, J., & Chan, S. (2007). Function , Structure , and Evolution of the RubisCO-Like Proteins and Their RubisCO Homologs †. 71(4), 576–599. https://doi.org/10.1128/MMBR.00015-07

Takeuchi, R., Masaki, T., Saito, K., Yui, T., & Yagi, M. (n.d.). Carbonate ions induce highly performed electrocatalytic water oxidation by. https://doi.org/10.1002/cssc.201601494

Tayeb, A. H., Amini, E., Ghasemi, S., & Tajvidi, M. (2018). Cellulose nanomaterials-binding properties and applications: A review. Molecules, 23(10), 1–24. https://doi.org/10.3390/molecules23102684

Tomimatsu, H., & Tang, Y. (2016). Effects of high CO_2 levels on dynamic photosynthesis: carbon gain, mechanisms, and environmental interactions. Journal of Plant Research, 129(3), 365–377. https://doi.org/10.1007/s10265-016-0817-0

Transport, R. I. (2018). Transport of water and urea in red blood cells. 246.

Tremblay, P., & Zhang, T. (2015). Electrifying microbes for the production of chemicals. 6(March), 1–10. https://doi.org/10.3389/fmicb.2015.00201

Uddin, N., Kim, J., Sung, B. J., Choi, T. H., Choi, C. H., & Kang, H. (2014). Comparative proton transfer efficiencies of hydronium and hydroxide in aqueous solution: Proton transfer vs Brownian motion. Journal of Physical Chemistry B, 118(47), 13671–13678. https://doi.org/10.1021/jp5093114

Uma Vanitha, M., Natarajan, M., Sridhar, H., & Umamaheswari, S. (2017). Microbial fuel cell characterisation and evaluation of Lysinibacillus macroides MFC02 electrigenic capability. World Journal of Microbiology and Biotechnology, 33(5), 1–9. https://doi.org/10.1007/s11274-017-2252-3

Volkers, R. J. M., Snoek, L. B., Ruijssenaars, H. J., & De Winde, J. H. (2015). Dynamic response of pseudomonas putida S12 to sudden addition of toluene and the potential role of the solvent tolerance gene trig. PLoS ONE, 10(7), 1–17. https://doi.org/10.1371/journal.pone.0132416

Wang, J., Cui, W., Liu, Q., Xing, Z., Asiri, A. M., & Sun, X. (2016). Recent Progress in Cobalt-Based Heterogeneous Catalysts for Electrochemical Water Splitting. 215–230.

https://doi.org/10.1002/adma.201502696

Widdel, F. (1987). Microbiolngy. 286–291.

Worsey, M. J., & Williams, A. P. (1975). Metablism of toluene and xylenes by Pseudomonas putida (arvilla) mt 2: evidence for a new function of the TOL plasmid. Journal of Bacteriology, 124(1), 7–13. https://doi.org/10.1128/jb.124.1.7-13.1975

William F Martin, Donald A Bryant, J Thomas Beatty, A physiological perspective on the origin and evolution of photosynthesis, FEMS Microbiology Reviews, Volume 42, Issue 2, March 2018, Pages 205–231, https://doi.org/10.1093/femsre/fux056

Wyss, O., & Wilson, P. W. (1941). Mechanism of Biological Nitrogen Fixation: VI. Inhibition of Azotobacter by Hydrogen. Proceedings of the National Academy of Sciences of the United States of America, 27(3), 162.

Young, L. Y. (1995). Degradation of Monochlorinated and Nonchlorinated Aromatic Compounds under Iron-Reducing Conditions Degradation of Monochlorinated and Nonchlorinated Aromatic Compounds under Iron-Reducing Conditions. June 2014. https://doi.org/10.1128/AEM.61.11.4069-4073.1995

Yuan, H., Ge, T., Chen, C., Anthony, G., Donnell, O., & Wu, J. (2012). the Sequestration of Soil Carbon Significant Role for Microbial Autotrophy in the Sequestration of. 78(7). https://doi.org/10.1128/AEM.06881-11

Yang, J., Liu, H., Martens, W. N., & Frost, R. L. (2010). Synthesis and characterization of cobalt hydroxide, cobalt oxyhydroxide, and cobalt oxide nanodiscs. The Journal of Physical Chemistry C, 114(1), 111-119.

Yang, S., Sun, L., An, X., & Qian, X. (2020). Construction of flexible electrodes based on ternary polypyrrole@ cobalt oxyhydroxide/cellulose fiber composite for supercapacitor. Carbohydrate polymers, 229, 115455.

Zanardini, E., May, E., Purdy, K. J., Murrell, J. C., Technology, H., & Campus, G. H. (n.d.). This article is protected by copyright. All rights reserved. https://doi.org/10.1111/1758-2229.12707

Zhong, D. K., & Gamelin, D. R. (2010). Photoelectrochemical Water Oxidation by Cobalt Catalyst (“ Co - Pi ”)/ r -Fe 2 O 3 Composite Photoanodes : Oxygen Evolution and Resolution of a Kinetic Bottleneck. 15, 4202–4207.

Ladd, M. F. C., Palmer, R. A., & Palmer, R. A. (1985). Structure determination by X-ray crystallography (p. 71). New York: Plenum Press.

APPENDICES

Appendix I

Composition of Luria Bertani Broth, Miller (LB):

Ingredients	gm/l
Casein enzymic hydrolysate	10.00
Yeast extract	5.00
Sodium chloride	10.00
p^H at 25^oc	7.5 +0.2
Total	1000ml

Vitamin mixture composition

Ingredients	mg/l
Biotin	2
Folic acid	2
Pyridoxine	5
Thiamine	5
Nicotonic acid	5
Pantothenic acid	5
Vitamin B12	0.1
P-amino benzoic acid	5
Total	1000ml

Mineral mixture composition

Ingredients	g/l
Manganese sulphate	0.5
Magnesium sulphate	3
Sodium chloride	1
Ferrous sulphate	0.1
Calcium chloride	0.1
Cobalt chloride	0.1
Zinc chloride	0.13
Aluminium Potassium sulpahate	0.01
Boric acid	0.01
Sodium molybdate	0.025
Total	1000ml

Modified Nfb media composition

Ingredients	gm/l
Sodium carbonate (Na_2CO_3)	3.953
Di-potassium hydrogen phosphate (K_2HPO_4)	0.5
Magnesium sulphate ($MgSO_4.7H_2O$)	0.2
Sodium chloride (NaCl)	0.1
Calcium Chloride ($CaCl_2.H_2O$)	0.02
Ferrous sulphate ($FeSO_4$)	0.05
Bromothymol Blue (0.5% in 2N KOH)	2 ml
Micronutrient solution	2 ml
Vitamin mix	1 ml
Total	1000 ml
P^H	6.8

Modified Nfb media with added cobalt nanoparticle

Ingredients	g/l
Sodium carbonate (Na_2CO_3)	5.3
Cobalt nano particle (CoOOH)	1.838
Di-potassium hydrogen phosphate (K_2HPO_4)	0.5
Magnesium sulphate ($MgSO_4.7H_2O$)	0.2
Sodium chloride (NaCl)	0.1
Calcium Chloride ($CaCl_2.H_2O$)	0.02
Ferrous sulphate ($FeSO_4$)	0.05
2N KOH	2 ml

Micronutrient solution	2 ml
Vitamin mix	1 ml
Total	1000 ml
P^H	6.8

Composition of modified GS media:

Ingredients	gm/l
Potassium dihydrogen phosphate (kH_2PO_4)	1.5
Potassium hydrogen phosphate (k_2HPO_4)	0.3
Nacl	0.1
Mineral mix	10 ml
Vitamin mix	10 ml
Potassium carbonate (K_2CO_3) (30 mM)	4.15
Total	1000 ml
pH	6.8

Composition of Nitrogen Carbon free (NCF) media:

Ingredients	gm/l
Potassium hydrogen phosphate (k_2HPO_4)	0.5
Magnesium sulphate ($MgSO_4.7H_2O$)	0.2
Nacl	0.1
Calcium chloride ($CaCl_2.H_2O$)	0.02
Ferrous sulphate ($FeSO_4$)	0.005

Micronutrient	2 ml
Total	1000 ml
pH	6.8

Appendix II

Created with

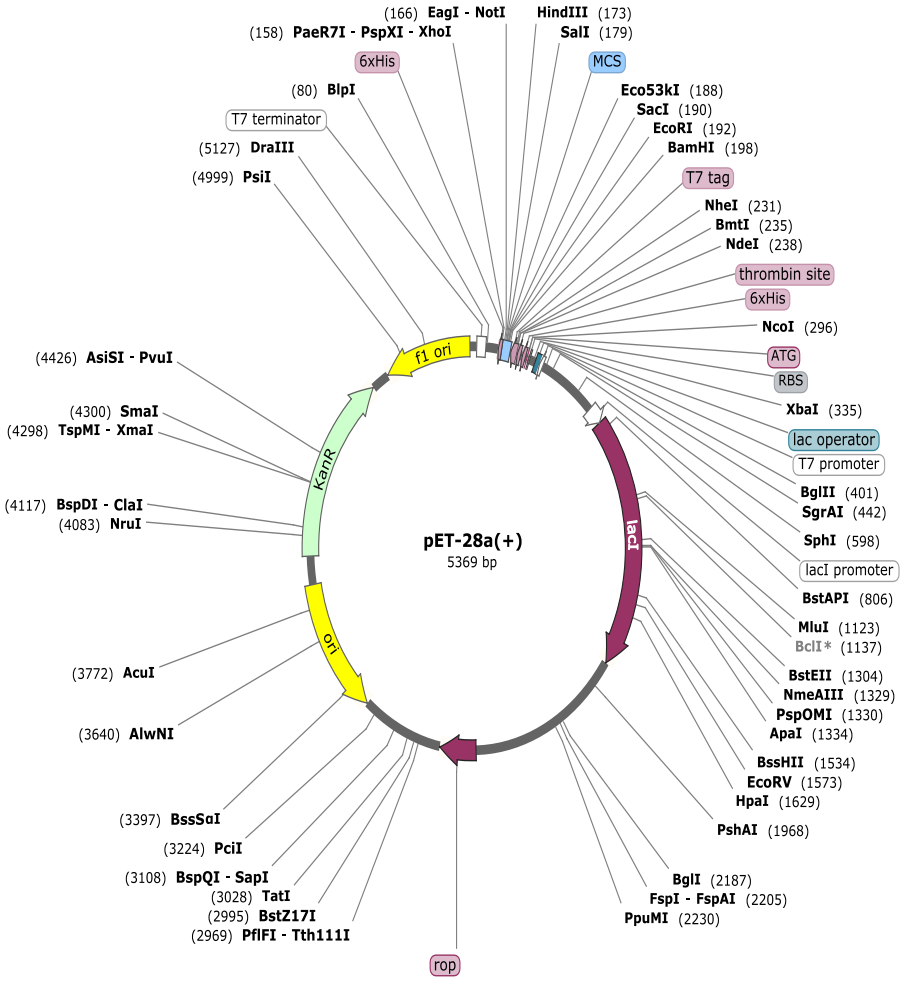

Figure (49): Vector (pET28a+) map source from snap gene app

Appendix III

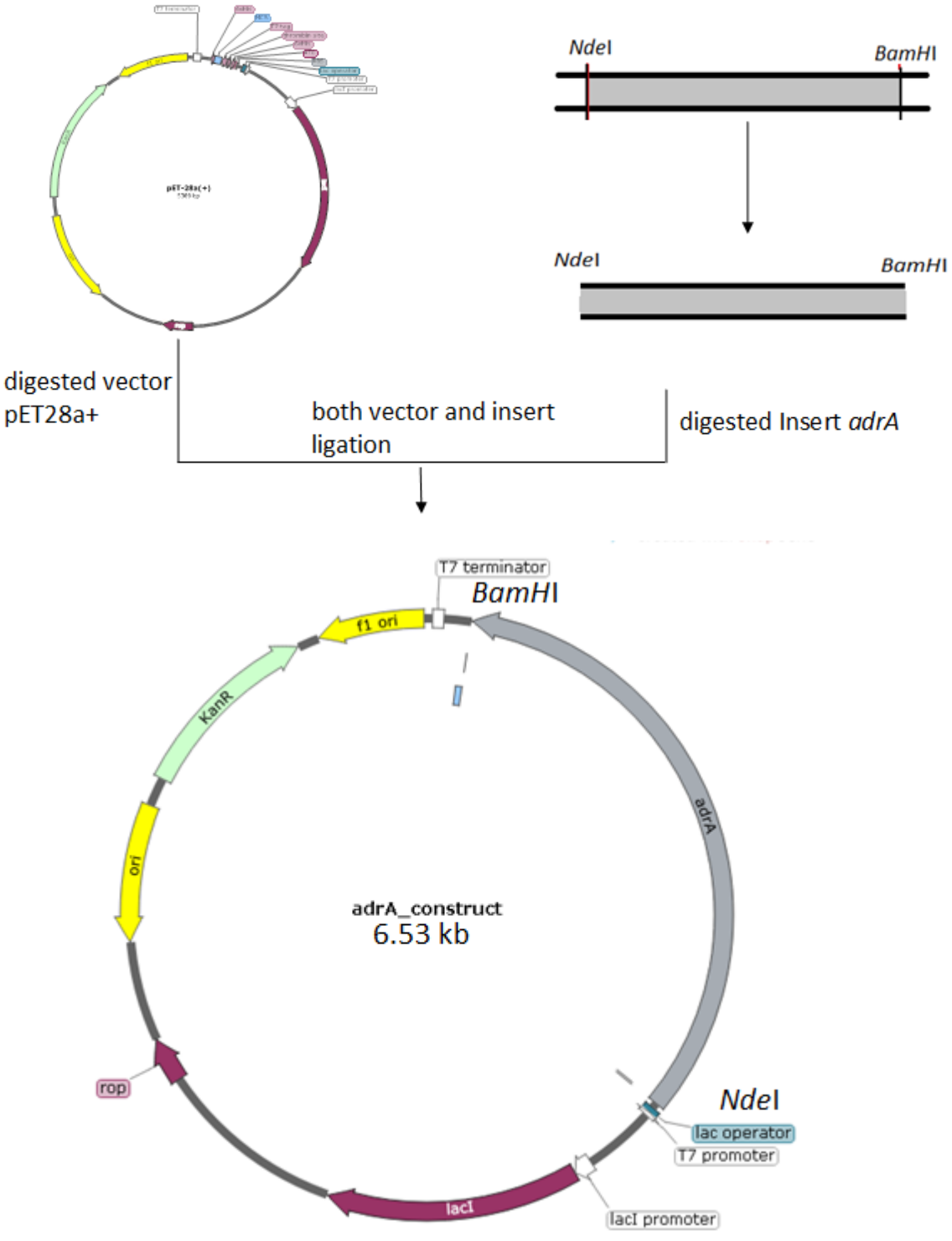

Figure (50): Schematic diagram of monocistronic construct of *adrA* gene, transformed into using suitable vector pET28a+

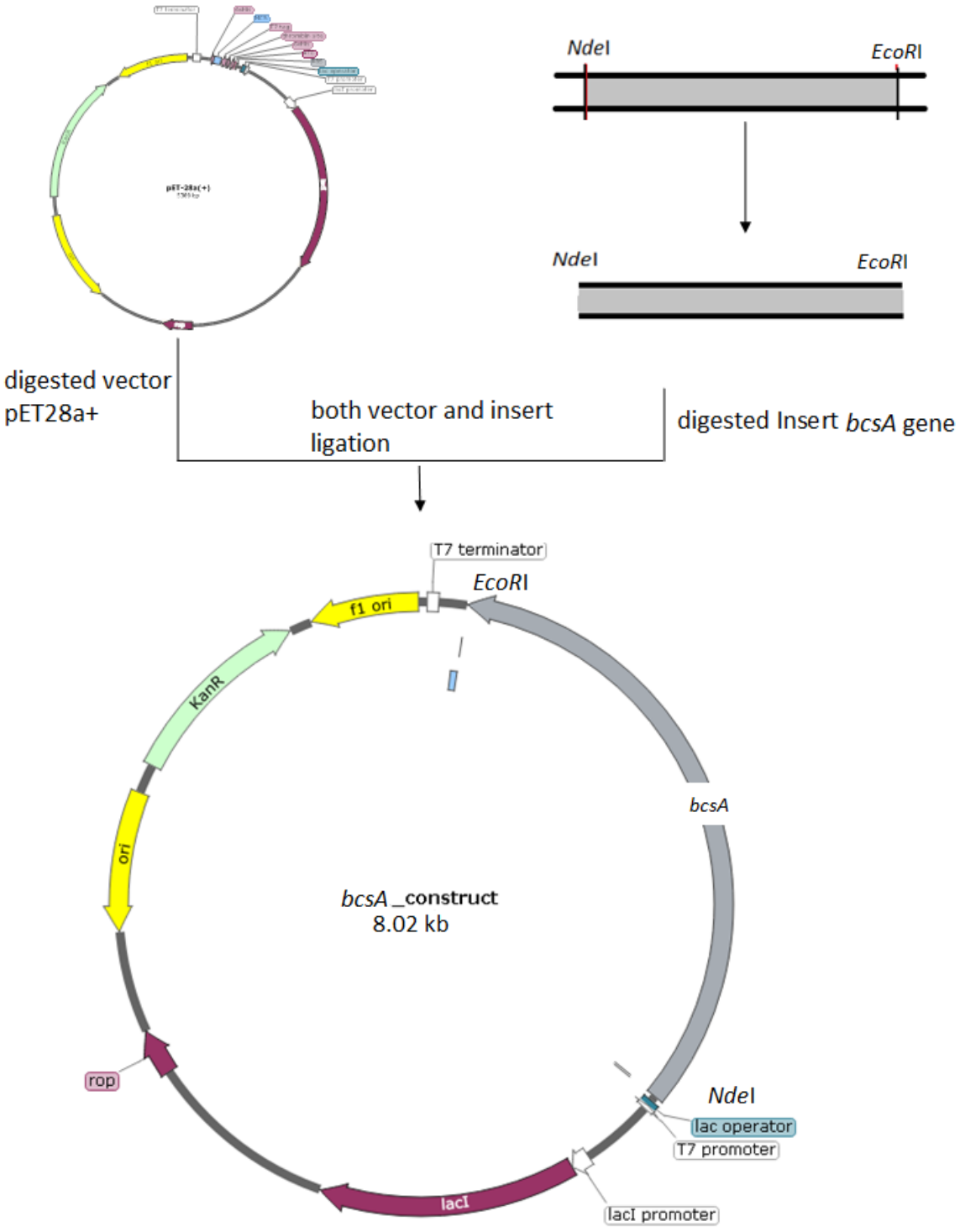

Figure (51): Schematic diagram of monocistronic construct of *bcsA* gene, transformed into using suitable vector pET28a+